

https://dspace.org/

Characterization of the DWNN domain and ring finger-like motif within the DCM of the Drosophila melanogaster SNAMA protein

Antunes, Ricardo Jorge

2009-05-25T13:03:09Z
http://hdl.handle.net/10539/6981

Downloaded from a DSpace repository. https://dspace.org/

CHARACTERIZATION OF THE DWNN DOMAIN AND RING FINGER-LIKE MOTIF WITHIN THE DCM OF THE *Drosophila melanogaster* SNAMA PROTEIN

Ricardo Jorge Antunes

A dissertation submitted to the School of Molecular and Cell Biology, Faculty of Science, University of the Witwatersrand, in fulfilment of the requirements for the degree of Master of Science.

Johannesburg, 2008

DECLARATION

I declare that this dissertation is my own, unaided work. It is being submitted for the degree of Master of Science to the University of the Witwatesrand, Johannesburg. It has not been submitted before for any degree or examination at any other institution, and all sources of information have been acknowledged by complete references.

_____

Ricardo Jorge Antunes

_____ day of _____, 2008

ABSTRACT

SNAMA is a 139 kDa *Drosophila melanogaster* protein belonging to the Retinoblastoma Binding Protein 6 (RbBP6) superfamily. Mammalian RbBP6 interacts with both p53 and Rb and plays a critical role in embryonic development and tumorigenesis as a negative regulator of p53. All RbBP6 members contain a 5´ DWNN Catalytic Domain (DCM) consisting of a DWNN (domain with no name) domain followed by a zinc finger and RING (really interesting new gene) finger motif. RING finger and U-box ubiquitin ligases are dependent on their RING finger conformation for their ubiquitin ligase activity. The main focus of this work was to further elucidate the functional characteristics of the DCM within SNAMA. This was achieved by examinining transcription regulation of the *SNAMA* gene and determining whether SNAMA exhibits ubiquitin ligase activity. 5´ Rapid amplification of cDNA ends (RACE) was used to determine the core promoter elements of *SNAMA* through the discovery of the transcription initiation site. Ubiquitin conjugation assays using pure recombinant SNAMA as the ubiquitin ligase were performed to analyze the ubiquitin ligase activity of the protein. Transcriptional regulation of the *SNAMA* gene is achieved through a single TATA-less promoter that gives rise to a single transcript of 3.9 kb. Furthermore, this work shows that SNAMA is a unique RING finger ubiquitin ligase that is capable of auto-ubiquitination in the absence of zinc ions. This activity is dependent on its RING finger-like motif, which has greatest specificity to the UbcH5a conjugating enzyme. Furthermore, SNAMA relies on E1, E2, ATP, and ubiquitin for its E3 activity. Thus, SNAMA is the first member of the RbBP6 family to portray RING finger ubiquitin ligase activity and represents a "drugable" target for pharmaceutical intervention.

ACKNOWLEDGEMENTS

I would like to thank my supervisor, Dr. Monde Ntwasa, for his guidance and support throughout the past few years. He has supplied me with much knowledge and inforced a strategic way of thinking in order to achieve an ultimate goal.

I would also like to thank all the members of the Fly Lab in recent years. In particular, I would like to thank Christopher Arnot for showing me the ropes and Rodney Hull for sharing his knowledge and for his companionship in the lab.

A big thank you to my family and friends for their love, and always being there to celebrate when things went well and mourn when stuff just wouldn't work.

Lastly, I would like to thank the National Research Foundation of South Africa as well as the University of the Witwatersrand for their financial support.

TABLE OF CONTENTS

DECLARATION……..…….. 2
ABSTRACT…….. 3
ACKNOWLEDGEMENTS……...4
TABLE OF CONTENTS…….. 5
LIST OF FIGURES……... 9
LIST OF TABLES……10
ABBREVIATIONS……... 11

1. INTRODUCTION……... 13
1.1 *Drosophila melanogaster* as a Model Organism…….……..13
1.2 Programmed Cell Death Within *Drosophila melanogaster*…….….14
1.2.1 Pro-apoptotic activator genes……..…….……14
1.2.2 Caspases……..…….……15
1.2.3 Inhibitor of apoptosis proteins (IAPs)……..……17
1.2.4 The Grim Reaper pathway……..…….……17
1.2.5 The Hippo pathway……..……18
1.2.6 The JNK pathway…… 20
1.3 *Drosophila melanogaster* p53 (Dmp53)……..…… 20
1.3.1 Identification of Dmp53…….. 20
1.3.2 Dmp53 activity…… 22
1.3.3 Regulation of Dmp53…….. 23
1.3.4 DNA damage-induced targets of Dmp53…… 23
1.4 Mammalian p53……..……. 25
1.5 SNAMA..…… 29
1.5.1 The domain with no name (DWNN)……... 32
1.5.2 The zinc finger…….34
1.5.3 The RING finger-like domain: C3SC4……34
1.6 The Retinoblastoma Binding Protein 6 (RbBP6) Superfamily…….35
1.6.1 RbBP6 function: a role in apoptosis…… 37
1.7 Ubiquitin……...…….37

1.8 Ubiquitin-Proteasome Pathway…… 39
1.9 Ubiquitin Ligases, the E3s…… 41
1.9.1 RING finger E3s…… 42
1.9.2 U-Box domain ubiquitin ligases, E4s…… 44
1.10 Deubiquitinating Enzymes (DUBs)…… 45
1.11 The Ubiquitin-like Superfamily…… 46
1.11.1 Ubiquitin-like proteins (UBLs)…… 46
1.11.2 Ubiquitin domain proteins (UDPs)…… 48
1.12 Aims…… 50

2. MATERIALS AND METHODS…… 52
2.1 Growth Media…… 52
2.2 Buffers and Solutions…… 52
2.3 Chemicals and Kits…… 53
2.4 Bacterial Strains…… 55
2.5 Oligonucleotides…… 55
2.6 Total RNA Extraction From Wild-Type *D. melanogaster*…… 56
2.7 5´ Rapid Amplification of cDNA Ends (5´ RACE)…… 56
2.8 Agarose Gel Electrophoresis…… 57
2.9 DNA Extraction from Agarose Gel…… 58
2.10 Cloning…… 58
2.10.1 Ligation…… 59
2.10.2 Preparation of chemically competent cells…… 59
2.10.3 Transformation…… 60
2.11 Small Scale Preparation of Plasmid DNA (Miniprep)…… 60
2.12 Polymerase Chain Reaction (PCR)…… 61
2.13 Quantification of Nucleic Acid…… 62
2.14 Restriction Digestion of DNA…… 62
2.15 SDS-PAGE…… 62
2.16 Recombinant Protein Expression in *E. coli*…… 63
2.17 Recombinant Protein Extraction from *E. coli*…… 64
2.17.1 Protein extraction using BugBuster® reagent…… 64

2.17.2 Protein extraction using lysis buffer……..……... 64
2.18 iFOLD^{TM} Protein Refolding System 1……..……65
2.19 Inclusion Body Solubilization…….……. 65
2.20 Purification of Recombinant Protein…….……... 66
2.20.1 His-tag purification…….. 66
2.20.2 GST-tag purification…… 67
2.21 Dialysis.…… 67
2.22 Quantification of Protein……..…….67
2.23 Circular Dichroism (CD) Spectroscopy……..……...68
2.24 Ubiquitin Conjugation Assay……..……..69
2.25 Bioinformatic Tools….……69

3. TRANSCRIPTIONAL REGULATION OF *SNAMA*……70
3.1 5´ Rapid Amplification of cDNA Ends (5´ RACE)…..……....72
3.2 Cloning of 5´ RACE Products……...……... 74
3.3 Sequence Alignments of the 5´ RACE Clones……..…….. 75

4. DOES SNAMA EXHIBIT UBIQUITIN LIGASE ACTIVITY?…….79
4.1 Recombinant Expression and Extraction of SNAMA…...……... 80
4.2 His-Tag Purification of Denatured Recombinant SNAMA……...…...81
4.3 Optimal Refolding Conditions for SNAMA……...……..83
4.4 Refolding the Pure, Denatured SNAMA……...……... 87
4.5 Confirmation of Correctly Refolded SNAMA Protein……...……..87
4.6 Ubiquitin Conjugation Assays Using SNAMA as the E3…...……. 92
4.6.1 Specificity of SNAMA activity to various E2s……92
4.6.2 Key components involved in SNAMA E3 ubiquitination……... 94

5. DISCUSSION……... 97
5.1 A single TATA-less Promoter Regulates Expression of *SNAMA*.……98
5.2 SNAMA Exhibits Ubiquitin Ligase Activity……..……..100
5.2.1 SNAMA has E3 activity capable of auto-ubiquitination……. 100
5.2.2 SNAMA demonstrates optimal activity with UbcH5a…… 101

5.2.3 SNAMA is a classical RING finger E3……..…….. 101
5.3 Conclusion……...……. 104
5.4 Future Work……...……...104

6. APPENDIX……...106
6.1 Appendix I (The SNAMA Protein and cDNA Sequence).……106
6.2 Appendix II (Chromosome Map of the 5´ RACE Products)……. 111
6.3 Appendix III (iFOLD^{TM} Protein Refolding System Plate Layout)….. 112
6.4 Appendix IV (Secondary Structure Prediction for SNAMA DCM)… 113
6.5 Appendix V (TA Cloning Vectors)….…… 114
6.6 Appendix VI (pET41(a) Expression Vector Map and MCS)…..…….. 116
6.7 Appendix VII (CD Spectra of Characteristic Secondary Structures)... 117
6.8 Appendix VIII (The Molecular Weight Markers)…….. 118

7. REFERENCES…….119

LIST OF FIGURES

Figure 1: Programmed cell death in *Drosophila melanogaster*

Figure 2: *Drosophila melanogaster* p53 isoforms: dp53L, dp53, and dp53n

Figure 3: Regulation of p53 and Mdm2 during cell survival and apoptosis

Figure 4: Schematic representation of the *Drosophila* SNAMA protein

Figure 5: The domain structure of the RbBP6 family of proteins

Figure 6: Multiple alignment of DWNN from various organisms

Figure 7: The "cross-brace" structure of RING finger motifs

Figure 8: The native structure of ubiquitin

Figure 9: Degradation of proteins via the ubiquitin-proteasome pathway

Figure 10: 5´ Rapid amplification of cDNA ends using *Drosophila* RNA

Figure 11: PCR amplification to verify cloning of 5´ RACE products

Figure 12: Multiple sequence alignment of cloned 5´ RACE products

Figure 13: The 5´ region of the *SNAMA* gene that is ultimately translated into the DWNN catalytic module

Figure 14: Recombinant expression of GST-fusion SNAMA protein

Figure 15: His-tag purification of denatured recombinant SNAMA protein

Figure 16: Refolding conditions for the recombinant SNAMA protein

Figure 17: Dialysis of His-tag purified SNAMA protein

Figure 18: Glutathione affinity chromatography of refolded GST-S protein

Figure 19: CD spectra for the recombinant GST-S and GST proteins

Figure 20: The test for ubiquitin ligase activity of SNAMA, and its specificity towards various E2s

Figure 21: The dependence of SNAMA E3 activity on key ubiquitination factors

Figure 22: The effect of ATP on SNAMA E3 activity

Figure 23: Multiple alignment of RING finger motifs from the RbBP6 superfamily

LIST OF TABLES

Table 1: Ubiquitin ligases specific for p53 ubquitination and degradation

Table 2: Growth media

Table 3: Molecular biology buffers and solutions

Table 4: Chemicals, kits and their suppliers

Table 5: Bacterial strains

Table 6: Oligonucleotides used during PCR, RT-PCR, and sequencing

Table 7: Buffers used during His-tag purification under denaturing conditions

Table 8: Web addresses for various bioinformatic tools used

Table 9: The most effective refolding buffers for recombinant SNAMA

ABBREVIATIONS

5´ RACE	5´ rapid amplification of cDNA ends
BIR	baculoviral IAP repeat
CD	circular dichroism
CHO	Chinese hamster ovary
DCM	DWNN Catalytic Module
Dmp53	*Drosophila melanogaster* p53
DPM	downstream promoter element
DUB	deubiquitinating enzymes
DWNN	domain with no name
EGFR	epidermal growth factor receptor
GR	GeneRacer
GST	glutathione S-transferase
GuHCl	guanidinium hydrochloride
HECT	homology to E6AP C-terminus
IAP	inhibitor of apoptosis proteins
Inr	initiator
IPTG	isopropyl-β-D-thiogalactoside
IR	ionizing radiation
JNK	c-jun N-terminal kinase
kDa	kilodalton
MAPK	mitogen-activated protein kinase
Mdm2	mouse double minute 2
MNK	maternal nuclear kinase
MST	mammalian sterile twenty-like
MTE	motif ten element
NMR	nuclear magnetic resonance
P2P-R	proliferation potential protein-related
PACT	p53-associated cellular protein-testes derived
PHD	plant homeo-domain
RbBP6	retinoblastoma binding protein 6

RBQ	Rb-binding Q-protein
RHG	Reaper Hid Grim
RING	really interesting new gene
RF	RING finger
RFL	RING finger-like
RUB	related to ubiquitin
SDS-PAGE	sodium dodecyl sulphate-polyacrylamide gel electrophoresis
SUMO	small ubiquitin-like modifier
TNF	tumour necrosis factor
UBL	ubiquitin-like protein
UDP	ubiquitin domain protein
USP	ubiquitin specific protease
UTR	untranslated region

1. INTRODUCTION

1.1 *Drosophila melanogaster* as a Model Organism

Drosophila melanogaster (meaning dark-gut dew-lover) is a common fruit fly belonging to the family Drosophilidae and found in the order Diptera. It is therefore classified as an insect. It was first used as a model organism in the early 1900's by Nobel Prize winner Thomas Hunt Morgan for his genetic research on sex-linkage and genetic recombination (Morgan et al., 1915).

Drosophila is a very popular and successful model organism due to the great number of properties that it possesses. It has a short generation time of 10-12 days making it possible to study numerous generations in an academic year (Kramer, 1986; Sofer and Tompkins, 1994). It is easily cultured and inexpensive to house in large numbers (Jeszenszky, 1997; Kramer, 1986). Due to its small size *Drosophila* is suitable for cultivation in laboratories yet it is large enough for many attributes to be seen with the naked eye or under low-power magnification (Sofer and Tompkins, 1994). It has a high rate of reproduction with a female laying hundreds of fertilized eggs during her brief life span. Giant polytene chromosomes that show far more structural detail than do normal chromosomes are found in the salivary and other glands of the mature larvae (Mortin and Sedat, 1982). Furthermore, the *Drosophila* embryo grows outside the body and can be easily studied at every stage of development.

Since Thomas Hunt Morgan, for over a century *Drosophila* has been used as a popular model organism in heredity and biomedical research where the aims are to understand human genetics and developmental processes (Celniker, 2000). This is possible due to *Drosophila* showing the same developmental plasticity as that seen in humans but having less redundancy, allowing for easier dissection of function (Richardson and Kumar, 2002). More recently *Drosophila* has been used for what it does best: identifying novel oncogenes and tumor suppressors, and linking cancer-related genes together into complex signalling pathways

(Vidal and Cagan, 2006). This was facilitated by the completion of the *Drosophila* euchromatic genomic sequence (Celniker, 2000), which revealed that two thirds of genes involved in human cancers have counterparts in *Drosophila* (Vernooy et al., 2000).

Perhaps the greatest advantage of *Drosophila* is its powerful genetics. This can be used to generate mutations and transgenic lines that ectopically overexpress genes, examine genetic interactions, and carry out dominant genetic modifier screens to uncover novel genes (Richardson and Kumar, 2002). All of these genetic approaches have been used for comparative study of programmed cell death between *Drosophila* and humans.

1.2 Programmed Cell Death Within *Drosophila melanogaster*

Regulation of programmed cell death or apoptosis is a delicately controlled process, one which is critical to a wide variety of developmental processes. This includes removal of unnecessary anatomical structures, control of cell number, morphological sculpting, and elimination of injured or dangerous cells (Jacobson et al., 1997). Regulation of cell number is critical for proper organism development and homeostasis. In *Drosophila*, programmed cell death can be controlled intrinsically through caspase-dependent pathways such as the Grim Reaper or Hippo pathways (Figure 1). The intrinsic cell death system is controlled predominantly by: pro-apoptotic activators (*H99* genes), caspases, inhibitor of apoptosis proteins (IAP), and tumour suppressors. Alternatively, an extrinsic cell death-inducing mechanism is used whereby the physiological ligand Eiger stimulates cell death via the JNK pathway (Igaki et al., 2002).

1.2.1 Pro-apoptotic activator genes

Only five pro-apoptotic activators have been discovered in *Drosophila* thus far, they are *reaper* (*rpr*), *grim, head involution defective* (*hid*), *sickle (skl),* and *jafrac2* (Cashio et al., 2005). *Rpr, grim* and *hid* are three closely linked genes

contained within the *H99* cell death locus (Chen et al., 1996), while *skl* is found just outside the *H99* locus (Srinivasula et al., 2002; Wing et al., 2002). In contrast, *jafrac2* is found in a very different position of the genome that still contains *H99*-like characteristics (Tenev et al., 2002). The domain structure of these pro-apoptotic genes and the functional human homologue, Smac, share a conserved N-terminal region known as the RHG (Reaper Hid Grim) motif (Wing et al., 2001). Outside this motif they are not similar and vary significantly in size. The RHG motif has been shown to competitively bind a domain in the IAP family and in so doing prevents inhibition of caspase activity. It is thus clear that the RHG motif is important in the pro-apoptotic function of the activator proteins.

Rpr expression is regulated by the steroid hormone ecdysone and by developmental signals (Jiang et al., 2000; Nordstrom et al., 1996). Grim, like Rpr, is also expressed in cells destined for death whereas Hid has a more general expression pattern (Chen et al., 1996). *Hid* is negatively regulated at both transcriptional and posttranscriptional levels by the epidermal growth factor receptor (EGFR)-Ras-Raf-MAPK signaling pathway (Grether et al., 1995; Bergmann et al., 1998; Kurada and White, 1998). Additional *in vivo* analysis of these *H99* pro-apoptotic genes is needed in order to determine the factors that control its expression.

1.2.2 Caspases

Caspases are commonly implemented during the process of apoptosis. These caspases are highly conserved cysteine proteases that specifically target and cleave substrates after an aspartate residue (Cashio et al., 2005). Caspases are expressed as inactive zymogen precursors that consist of a variable length prodomain followed by a large (p20) and small (p10) unit, which are responsible for substrate recognition and catalysis. Activation occurs through the incorporation of the caspase into large protein complexes, or through the separation of the p10 and p20 subunits and reassembly into an active

heterotetramer. Once activated, they literally break down the protein scaffolding holding the cell together leading to the destruction of the cell and ultimate death (Degterev et al., 2003).

Caspases are divided into two general classes: apical caspases (Class I) and effector caspases (Class II). Caspases are activated in an amplifying proteolytic cascade with cleavage of one another in sequence (Cashio et al., 2005). It therefore makes sense that the apical caspases are activated early at the onset of apoptosis while downstream effector caspases are activated later by already active apical caspases via proteolytic processing. Apical caspases are usually characterized according to their long N-terminal prodomain, which contain protein-protein binding motifs that are essential for their caspase activity (Degterev et al., 2003).

Thus far seven caspase-encoding genes have been identified in the *Drosophila* genome: *dcp-1*, *dredd*, *drice*, *dronc*, *decay*, *strica*, and *damm* (Kumar and Doumanis, 2000; Salvesen and Abrams, 2004). Based on the prodomain structure, Dcp-1, Drice, Decay, and Damm are effector caspases whilst Dronc (*Drosophila* Nedd-2 like Caspase) and Dredd (death related CED-3/Nedd2-like protein) are classified as apical caspases. Dronc contains a CARD (Caspase Activation and Recruitment Domain) motif in its prodmain and is most similar to caspase-2 and -9 in mammals (Dorstyn et al., 1999). Dredd contains a pair of DEDs (death effector domain), and although it similar to mammalian caspase-8, Dredd doesn't seem to play a role in the apoptotic immune response (Leulier et al., 2000). Strica contains a long prodomain but does not contain any known protein-protein interaction motifs, nor are there any mutants for *strica* that could be used to clarify its function (Doumanis et al., 2001). Thus, with the role of Strica still unclear it seems as though Dronc is the only "classical" apical caspase. Furthermore, various studies have been done that establish Dronc as an essential caspase in *Drosophila* apoptosis (Meier et al., 2000; Quinn et al., 2000; Muro et al., 2002).

1.2.3 Inhibitor of apoptosis proteins (IAPs)

The key role of IAPs in both mammals and *Drosophila* is to bind to caspases thereby rendering them biochemically inactive and ultimately preventing apoptosis from taking place (Salvesen and Duckett, 2002). IAPs are highly conserved throughout all eukaryotes and share several structural motifs (Miller, 1999). An example is the presence of between one and three tandem baculoviral IAP repeat (BIR) motifs, which is indicative of an IAP family member (Salvesen and Duckett, 2002). The BIR motif is essentially a Zn-binding fold of approximately 80 residues that is pivotal for the anti-apoptotic function of IAPs. In addition, some IAPs contain a RING (Really Interesting New Gene) finger domain that confers E3 ubiquitin ligase activity, leading to ubiquitin-mediated protein degradation. Targets for ubiquitination include the caspases, the H99 proteins and the IAPs themselves. IAPs appear to interact with only a certain subset of caspases and it does so through the BIR motifs. Those with more than one BIR motif fold into functionally independent structures, each with different substrate specificity (Cashio et al., 2005). This has been illustrated in *Drosophila* where the BIR1 motif of *Drosophila* IAP1 (DIAP1) specifically inhibits Dcp-1 and Drice, whereas BIR2 inhibits Dronc (Zachariou et al., 2003; Chai et al., 2003; Yan et al., 2004).

There are four IAPs encoded by the *Drosophila* genome: *diap1*, *diap2*, *deterin* and *dBruce*. Of these the *diap1* gene appears to be most important and thus most extensively studied. This gene encodes for an IAP with two BIR motifs and a single RING domain (Hay et al., 1995). Loss of *diap1* results in uncontrolled caspase activation causing massive and widespread apoptosis that ultimately leads to embryonic lethality (Wang et al., 1999).

1.2.4 The Grim Reaper pathway

The most popular and extensively studied cell death system in *Drosophila* is that involving the activation of the pro-apoptotic genes in the Grim Reaper pathway.

In *Drosophila* cells that have not received apoptotic stimuli, the BIR2 domain of DIAP1 binds to the prodomain of Dronc, thus preventing the association of Dronc with the human Apaf-1 homologue Dark (Zachariou et al., 2003) (Figure 1). This DIAP1-Dronc complex allows the RING domain of DIAP1 to catalyze the ubiquitination and subsequent degradation of Dronc thereby inactivating it. Dronc therefore requires inhibition of complex formation with DIAP1 in order to become active. Upon apoptotic stimulation pro-apoptotic H99 proteins (Rpr, Grim, Hid, Skl, Jafrac2), through their highly conserved RHG motif, bind with high affinity to the BIR2 domain of DIAP1 (Cashio et al., 2005). This prevents DIAP1 from forming a complex with the apical caspase Dronc.

In this way H99 proteins function as IAP antagonists. However, it is unclear whether this competition leads to displacement of Dronc from DIAP1 or whether there is inactivation of free DIAP1 upon H99 protein binding. In either case Dronc is free to bind with the adaptor protein Dark and gain activity thus becoming “the executioner” of the cell suicide program through the specific cleavage of target proteins (Cashio et al., 2005). Meanwhile, DIAP1 undergoes degradation through self-ubiquitination (Cashio et al., 2005) and is thought to degrade the bound H99 proteins in the same way (Olson et al., 2003).

1.2.5 The Hippo pathway

The Hippo pathway is a recently discovered cell signaling event that coordinately controls cell proliferation and apoptosis in *Drosophila* (Edgar, 2006). It consists of six pro-apotoptotic components: Merlin, Expanded, Hippo (Hpo), Salvador (Sav), Warts/Lats (Wts), and Mob1 as a tumour suppressor (Mats), as well as a single anti-apoptotic component: Yorkie (Yki) (Thompson and Cohen, 2007). Merlin and Expanded are related FERM-domain proteins that are located at the cytoskeleton and are the most upstream components of the pathway. Hpo is a MST-family kinase that functions with the adaptor protein Sav to either: phosphorylate and decrease stability of DIAP1, or phosphorylate and activate Wts. Wts is a NDR-family kinase that functions with the adaptor

protein Mats to phosphorylate and inactivate Yki (Colombani et al., 2006). Yki is a transcriptional cofactor that functions in promoting cell cycle regulation through Cyclin E transactivation and inhibiting apoptosis through expression of DIAP1 (Huang et al., 2005). In addition, Yki also activates Merlin and Expanded as part of a negative feedback loop (Hamaratoglu et al., 2006). Activation of the Hippo pathway in response to irradiation leads to the activation of the apical caspase Dronc, and ultimately cell death through proteolytic processing. Furthermore, all the components of the Hippo pathway are conserved in humans and several have been implicated in human cancer.

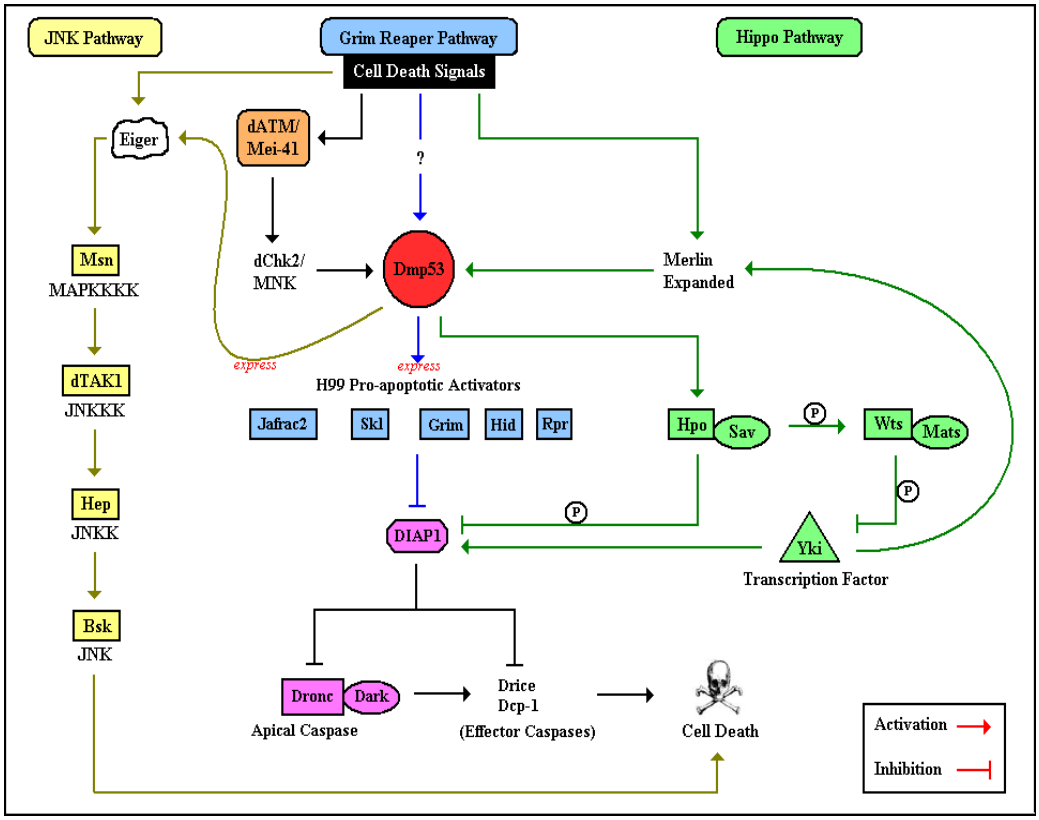


Figure 1. Programmed cell death in *Drosophila melanogaster*. Apoptosis is controlled intrinsically through caspase-dependent pathways such as the Grim Reaper or Hippo pathways. The intrinsic cell death system is controlled by pro-apoptotic activators (*H99* genes), caspases, IAPs, and tumour suppressors. Alternatively, apoptosis can occur extrinsically through Eiger via the JNK pathway. Dmp53 has a pivotal role in *Drosophila melanogaster* programmed cell death and is linked to both the extrinsic and intrinsic cell death systems.

1.2.6 The JNK pathway

A search for cell death-inducing factors, responsible for reduced eye size in *Drosophila*, led to the discovery of the first invertebrate tumour necrosis factor (TNF) ligand, Eiger (Igaki et al., 2002). Overexpression of Eiger results in severe developmental defects that are distinct from that of Reaper. Eiger induces IAP-sensitive cell death through activation of the *Drosophila* JNK pathway and does not require caspase activity (Igaki et al., 2002). Furthermore, the structure and function of Eiger suggests that this extrinsic cell death-inducing mechanism may be evolutionarily conserved in *Drosophila*. Eiger binds an Eiger receptor containing a TNF receptor homology domain and a transmembrane domain. This results in the activation of downstream Misshapen (Msn), a *Drosophila* MAPKKKK, which in turn activates dTAK1, a *Drosophila* JNKKK. dTAK1 then activates the *Drosophila* JNKK, Hemipterous (Hep), which ultimately activates the JNK, Basket (Bsk). Bsk is responsible for inducing cell death, possibly through JNK-mediated release of mitochondrial caspase-independent cell death factors (Igaki et al., 2002). Recent analysis has shown that while overexpression of *Eiger* is sufficient to induce apoptosis, it is not required for ionizing radiation (IR)-induced apoptosis (Brodsky et al., 2004).

1.3 *Drosophila melanogaster* p53 (Dmp53)

1.3.1 Identification of Dmp53

Dmp53 was identified by three groups while performing homology searches in *Drosophila* using the human homologue p53 (Ollmann et al., 2000; Brodsky et al., 2000; Jin et al., 2000). It was initially described as a 42 kDa *Drosophila melanogaster* protein of 385 amino acids. Year's later, after the discovery of a conserved internal promoter in mammalian *p53*, experiments were performed to identify an internal promoter in *Drosophila p53* (Bourdon et al., 2005). In so doing it was discovered that in fact the *Dmp53* gene encodes for three Dmp53

isoforms *in vitro*: dp53L (495 amino acids), dp53 (385 amino acids), and dp53n (123 amino acids) (Figure 2).

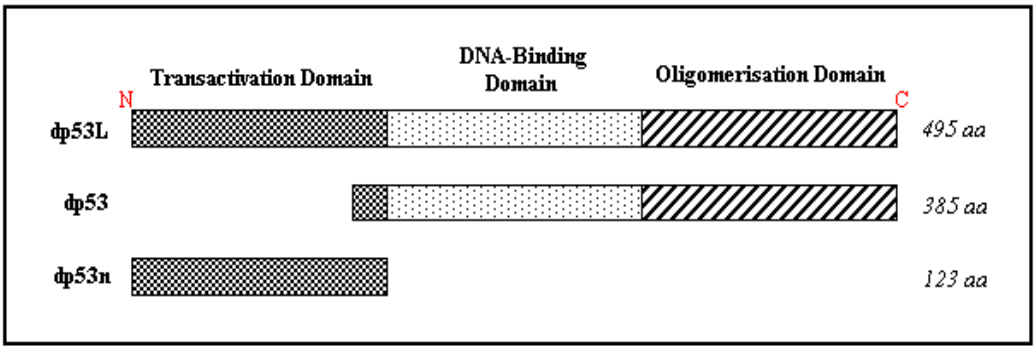


Figure 2. *Drosophila melanogaster* p53 isoforms: dp53L, dp53, and dp53n. dp53 is a N-terminally truncated isoform of an internal promoter and is identical to that first published. dp53L is initiated at exon A, 580 bp upstream of the internal promoter, and contains the conserved N-terminal domain FxxψW. This domain is not found within dp53 and is required to activate gene transcription. The third isoform, dp53n, is a splice variant of dp53L with no slicing of intron B (Bourdon et al., 2005).

dp53 is initiated at exon 1 and is identical to that first published. In contrast, dp53L contains two extra exons (exons A and B) and is initiated 580 bp upstream of exon 1. dp53n is a splice variant of dp53L where there is no slicing of intron B. Because expression of dp53L is initiated at exon A it contains a longer N-terminal domain whereas dp53 is a N-terminally truncated isoform produced from an internal promoter (Bourdon et al., 2005). This confirms the hypothesis made by Bourdon and his colleagues of a conserved internal promoter existing within *Drosophila p53*, and strongly suggests an essential role in the control of *p53* family activities.

Alignment of p53 proteins from various families revealed that the only domain conserved through evolution within the N-terminal end is the sequence FxxψW (Bourdon et al., 2005). It is this domain that is required to activate gene

transcription. The dp53L isoform but not the dp53 isoform contains the domain FxxψW, indicating that dp53L is homologous to full length p53 and p53-related proteins and strongly suggests that dp53L is able to transactivate genes.

Although the overall homology between Dmp53 and human p53 is found to be very low, significant similarity has been shown in the central DNA-binding domain (Brodsky et al., 2000). This includes residues identified in human p53 that are critical for DNA sequence recognition and coordination of a zinc ion. In contrast, the C- and N-termini of Dmp53 show little similarity with human p53 (Sutcliffe et al., 2003). Dmp53 does, however, contain secondary structures and enriched basic residues at its C terminus and a high proportion of acidic residues at its N terminus. These residues at the C- and N-termini of Dmp53 are shared in human p53 where they regulate sequence-specific DNA binding and function in transcriptional activation respectively (Sutcliffe and Brehm, 2004). Furthermore, like human p53 the dp53L isoform contains the highly conserved FxxψW at its N-terminus, which is thought to activate gene transcription.

1.3.2 Dmp53 activity

The effect of a dominant-negative Dmp53 on radiation-induced arrest of cell cycle progression shows that entry into mitosis is not affected by this mutation (Brodsky et al., 2000). More specifically Dmp53 does not engage checkpoint controls through the cell cycle such as its human counterpart p53, which mediates G1 cell cycle arrest through induction of p21 (Ollmann et al., 2000). This is consistent with the observation that the *Drosophila* p21/p27 homolog, *dacapo*, is not induced by IR (Brodsky et al., 2004). Null mutations in Dmp53 do not show dramatic effects with flies being viable and semi-sterile (Lee et al., 2003). However, upon exposure to a DNA damaging stimulus such as radiation, Dmp53 is required for apoptosis in the wing (Brodsky et al., 2000). Overexpression of Dmp53 is also sufficient to induce apoptosis, but the response is either qualitatively or quantitatively different from the apoptotic response to DNA damage (Brodsky et al., 2000). Thus, the role of Dmp53 in apoptosis

induction has been shown to be conserved. Recently, a genome-wide analysis involving IR-induction showed that Dmp53 is not only involved in apoptotic regulation but also other cellular pathways that include cell-cell signaling and DNA repair (Brodsky et al., 2004).

1.3.3 Regulation of Dmp53

Not much is known about the regulation of Dmp53 but the information accumulated thus far suggests that Dmp53 is regulated in a partially conserved, ancestral way. Upstream regulators of Dmp53 activation include Mei-41 and MNK (maternal nuclear kinase), the *Drosophila* homologs of mammalian ATM (ataxia-telangiectasia-mutated) and Chk2 (checkpoint-homologs 2) respectively. Both these kinases are involved in DNA damage responses (Brodsky et al., 2000), with MNK shown to directly activate Dmp53 (Peters et al., 2002).

MNK/*d*Chk2 is required for both induction of cell cycle arrest and apoptosis in response to DNA damage (Xu et al., 2001). Furthermore, overexpression of Dmp53 results in apoptosis that is enhanced by the co-expression of MNK, but not the kinase-inactive form of MNK (Peters et al., 2002). This effect is specific, with no change in apoptotic levels when Dmp53 is co-expressed with wild-type and mutant *Drosophila* Chk1, Grape (Sutcliffe et al., 2003; Brodsky et al., 2004). Like its human counterpart, Dmp53 is phosphorylated by MNK indicating that posttranslational modification is necessary for Dmp53 activation and consequent induction of apoptosis (Brodsky et al., 2004). However, unlike its human counterpart, Dmp53 levels remain constant following activation (Sutcliffe et al., 2003).

1.3.4 DNA damage-induced targets of Dmp53

Analysis of Dmp53 targets in response to IR identified far less genes in *Drosophila* than p53 gene targets in mammals (Brodsky et al., 2004). Targets of mammalian p53 have been identified in many different cell types following different sources of DNA damage or simply overexpression of p53. It is

therefore likely that additional targets of Dmp53 will be identified when using different causes of cellular stresses in different cell types or developmental stages.

Dmp53 regulated apoptosis: Intrinsic mechanism

The most prominent group of Dmp53 targets discovered thus far are the pro-apoptotic genes of the Grim Reaper pathway. Initially, *reaper* was found to be the only effector of the pro-apoptotic function of Dmp53 (Brodsky et al., 2000). More recently it has been shown that activated Dmp53 induces programmed cell death by expressing additional proapoptotic genes including *Hid* and *sickle* (Brodsky et al., 2004). Dmp53 transactivates expression of these proapototic genes, which leads to the activation of apical caspases through the inhibition of IAPs (Wang et al., 1999). In this way caspase activity is increased illustrating one way in which Dmp53 induces apoptosis in *Drosophila* (Brodsky et al. 2000). Alternatively, activation of apical caspases is accomplished by the activation of Dark, the human Apaf-1 homolog, which is activated by the reaper protein (Nordstrom and Abrams, 2000).

Although the pro-apoptotic genes *reaper, hid, and sickle* are Dmp53 transcriptional targets, removal of these three proteins through chromosomal deficiencies only partially suppresses the cell-death effects of IR in embryos (White et al., 1994). This implies that there are additional death signals that are independent of the Grim Reaper pathway. Recently it has been shown that it is possible for the Hippo apoptotic pathway to be activated by IR in a Dmp53-dependent manner (Colombani et al., 2006). Hpo is required, although not entirely, for the cell death response to DNA damage or Dmp53 ectopic expression.

Dmp53 regulated apoptosis: Extrinsic mechanism

It has recently been shown that the *Drosophila* TNF homolog, *Eiger*, is transactivated by Dmp53 during IR induction (Brodsky et al., 2004). As mentioned earlier, overexpression of Eiger leads to apoptosis through the activation of the *Drosophila* JNK pathway, however, it is not required for IR-induced apoptosis (Igaki et al., 2002; Brodsky et al., 2004). Thus, it is still unclear how transcriptional activation of *Eiger* by Dmp53, and apoptosis, are related following IR induction. It is possible that the conserved activation of the JNK pathway by Dmp53 is required for the induction of apoptosis under specific conditions that have not been tested for yet. In this way, Dmp53 is thought to be involved in cell-cell signaling that ultimately leads to apoptosis in response to DNA damage.

1.4 Mammalian p53

Human p53 consists of a N-terminal transactivation domain, a central sequence-specific DNA binding domain, and a C-terminal oligomerization domain (Sutcliffe and Brehm, 2004). p53 is a tumor suppressor protein that is characterized primarily as a sequence-specific transcription factor (Lee et al., 2003). In normal unstressed cells, p53 is an inactive short-lived protein, which is maintained at very low, almost undetectable levels in the cell. Cellular stresses, such as DNA damage, hypoxia, or abnormal oncogene activation, activate and increase p53 levels, which lead to inhibition of growth through activities that reversibly arrest the cell cycle or promote apoptosis (Vousden, 2000). Activation of p53 occurs as a result of post-translational modifications that include acetylation and phosophorylation (Oren, 2003). Mutations in p53 are responsible for more than half of all human cancers (Levine, 1997; Ryan et al., 2001).

p53-specific E3 ligases such as Mdm2 play a pivotal role in regulating p53 levels in cells under normal conditions. Mdm2 is involved in an autoregulatory negative feedback loop with p53, whereby p53 induces *Mdm2* expression and

Mdm2 represses p53 activity (Wu et al., 1993). This serves as a vital mechanism for restraining p53 function in normal cells without stress (Midgley and Lane, 1997; Michael and Oren, 2002). The N-terminal region of Mdm2 binds p53 to form a tight complex that controls p53 function either through the physical inhibition of p53-mediated transcriptional activity (Chen et al., 1995), or by p53 degradation (Haupt et al., 1997). The RING finger motif at the N-terminal of Mdm2 allows it to function as an E3 ubiquitin ligase that ubiquitinates p53, thereby targeting it for degradation by proteasome (Honda et al., 1997) (Figure 3). Interestingly, in addition to p53, Mdm2 catalyzes ubiquitination of itself (Fang et al., 2000).

Recent studies have shown that Mdm2-mediated ubiquitination is not the only regulator of p53, although it is the most important. An *in vivo* mutant of p53, that lacks major Mdm2 ubiquitination binding sites, has been shown to contain a normal half-life that is stabilized and activated in response to stress (Feng et al., 2005; Krummel et al., 2005). Furthermore, E3 ligases other than Mdm2 have been shown to specifically bind p53 and promote its degradation via ubiquitination (Brooks and Gu, 2006). Pirh2, a RING-H2 domain-containing protein, interacts with p53 and promotes Mdm2-independent p53 ubiquitination and degradation (Leng et al., 2003). Like Mdm2, Pirh2 is a p53 responsive gene that participates in a similar autoregulatory negative feedback loop. Another E3 ligase, COP1, is also a p53-inducible gene that can ubiquitinate and degrade p53 (Dornan et al., 2004). ARF-BP1, a HECT domain containing E3 ligase, was recently identified and is also capable of p53 ubiquitination and degradation (Chen et al., 2005). However, the ARF-BP1 ligase lacks a feedback loop that is present in the other ligases examined. Together, Mdm2, COP1, Pirh2, and ARF-BP1 represent an array of E3 ligases that the cell can call upon to regulate and maintain p53 levels (Figure 3). This suggests that both Mdm2-dependent and –independent mechanisms are used cooperatively by the cell for tight p53 regulation.

The genomes of *H. sapiens*, *M. musculus*, *D. melanogaster*, and *C. elegans* were screened for putative homologs of the aforementioned p53-specific E3 ligases (Brooks and Gu, 2006) (Table 1). Lower organisms such as *C. elegans* and *D. melanogaster*, which have fully functional p53, lacked the Mdm2 ortholog. Counterparts of the COP1 ligase were also absent in these lower organisms, although a homolog for Pirh2 was identified in *Drosophila* (Yi and Deng, 2005; Bernards and Hariharan, 2001). The ARF-BP1 gene is well conserved in all organisms.

Table 1. Ubiquitin ligases specific for p53 ubquitination and degradation. Genomes of *H. sapiens*, *M. musculus*, *D. melanogaster*, and *C. elegans* were screened for putative homologs to a number of E3 ligases that included Pirh2, COP1, Mdm2, and ARF-BP1 (Brooks and Gu, 2006).

	H. Sapiens	*M. Musculus*	*D. melanogaster*	*C. elegans*	Type
Pirh2	+	+	+	-	RING
COP1	+	+	-	-	RING
Mdm2	+	+	-	-	RING
ARF-BP1	+	+	+	+	HECT

DNA damage activates p53 through post-transcriptional modifications that include acetylation and phosophorylation (Oren, 2003). Acetylation of residues at the C-terminus of p53 during times of cell stress serves to block protein degradation by ubiquitination and stabilize p53 (Brooks and Gu, 2006). In addition Mdm2 can be acetylated at residues in its RING finger domain thereby inactivating the protein and increasing p53 transcriptional activity. Mdm2 can only bind to dephosphorylated p53, therefore under stressful conditions when there is a need for increased p53 activity, Mdm2 binding is prevented by p53 phosphorylation (Figure 3). Hence, the interaction between Mdm2 and p53 is disrupted, and Mdm2 can no longer target p53 for ubiquitination.

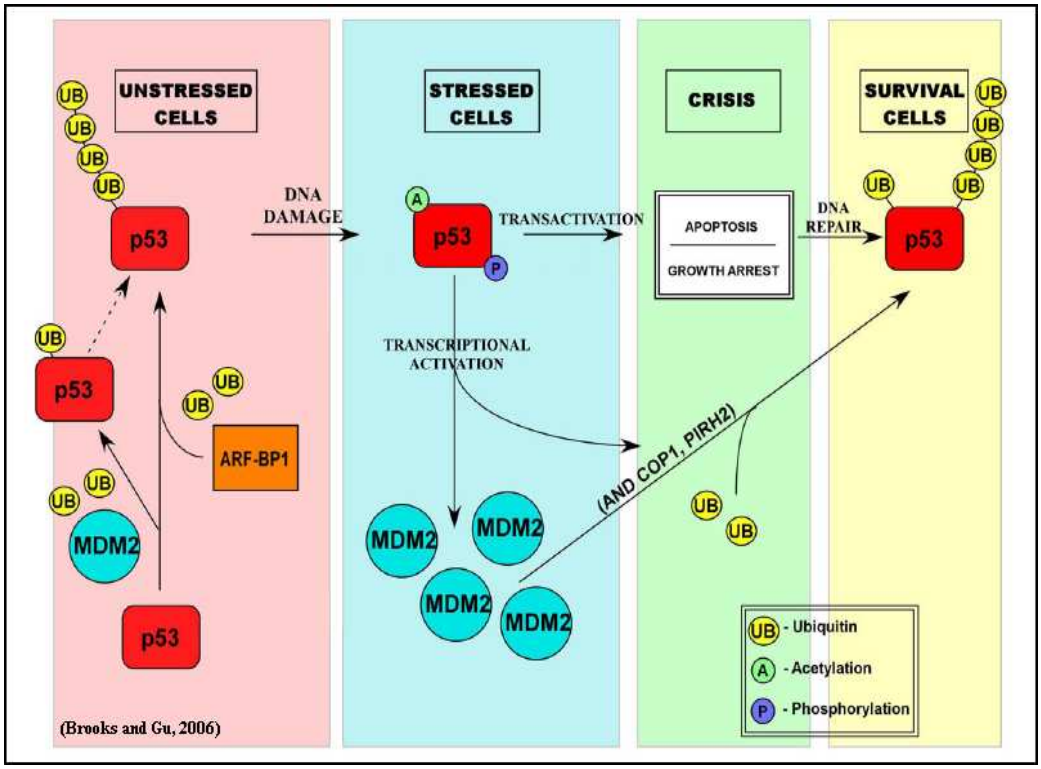


Figure 3. Regulation of p53 and Mdm2 during cell survival and apoptosis. In normal cells under no stress, extremely low levels of p53 are evident due to ubiquitination and degradation of p53 by E3 specific ligases such as Mdm2. Upon cell stress through DNA damage, p53 becomes stabilized and activated by post-translational modifications (Brooks and Gu, 2006).

Direct or indirect phosphorylation of p53 is controlled by DNA damage-induced kinases such as ATM, Chk1, and Chk2, which leads to p53 activation (Canman et al., 1998; Shieh et al., 2000). Once activated, p53 moves into the nucleus where it binds to specific enhancers and regulates transcription of adjacent genes (Oren, 2003). p53 target genes include *p21*, which regulates cell cycle progression, *RNR2*, *GADD45*, which enhances DNA repair, *bax*, which has role in apoptosis (Miyashita and Reed, 1995), and p53-specific E3 ligases, which act in a negative feedback pathway to downregulate p53 activity (Brodsky et al., 2004). At least ten p53 target genes encode potential proapoptotic proteins that include regulators of the intrinsic apoptotic mechanism, such as Apaf1, HTRA2, and BH3-containing proteins, as well as members of the TNF receptor family that regulate the extrinsic apoptotic mechanism (Brodsky et al., 2004). Why so

many proapoptotic genes are regulated by p53 and the relative contributions of these genes to damage-induced apoptosis is unclear.

A better understanding of p53-regulated pathways could lead to improved strategies for treating p53-deficient tumors. However, the apparent complexity of p53 function in vertebrates has hampered efforts to elucidate these pathways (Ollmann et al., 2000). Furthermore, the way in which p53 determines the type of genes (cell cycle arresting or apoptotic) to activate in these given pathways is not well understood (Sutcliffe et al. 2003). Understanding the way in which Dmp53 controls apoptosis in the fly, where there is no cell cycle mediation, could provide insight and clarity as to how p53 regulates apoptosis and its role in the various regulatory pathways in humans. This would aid in the battle to prevent tumorogenesis through p53 regulation.

1.5 SNAMA

SNAMA, a Xhosa word referring to something that sticks like glue, is a 1231 amino acid *Drosophila melanogaster* protein with a molecular weight of 139 kDa. It contains a highly conserved N-terminal region, which I refer to as the DWNN Catalytic Module (DCM) (Figure 4). The DCM is comprised of an ubiquitin-like domain known as DWNN (Domain With No Name), followed by a zinc finger motif and a RING finger-like motif (Mather et al., 2005). At its C-terminus SNAMA contains two lysine-rich regions.

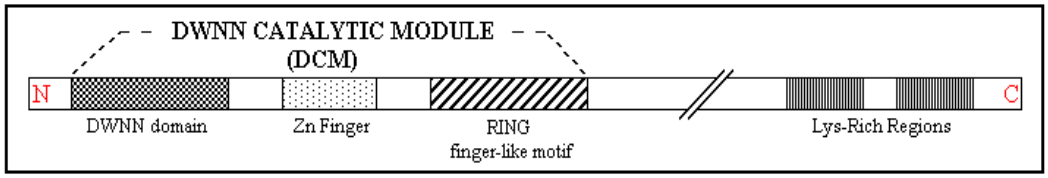


Figure 4. Schematic representation of the *Drosophila* SNAMA protein. SNAMA contains a highly conserved N-terminal region known as the DWNN Catalytic Module (DCM) encompassing a DWNN domain, Zn finger, and RING finger-like motif.

SNAMA was identified through homology searches using a highly conserved N-terminal domain known as DWNN (Mather et al., 2005). Orthologues of SNAMA include yeast Mpe1, which is involved in 3´ end mRNA processing (Vo et al., 2001), as well as RbBP6 (retinoblastoma binding protein 6) and its derivatives (Sakai et al., 1995; Simons et al. 1997). These SNAMA orthologues, including all members of the RbBP6 protein family studied thus far, contain the N-terminal DCM (Figure 5). The DCM is highly conserved throughout all eukaryotes but absent in prokaryotes (Pugh et al., 2006). Furthermore, the DCM is expressed independently in higher organisms and is therefore likely to have a conserved function in protein modification and regulation.

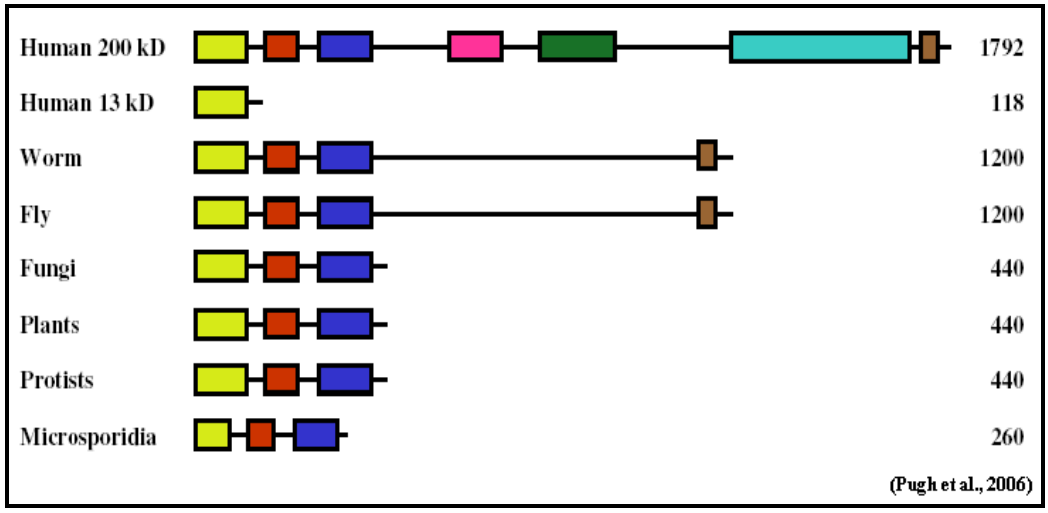


Figure 5. The domain structure of the RbBP6 family of proteins. The highly conserved DCM of the RbBP6 superfamily is shown by the DWNN domain (yellow), zinc finger motif (red) and RING finger motif (blue). Both the DCM and DWNN domain are expressed as individual polypeptides. Human RbBP6 contains additional domains that include the Rb-binding domain (green) and p53-binding domain (light blue) (Pugh et al., 2006).

Comparative analysis of SNAMA cDNA and genomic DNA shows that the transcriptional unit is made up of nine exons and eight introns (Mather et al., 2005). All introns are very short with the exception of introns 1 and 6, which are 0.84 kb and 0.3 kb respectively. An unorthodox translational start site was

determined at position 1702 of the genomic sequence (Cavener, 1987), due to no other upstream methionine codon being present and there being an upstream, in frame stop codon. The transcriptional start site for SNAMA has not been determined experimentally. However, it was predicted using the BDGP Neural Network Promoter prediction programme (http://www.fruitfly.org/seq_tools/promoter.html), to be approximately 2.2 kb upstream of the translational start site.

SNAMA is located at position 60B9 on the right arm of chromosome 2 in the *Drosophila* genome (Flybase). *SNAMA* is expressed as a 3.9 kb transcript throughout development along with an uncharacterized 1.8 kb fragment (Jones et al., 2006). Expression levels are extremely low in adult flies and unlike Dmp53 that is expressed at high levels in females (Jin et al., 2000), SNAMA levels are low in both males and females (Mather et al., 2005). SNAMA mutants die during embryogenesis when homozygous. In addition, *Drosophila* mutants with a P-element insertion in the first intron, exhibit an early occurrence of ectopic apoptosis in the blastoderm (Mather et al., 2005). This pattern was not present in wild type embryos or after the P-element was precisely excised. Furthermore, reduced levels of SNAMA mRNA is visible during late stages of development when normal apoptosis is taking place.

Rb and p53 play a central role in cell cycle regulation and programmed cell death. It is believed that that RbBP6 and its derivatives are involved in these processes and may affect apoptosis due to their association with Rb and p53. SNAMA, like other members of the RbBP6 family of proteins, is believed to regulate Dmp53 stability (Du and Dyson, 1999), whereby Dmp53 and/or RBF (the *Drosophila* homologue of Rb) act as the substrates for DWNN in protein-protein interactions. This is plausible, especially in the absence of Mdm2 or a p53-specific ligase in the fly. In addition, preliminary work shows that Dmp53 binds SNAMA. This suggests that SNAMA is a member of a distinct family of proteins that plays a role in *Drosophila* development and apoptosis, probably as a suppressor of apoptosis or negative regulator of an activator of apoptosis.

1.5.1 The domain with no name (DWNN)

The DWNN domain was initially identified by Professor Jasper Rees through a promoter trap mutagenesis screen for apoptotic genes in CHO (Chinese Hamster Ovary) cells (Pugh et al., 2006). It was characterized using the RbBP6 protein as a template and described as an ubiquitin-like N-terminal domain of 81 amino acid residues (Pugh et al., 2006). Similarly, it was shown that DWNN secondary structure in SNAMA has the highest score of similarity with ubiquitin, followed closely by ubiquitin-like proteins including Nedd8 and Rub1 (Mather et al., 2005). Thus, although there is only 18-22% sequence identity between DWNN and ubiquitin, the structural fold of DWNN is significantly similar to that of ubiquitin. Furthermore, DWNN contains the exposed ubiquitin-like C-terminal tail extending beyond the β-sheet. Unlike ubiquitin, however, DWNN lacks the smaller 3_{10} α-helix normally found, and is believed to contain an additional short piece of anti-parallel β-sheet immediately prior to the α-helix (Mather et al., 2005; Pugh et al., 2006).

The G^{75} and G^{76} residues found in ubiquitin molecules are required for recognition by specific hydrolases, which cleave between the di-glycine residues. This initiates the process of conjugation, thus allowing for protein modification to occur. These di-glycine residues are absent in the DWNN domain of SNAMA and yeast but present at positions 78 and 79 of human and mice DWNN (Figure 6). Thus it is believed that the DWNN domains containing the di-glycine motif are involved in a similar process of conjugation as ubiquitin, which is referred to as DWNNylation (Pugh et al., 2006). A highly conserved proline has replaced the G^{76} in DWNN. When this conserved glycine is replaced by a proline, as in DSK2 from yeast, cleavage by deubiquitinating enzymes does not occur (Biggins et al., 1996). Thus, it is possible that DWNN domains where there is no di-glycine motif present (such as in SNAMA) do not modify other proteins, at least in a way that requires cleavage by the known and specific hydrolases. Alternatively, DWNN could be cleaved by a different set of uncharacterized enzymes. The DWNN domain lacks the conserved equivalents

of K^{48} and K^{63} that are usually found in ubiquitin, although K^{6} and K^{29} are highly, although not absolutely, conserved. Both K^{48} and K^{29} are required for poly-ubiquitin chain formation and targeting modified proteins for 26S proteasome degradation (Pugh et al., 2006).



Figure 6. Multiple alignment of DWNN from various organisms. Dros-DWNN = SNAMA, Dros-Ub = *Drosophila* ubiquitin, Human-DWNN1 = long human homolog, Human-DWNN2 = short human homolog, Yeast-DWNN = *S. cerevisiae* homolog (Mather et al., 2005).

Protein sequence alignment of many different DWNN homologs from eukaryotes showed great similarity to each other and no similarity to any other sequences within the database, including prokaryotes (Mather et al., 2005; Pugh et al., 2006). Thus, it is believed that DWNN is a novel protein motif that emerged soon after the emergence of eukaryotes. Furthermore, the DWNN domain is independently expressed in higher vertebrates providing further evidence that it functions as a novel ubiquitin-like modifier of other proteins (Pugh et al., 2006). This is consistent with the discovery of a superfamiliy of ubiquitin-like domains in recent years (Schwartz and Hochstrasser, 2003). This superfamily is separated into the ubiquitin-like proteins (UBL's), that contain the ubiquitin-like domain only, and ubiquitin domain proteins (UDP's), that are larger proteins containing one or more ubiquitin-like domains. DWNN is the first example of a ubiquitin-like domain that is alternatively expressed both as a UBL and as a UDP (Pugh et al., 2006).

1.5.2 The zinc finger

Zinc fingers can best be described as small protein domains that are structured around a zinc ion, which forms part of the domain core and is sequestered from the solvent by cysteine and histidine residues (Krishna et al., 2003). The zinc finger, CCHC, like that found in SNAMA is known as a "zinc knuckle" (Klein et al., 2000; Darlix et al., 1995). This is because it is composed of two short β-strands connected by a turn (zinc knuckle), followed by a short helix or a loop (Krishna et al., 2003). Zinc knuckles have been found in a number of mRNA-associated proteins that include the splicing factors SLU7, h9G8, and hSF1 (Lopato et al., 1999). In general, zinc finger motifs tend to promote protein-protein and protein-DNA interactions (Matthews et al., 2000). This is interesting as this could support its "neighbor", DWNN, which contains an ubiquitin-like structure and is thought to be involved in protein interactions.

1.5.3 The RING finger-like domain: C3SC4

The RING finger domain of SNAMA differs from characteristic RING fingers due to the substitution of the histidine residue, normally present in the fourth ligand, with a serine residue (Mather et al., 2005). Thus, SNAMA contains a C3SC4 RING finger-like domain with sequence Cys-X_2-Cys-X_{11}-Cys-X_1-Ser-X_2-Cys-X_2-Cys-X_{12}-Cys-X_2-Cys, instead of the classical C3HC4 consensus (Figure 7). RING finger ligases are dependent on their RING finger motif for activity, as they play an essential role in conjugation of ubiquitin to target proteins (Joazeiro and Weissman, 2000). Although SNAMA contains an uncharacteristic RING finger motif it is still suspected that the RING finger-like domain will function as an ubiquitin ligase. This hypothesis is supported by the fact that proteins with uncharacteristic C4C4 RING finger-like domains still portrayed ubiquitin ligase activity. This was the case with the transcription-associated proteins CNOT4 (Albert et al., 2002) and p44 (Fribourg et al., 2000), which contain C4C4-type RING fingers. Furthermore, a threonine residue, an amino acid with a hydroxyl group in its side chain like serine, replaces Cys_3 in

the Mdm2 RING finger without affecting the overall structure or its ubiquitin ligase activity (Saurin et al., 1996).

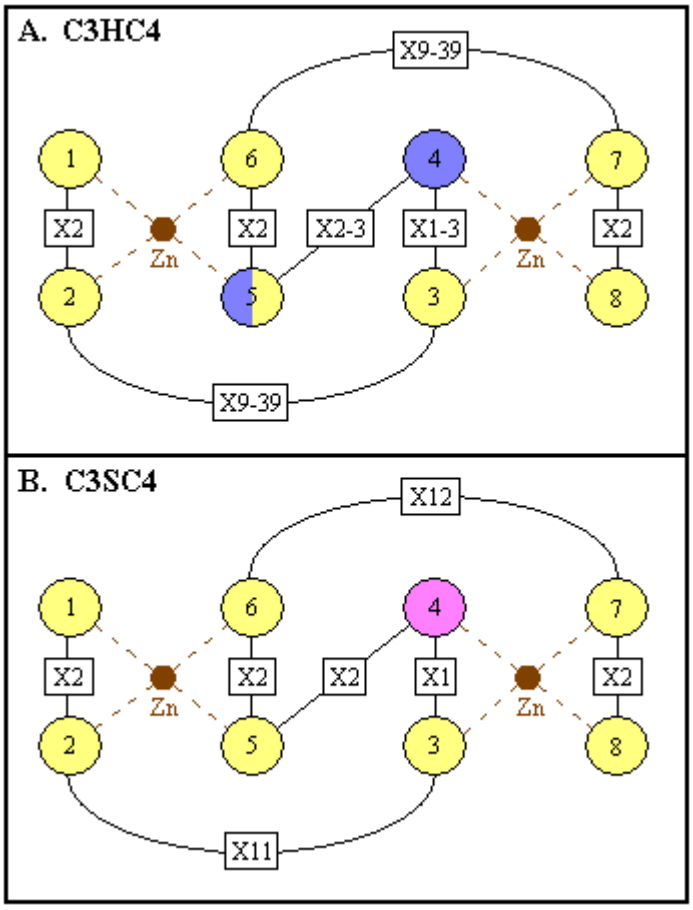


Figure 7. The "cross-brace" structure of RING finger motifs. (A) The classical C3HC4 RING finger, where two zinc ions are co-ordinated by cysteine residues (yellow spheres) and a histidine residue (blue sphere). (B) The uncharacteristic C3SC4 RING finger-like motif found within the DCM of SNAMA. Two zinc ions are co-ordinated by cysteine residues and a serine residue (pink sphere), (Mather et al., 2005).

1.6 The Retinoblastoma Binding Protein 6 (RbBP6) Superfamily

RbBP6 is one of the few proteins studied that is shown to interact with both p53 and Rb (Sakai et al., 1995; Simons et al., 1997). Thus, it is likely that this protein plays a role in the induction of apoptosis and regulation of the cell cycle. Three

partial cDNA's from the full length RbBP6 transcript were originally cloned and sequenced in different studies. RBQ-1 from humans (Sakai et al., 1995), corresponding to residues 150-1146 of the human protein, and PACT (p53-associated cellular protein-testes derived) from mice (Simons et al., 1997), corresponding to residues 207-1792, were cloned on the basis that they bind Rb and p53. P2P-R (proliferation potential protein-related), corresponding to residues 199-1792, was cloned due to its recognition by two antibodies specific for heterogeneous nuclear ribonucleoproteins (hnRNPs) (Witte and Scott, 1997). Thus, RBQ-1, PACT, and P2P-R are in fact derivatives of the RbBP6 protein, which is the complete protein.

Full length RbBP6 is a 250 kDa splicing-associated protein that, like SNAMA, contains the N-terminal DCM comprised of a DWNN domain, zinc finger, and RING finger motif. However, unlike the fly, both human and mouse RbBP6 contain addition domains that include an SR domain, Rb-binding domain, and p53 binding domain (Simons et al., 1997; Witte and Scott, 1997) (Figure 5). As mentioned earlier, the presence of the di-glycine motif in the DWNN domain suggests that the domain may be involved in a similar process of conjugation as ubiquitin, which is known as DWNNylation (Pugh et al., 2006). Like SNAMA, RbBP6 contains an uncharacteristic RING finger motif, C3NC4, that is believed to exhibit ubiquitin ligase activity (Pugh et al., 2006).

In humans, RbBP6 is expressed as three transcripts of 6.1, 6.0, and 1.1 kb, as a result of combined alternative splicing and alternative poly-adenylation (Pugh et al., 2006). These transcripts give rise to proteins of 1792, 1758, and 118 amino acids, designated RbBP6 isoforms 1, 2, and 3 respectively. The RbBP6 variant 3 represents the DWNN domain that is expressed in vertebrates as a small protein of 118-150 residues containing a DWNN domain and a short C-terminal tail. Preliminary analysis suggests that the short form is present in all vertebrates but not in invertebrates, plants or fungi (Pugh et al., 2006).

1.6.1 RbBP6 function: a role in apoptosis

RbBP6 and its derivatives are associated with and bind p53 and Rb in both humans and mice. RbBP6 is localized to chromosomes during mitosis and forms nuclear speckles, thought to be the main sites of activity for pre-mRNA splicing and processing during interphase (Gao et al., 2002). Overexpression of RbBP6 has shown to lead to apoptosis (Gao and Scott, 2002; Scott et al., 2003). Knockdown of PACT (the truncated derivative of RbBP6) significantly decreases p53-Hdm2 interaction, reduces p53 poly-ubiquitination and degradation, and enhances p53 accumulation (Li et al., 2007). This increases p53 levels, which leads to both apoptosis and cell growth retardation. Furthermore, disruption of PACT in mice leads to early embryonic lethality (Li et al., 2007). It has also been shown that RbBP6 is highly up-regulated in oesophageal cancer, and is thus a promising target for immunotherapy against the disease (Yoshitake et al., 2004). Taken together, these results indicate that the RbBP6-p53 interaction plays a critical role in embryonic development and tumorigenesis and identifies RbBP6 as a member of negative regulators of p53.

1.7 Ubiquitin

Ubiquitin is a small, single domain protein of 76 residues. Its secondary structure consists of three and a half turns of alpha-helix, a short piece of 3_{10}-helix, seven reverse turns, and a mixed beta-sheet containing five strands (Figure 8). It thus forms a highly heat-stable, compact globular structure, with the last four C-terminal residues (Leu-Arg-Gly-Gly) extending away from the main body of the protein into aqueous space (Wilkinson et al., 1980). It is this “tail” that enables ubiquitin to covalently attach to other proteins and is thus vital in the functioning of ubiquitin. The ubiquitin structure was determined by X-ray crystallography and NMR (Vijay-Kumar et al., 1987; Weber et al., 1987). Ubiquitin folds by a simple two-state process in aqueous solution, uncomplicated by the formation of disulphide bonds or metal/cofactor binding

and with no accumulation of stable intermediates (Khorasanizadeh et al., 1993; Krantz and Sosnick, 2000).

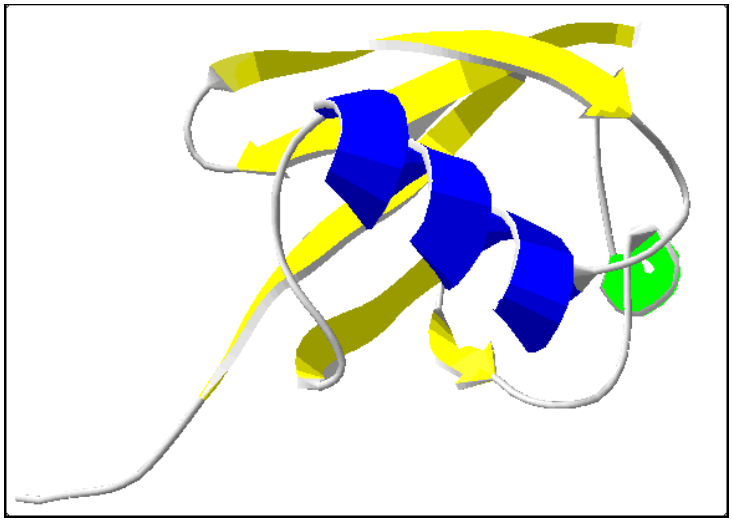


Figure 8. The native structure of ubiquitin. Ubiquitin consists of three and a half turns of α-helix (blue), a short piece of 3_{10}-helix (green), seven reverse turns (white strands), and a five stranded mixed β-sheet (yellow), (Vijay-Kumar et al., 1987).

Ubiquitin is a highly conserved polypeptide that is found in all eukaryotic organisms but not in either eubacteria or archaebacteria (Goldstein et al., 1975). It is found throughout the cell (hence its name) and can exist either in free form or as part of a complex with other proteins. In the latter case, ubiquitin is covalently attached to protein substrates and plays a fundamental role in the regulation of cellular function such as DNA repair, embryogenesis, cell cycle regulation, transcriptional regulation, and apoptosis (Lee and Tyers, 2001; Kirschner, 1999). In the nucleus, ubiquitin is covalently attached to histone 2A and is thought to participate in the regulation of transcriptional activity and/or chromatin structure. However, in the cytoplasm, ubiquitin targets protein substrates for degradation by the 26S proteasome (Pickart, 2001). The transfer of free ubiquitin onto a protein substrate is a multistep enzymatic process that ultimately leads to degradation of the target protein (Hershko and Ciechanover, 1998). Ubiquitin and some ubiquitin-like proteins are cleaved at their di-glycine motif (G^{75} and G^{76}) by specific hydrolases, thus initiating conjugation.

1.8 Ubiquitin-Proteasome Pathway

The ubiquitin-proteasome pathway plays an important role in the degradation of short lived regulatory proteins (Peters, 1998), thereby maintaining homeostasis in the cell by regulating protein levels. These include proteins involved in the cell cycle, cellular signaling in response to stress and extracellular signals, morphogenesis, the secretory pathway, and DNA repair (Hershko and Ciechanover, 1998; Weissman, 1997). Degradation of a protein via the ubiquitin-proteasome pathway involves two discrete and successive steps: tagging and degradation. The target protein is first "tagged" by the covalent attachment of multiple ubiquitin molecules. The "tagged" protein, which now contains a polyubiquitin chain, is then recognized by the 26S proteasome. The proteasome, which is a proteolytic complex, degrades the "tagged" protein and releases inactive peptides together with free, reusable ubiquitin (Ciechanover, 1998) (Figure 9).

The first step of the ubiquitin-proteasome pathway requires three enzymes that function in a cascade mechanism to allow the covalent attachment of the ubiquitin to the substrate (Figure 9). Initially, ubiquitin is activated by the ubiquitin activating enzyme (E1). This is an ATP-dependent reaction that results in a high-energy thioester bond forming between a cysteine, in the active site of E1, and the C-terminal glycine (G^{76}) of ubiquitin (Haas and Rose, 1982). The activated ubiquitin is then transferred from E1 to a specific ubiquitin conjugating enzyme (E2) through yet another thioester bond (Hershko et al., 1983). An ubiquitin ligase (E3), which interacts with both the E2 and the target protein, then catalyzes the isopeptide bond formation between the C-terminal glycine in ubiquitin and the lysine residue in the protein substrate (Hershko and Ciechanover, 1998). The isopeptide bond forms between the α-carboxyl group of the glycine and the ε-amino group of the lysine side chain.

Ubiquitin molecules are then attached in succession, through the binding of the terminal carboxyl of each ubiquitin with the lysine residue of the adjacent

ubiquitin, to form a polyubiquitin chain. A chain of 4 or more ubiquitin molecules, linked via K^{29} or K^{48}, targets proteins for degradation by the 26S proteasome. There are a number of different classes of E3 enzymes that serve to regulate the interaction between E2 proteins and the various protein substrates. Thus the ubiqutin ligases play a key role in ubiquitin conjugation pathway.

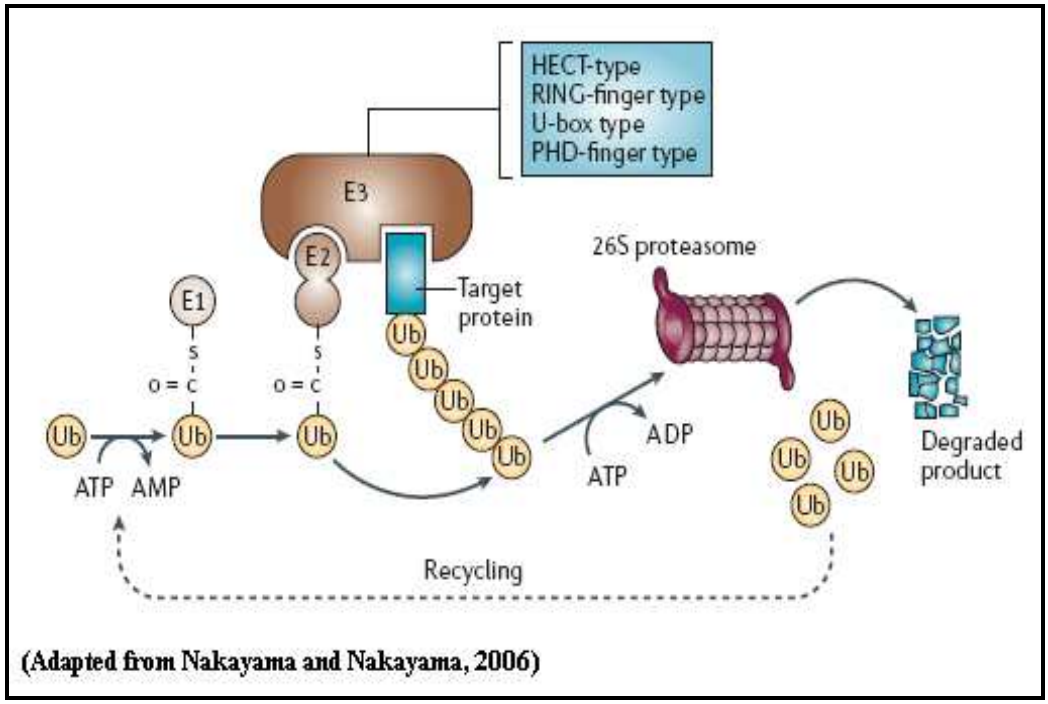


Figure 9. Degradation of proteins via the ubiquitin-proteasome pathway. Ubiquitin is transferred to the ubiquitin activating enzyme (E1) in an ATP-dependent manner. The ubiquitin is then transferred to an ubiquitin conjugating enzyme (E2). The ubiquitin ligase binds both the E2 and the target protein, thus allowing for the covalent attachement of the ubiquitin molecule to the target protein. Ubquitin molecules are then added in succession until a chain or 4 or more residues is reached, at which point the target protein is transported to the 26S proteasome for degradation.

1.9 Ubiquitin Ligases, the E3s

Ubiquitin ligases, E3s, are by definition enzymes that bind specifically to protein substrates, and promote the transfer of ubiquitin from a thioester intermediate to the target protein or ubiquitin molecules thus forming polyubiquitin chains (Hershko and Ciechanover, 1998). The E3s are a large family of proteins that exist as single polypeptides or multimeric complexes. They are separated into three major and structurally distinct classes: the N-end rule E3s, the E3s containing the HECT (Homology to E6AP C-Terminus) domain, and the RING finger E3s, which include its derivatives the U-Box and the PHD (Plant Homeo-Domain) (Sun, 2003). The N-end rule E3s are found rarely and are involved in ubiquitin conjugation to the N-terminal amino group of the protein substrate (Varshavsky, 2003). An example of an N-end rule E3 is DIAP1, which is involved in the *Drosophila* programmed cell death system (Ditzel et al., 2003).

HECT family E3s rely on the transfer of ubiquitin from the E2 to a cysteine residue in the active site of the E3, through a third high-energy thioester bond. The HECT E3 then transfers the ubiquitin molecule to the protein substrate (Glickman and Ciechanover, 2002). HECT family E3s include E6-AP (E6-associated protein), which targets p53 for ubiquitination in the presence of human papilloma virus E6 (Schneffner et al., 1993), and Nedd4.

The most common class of E3s, namely the RING finger E3s, catalyze the direct binding of the activated ubiquitin on E2 to the target protein (Figure 9). This is achieved through specific binding of both the E2 and the protein substrate to the RING finger, thus bringing the ubiqutin molecule into close enough proximity with the target protein for binding to occur. The U-box domain proteins, the E4s, also facilitate in the formation of polyubiquitin chains on target proteins, either independently of an E3 (Hatakeyama et al., 2001) or in some instances requiring an E3 (Koegl et al., 1999). The U-box domain forms a RING finger fold yet portrays ubiquitin ligase activity in the absence of divalent cations. Furthermore, U-box domains utilize lysine residues on ubiquitin for poly-ubiquitination like

that not used by HECT and RING finger domain E3s. Thus, there is much speculation of whether E4s form a new class of E3s, independent of the RING finger ligases, or whether they are derivatives of RING finger domain that form a subset of this class.

The PHD domain also resembles the RING finger domain but unlike the characteristic RING finger it contains eight conserved metal binding ligands with similar spacing (Lu et al., 2002). The PHD domain is found in many proteins involved in chromatin-mediated transcriptional regulation, however very little is known about their exact functions (Aasland et al., 1995).

E3s are enzymes that determine the specificity of protein substrates, and therefore represent a class of "drugable" targets for pharmaceutical intervention. Ubiquitin ligases are overexpressed in a number of human cancers and their inhibition leads to growth suppression or apoptosis (Sun, 2003). It is anticipated that ubiquitin ligases, in particular the RING finger ubiquitin ligases, will present an important new target platform for future mechanism-driven drug discovery due to their specificity for both the E2 and target protein.

1.9.1 RING finger E3s

Classical RING finger motifs are small zinc binding domains that are found within larger, functionally distinct proteins, often close to the N- or C-terminal. There are hundreds of known RING finger domain proteins (more than 350 in humans alone) (Furukawa et al., 2002), which were originally discovered by Paul Freemont and his colleagues (Freemont et al., 1991). Freemont showed that all RING finger domains contain the conserved sequence Cys-X_2-Cys-X_{9-39}-Cys-X_{1-3}-His-X_{2-3}-Cys/His-X_2-Cys-X_{9-39}-Cys-X_2-Cys, where X is any amino acid (Saurin et al., 1996) (Figure 7A). RING finger domains are defined by this pattern of conserved Cys and His residues that co-ordinate two zinc ions to form a "cross-brace" structure (Borden, 2000; Saurin et al., 1996). The varying length and sequence between the conserved Cys and His residues, as well as metal

chelating residues being substituted with others, accounts for the differences among RING finger domains.

As mentioned earlier, RING finger ubiquitin ligases interact with both the E2 and the target protein and catalyze the direct formation of a covalent bond between ubiquitin and the protein substrate (Figure 9). Crystal structures of RING finger ubiquitin ligases have shown that E2 binds to the RING domain through contacts between a groove in the RING domain and two loops in the E2 fold (Zhou and Howley, 1998). Furthermore, the structure reveals a rigid coupling between the target protein-E3 complex and the E2-E3 complex with a conserved surface channel leading from the target protein to the E2 active site. This indicates that RING finger ubiquitin ligases function as scaffolds that position the substrate and the E2 optimally for ubiquitin transfer. Following this discovery, the function of many more RING finger ligases have been shown to be dependent on their RING finger motif (Lorick et al., 1999). Thus, it is suspected that all RING finger containing proteins act as ubiquitin ligases that facilitate in the ubiquitination of target proteins.

RING finger ligases are separated into two distinct groups: the single subunit ubiquitin ligases and the multi-subunit ubiquitin ligases. The single subunit E3s are monomers or homodimers that contain both the RING finger domain and the substrate-binding site in the same molecule, such as Mdm2 and Parkin (Lorick et al., 1999; Shimura et al., 2000). The multi-subunit enzyme, which include the APC (anaphase-promoting complex), the VBC (von-Hippel Lindau-Elongins B and C), and the SCF (Skp1-Cullin/Cdc53-F-box protein), function in complexes with proteins of the cullin family and other ancillary proteins. The cullin proteins promote the assembly of these multi-subunit enzymes, whereas the other ancillary proteins function in substrate recognition.

1.9.2 U-Box domain ubiquitin ligase, E4s

The U-box is a domain of approximately 70 amino acids that is present in proteins from yeast to humans (Hatakeyama et al., 2001). The prototype U-box protein, yeast Ufd2 (ubiquitin fusion degradation), is essential for the assembly of polyubiquitin chains on artificial substrates that are targeted for degradation (Koegl et al., 1999). The U-box is essentially a modified RING finger that lacks many of the conserved metal chelating cysteine residues normally found in RING finger domains (Aravind and Koonin, 2000). Rather, the U-box fold, which mimics that of the RING finger, is stabilized by salt-bridges, hydrogen bonds, and conserved hydrophobic residues within its consensus.

Proteins that contain the U-box domain are referred to as E4s. Some believe that E4s form an additional subset of RING finger ligases (Koegl et al., 1999; Aravind and Koonin, 2000). Others believe that E4s define a new class of E3s, independent of the HECT and RING finger E3s (Hatakeyama et al., 2001). In either case, U box proteins facilitate the formation of polyubiquitin chains on target proteins due to its RING finger conformation (Koegl et al., 1999). E4s can function as ubiquitin ligases in the absence of an E3 (Hatakeyama et al., 2001), or in some instances they require an E3 (Koegl et al, 1999). At least six mammalian E4s have been shown to mediate polyubiquitination in the presence of an E1 and a specific E2 but absence of E3 (Hatakeyama et al., 2001). Furthermore, deletion of the U-box or mutation of conserved amino acids within its conserved sequence, abolishes ubiquitination activity.

The characteristic RING finger E3s require divalent cations for ubiquitin ligase activity (Freemont, 1993). In contrast, the E4s portray ubiquitin ligase activity in the absence of divalent ions such as zinc. The U-box proteins also appear to catalyze their own ubiquitination. Interestingly E4s have been shown to utilize multiple lysine residues of ubiquitin, in addition to normal K^{29}, K^{48}, or K^{63}, to mediate the formation of polyubiquitin chains (Hatakeyama et al., 2001). It is not clear yet whether E4s, like the RING finger E3s, are involved in recruiting

E2 or whether it binds to the short ubiquitin chain conjugated to the target protein.

1.10 Deubiquitinating Enzymes (DUBs)

Deubiquitinating enzymes (DUBs) are specific proteases that recognize ubiquitin and cleave the isopeptide bond formed by the last glycine residue in an ubiquitin molecule. There are at least five families of DUBs: ubiquitin C-terminal hydrolases (UCHs), ubiquitin specific proteases (USPs), MJD (Machado-Joseph disease) proteases, OTU (Otubain) proteases, and JAMM (JAB1/MPN/Mov34 metalloenzyme) motif metallo-proteases (Nijman et al., 2005). The first four families are cysteine proteases, while JAMMs are zinc-dependent metalloproteases. UCHs are 20-30 kDa enzymes that remove short or flexible peptide chains from the C-terminus of ubiquitin. UBPs are approximately 100 kDa enzymes that cleave the isopeptide bonds of ubiquitin-ubiquitin or ubiquitin-protein fusions. Both groups of enzymes contain conserved cysteine, histidine, and aspartate residues within their active site, but differ in that their consensus sequence is divergent (D'Andrea and Pellman, 1998). As mentioned earlier, ubiquitin is not synthesized directly as free ubiquitin but rather as linear fusions either to itself or to certain ribosomal proteins. DUBs function in maintaining the steady-state levels of free ubiquitin by cleaving ubiquitin from ubiquitin-protein or ubiquitin-ubiquitin complexes (Chung and Baek, 1999; D'Andrea and Pellman, 1998). Thus, DUBs play a role in the generation of ubiquitin, recycling of ubiquitin, editing polyubiquitin chains, and aiding in proteasome-dependent degradation.

Originally, the ubiquitin-proteasome pathway was thought to be unidirectional from substrate ubiquitination to degradation by the 26S proteasome. However, the discovery of deubiquitinating enzymes (DUBs) changed the global view of the enzymatic process and showed the incredible dynamics of this pathway. The finding that the herpes virus-associated ubiquitin-specific protease (HAUSP) could bind to and stabilize p53 illustrated the greater dynamics of the p53

proteasome-pathway and was one of the first indications that DUBs exhibited substrate specificity (Hu et al., 2002). A growing number of substrate-specific mammalian DUBs involved in tumorigenesis are continually being revealed such as USP1 and USP9X, which deubiquinate FANCD2 and β-catenin respectively (Nijman et al., 2005). In the proteasome there are regulatory particles that have DUB activity and are responsible for removal of ubiquitin from protein substrates (Eytan et al., 1993). In *Drosophila*, the regulatory particle subunit responsible for this activity is p37a (Hölzl et al., 2000).

1.11 The ubiquitin-like Superfamily

Following the discovery of ubiquitin a number of proteins have been identified that are related to ubiquitin, or function similarly to modify proteins through their covalent attachment to protein substrates. This ubiquitin-like superfamily is divided into two groups. Proteins within the first group are known as ubiquitin-like proteins (UBLs). UBLs are similar to ubiquitin in that they modify other proteins by covalent attachment of themselves to amino acid residues on the target protein. Furthermore, the conjugation pathway and sites of attachment of these proteins onto target proteins resemble the ubiquitin conjugation pathway. Proteins within the second group are referred to as ubiquitin domain proteins (UDPs). UDPs contain protein domains that are related to ubiquitin. However, these protein domains are not related to ubiquitin in sequence, nor are the proteins conjugated to other proteins like ubiquitin.

1.11.1 Ubiquitin-like proteins (UBLs)

UBLs, like ubiquitin, are expressed as inactive precursors that are activated by proteolytic cleavage of the C-terminus, thus exposing the C-terminal di-glycine motif needed for conjugation. The di-glycine motif is important for the recognition and activation of the conjugation process by the activation enzyme E1. The conjugation pathways for the UBLs are very similar to that of ubiquitin. Like ubiquitin, they require their own enzymes E1 and E2, and attach to the

target protein through an isopeptide bond with a lysine residue of the substrate. The activating enzyme, E1, activates the UBL followed by the transfer of the UBL to the conjugating enzyme, E2, via a thiol-ester bond. Although the steps and reactions involved in the activation of ubiquitin and UBL are similar, the E1 and E2 enzymes cannot replace each other. All known UBLs are homologous to ubiquitin in some regard, with the exception of APG12 and URM1 (ubiquitin related modifier). NEDD8/Rub1 shows 60% identity to ubiquitin, SUMO/Smt3p/sentrin shows ~20% identity to ubiquitin, and APG12/URM1 shows no sequence homology whatsoever. APG12 and URM1 are therefore only grouped with UBLs since they are small protein modifiers that are activated and conjugated to target proteins in a similar manner to ubiquitin.

SUMO

The transfer of SUMO (small ubiquitin-like modifier) to target proteins involves the E1 heterodimer Aos1-Uba2, a single E2 enzyme Ubc9 (Johnson et al., 1997; Johnson and Hochstrasser, 1997), and in yeast a specific E3 (Johnson and Gupta, 2001). Several SUMO molecules can attach to the target protein at distinct sites, but unlike ubiquitin, multi SUMO chains do not form on the substrate (Jentsch and Pyrowolakis, 2000). In addition, the attachment of SUMO to target proteins, referred to as sumoylation, does not target proteins for degradation. Sumoylated proteins are however found in the nucleus or nuclear envelope, as shown with sumoylated PML (Kamitani et al., 1998), SP100, RanGAP1, p53, and $I_KB\alpha$ (Yeh et al., 2000). This suggests that attachment of SUMO to substrates targets them for transfer to the nucleus similarly to ubiquitinated proteins.

RUB

RUB (related to ubiquitin) shows 50% homology to ubiquitin with homologs found in all eukaryotes (Liakopoulos et al., 1998). These homologs include the *S. cerevisiae* protein Rub1, and the human protein NEDD8. Like SUMO, RUB is also related to the ubiquitin pathway as it is conjugated to proteins by process

known as rubylation. Rubylation occurs in the presence of a heterodimeric E1, ULA1/UBA1, and an E2, Ubc12 (Hori et al., 1999). The target proteins of RUB proteins are limited to a small number of proteins that are part of the cullin protein family. Rub1/NEDD8 conjugates to Cdc53/Cul-1, which are components of the SCF E3 ubiquitinating complex. This conjugation stabilizes the interaction between Cdc53/Cul-1 with E2s such as Cdc34 or Ubc4 and to a variety of F-box proteins (Kawakami et al., 2001; Liakopoulos et al., 1998). Thus, RUB ubiquitin-like proteins play a general role in down regulating SCF activity (Glickman and Ciechanover, 2002).

APG12 and URM1

APG12 conjugation to the target protein Apg5 involves the E1 enzyme Apg7, and the E2 enzyme Apg10. Interestingly, Apg7 is related in sequence to the E1 of the ubiquitin conjugation pathway, however the Apg10 differs from the ubiquitin E2s. The conjugated protein plays a role in autophagosome vesicle formation and delivery of cytoplasmic material to the lysosome (Furukawa et al., 2000). URM1 is a 99 amino acid protein ending with the di-glycine residue found in ubiquitin and other UBLs (Furukawa et al., 2000). This provides URM1 with a means of conjugation to target proteins through hydrolysis of the peptide bond. The identification of Apg12 and URM1 indicates that other UBLs may exist that cannot be identified by sequence homology to ubiquitin but rather need to be identified by functional similarities.

1.11.2 Ubiquitin domain proteins (UDPs)

UDPs are large proteins that contain a distinct ubiquitin-like domain within their sequence. The ubiquitin-like domain does not always end in the di-glycine motif and is thus not processed by DUB proteases as ubiquitin, but they do show sequence homology to ubiquitin and are linked to the ubiquitin conjugation pathway (Jentsch and Pyrowolakis, 2000). These UDPs include the *Xenopus* Scythe (Thress et al., 1998), Parkin (Morett and Bork, 1999), and the UIP28

protein (Martinez-Noel et al., 1999). One must keep in mind that UDPs such as Parkin and UIP28 contain an ubiquitin-like domain amongst other domains that include RING fingers. It is therefore possible that the activity portrayed by the protein is not entirely due to the ubiquitin-like domain but rather more due to other domains within the protein. It is likely the ubiquitin-like domain of most UDPs, especially those where the di-glyine motif is absent, facilitates processes such as ubquitination in terms of recognition and binding to target proteins or ubiquitin molecules.

UDPs have also been shown to play a role as adaptors linking the ubiquitin pathway to the proteasome, sometimes with the aid of chaperones (Kleijnen et al., 2000). This process occurs via the association between the ubiquitin-like domain within the UDPs and other characterized domains within the proteasome. Three such UDPs include Rad23, Dsk2, and Bag-1 (Lambertson et al., 1999; Lüders et al., 2000). The replacement of the ubiquitin-like domain in Rad23 with ubiquitin demonstrates the structural importance of this ubiquitin-like domain and not its sequence identity to ubiquitin in binding the proteasome (Watkins et al., 1993). The yeast Rad23 and Dsk2 UDPs overlap functionally with respect to their involvement in the spindle pole body duplication, with Rad23 having an additional role in DNA repair (Biggins et al., 1996).

HUB (homologous to ubiquitin) is a UDP that functions similarly to ubiquitin by attaching itself to target proteins. It has a 22% sequence homology to ubiqutitin but lacks the di-glycine motif at the C-terminal end of its ubiquitin-like domain (Lüders et al., 2003). However, the highly conserved HUB proteins contain a C-terminal di-tyrosine motif followed by a nonconserved single amino acid. Homologs in humans and yeast include UBL5 and HUB1 respectively (McNally et al., 2000), with HUB1 being shown to fold similarly to that of ubiquitin (Ramelot et al., 2003). Although HUB shows sequence similarity and folding to ubiquitin its mechanism of attachment to target protein does not involve covalent bonding. This was shown by HUB1, which forms SDS-resistant complexes with target proteins (Lüders et al., 2003). These complexes are not formed through

covalent C-terminal conjugation thus disagreeing with an ubiquitin-like conjugation mechanism for HUB1. It suggests rather that attachment of the HUB1 UDP occurs via a different, possibly non-enzymatic process.

1.12 Aims

The main focus of this work is to further elucidate the functional characteristics of the DCM within SNAMA. This will be achieved in two ways. Firstly, the way in which gene regulation of *SNAMA* is controlled will be examined. Secondly, and more importantly, it will be determined whether the DCM of SNAMA exhibits ubiquitin ligase activity and if so what factors affect this activity.

Transcriptional regulation of *SNAMA* will be determined by analysing the core promoter elements that surround the transcription start site of the gene. The transcription initiation site of *SNAMA* will be established by performing 5´ RACE using *Drosophila* RNA and gene specific primers. This will allow for analysis of the 5´ region of the *SNAMA* gene by ensuring the amplification of capped transcripts.

SNAMA ubiquitin ligase activity will be confirmed by ubiquitin conjugation assays using a pure and active recombinant SNAMA protein as the E3. This would allow SNAMA to catalyze the covalent attachment of ubiquitin to both itself as well as other target proteins. The dependence of SNAMA activity on its RFL motif will be examined in unison with determining the specific E2 that allows SNAMA to function with optimal activity. Thereafter, the dependence of SNAMA activity on key components of the ubiquitination process including E1, zinc ions, ATP, and ubiquitin, will be determined. In order to achieve this goal a pure and active form of the conserved N-terminal DCM of SNAMA will be needed. This promises to be challenging as heterologous protein expression of SNAMA in *E. coli* forms insoluble inclusion bodies.

This characterization of the RFL motif and DWNN domain will facilitate the determination of the overall function of SNAMA and provide insight into its role in apoptosis, particularly its relationship to Dmp53. Since the mechanisms and regulation of apoptosis are highly conserved throughout evolution, studies of apoptosis in *Drosophila* may provide new insight for understanding defective regulation of apoptosis in diseases such as cancer.

2. MATERIALS AND METHODS

2.1 Growth Media

Table 2. Growth media.

Media	Composition
Apple juice agar	1.25% sucrose; 2% agar; 0.025% streptomycin; 0.15% methylparaben (3g dissolved in 30 ml ethanol and made up to a litre); 25% apple juice (v/v).
Luria-Bertani broth (LB)	1% tryptone powder; 0.5% yeast extract powder; 1% NaCl; mix and autoclave.
LB agar (LA)	LB + 1.5% agar; autoclave.

2.2 Buffers and Solutions

Table 3. Molecular biology buffers and solutions. All reagents were stored at room temperature and made up with deionised water unless otherwise indicated.

Buffer	Composition
Coomassie blue stain	0.1% Coomassie blue R-250; 40% ethanol; 10% glacial acetic acid.
Denaturation buffer	8 M Urea; 50 mM sodium phosphate buffer, pH 8.0; 100 mM NaCl; 1 mM PMSF and 2 mM DTT on day of use.
Dialysis (refolding) buffer	50 mM Sodium phosphate buffer, pH 8.0; 100 mM NaCl; 5 mM EDTA; 5 mM cycolodextrin; 50 mM arginine.
DNA loading dye (10X)	0.21% Bromophenol blue; 0.21% xylene cyanol FF; 50% glycerol; 0.2 M EDTA,

	pH 8.0; store at 4ºC.
Electrode (running) buffer (5X)	125 mM Tris base; 1 M glycine; 17 mM SDS; pH to 8.3 with HCl.
Lysis buffer	50 mM Tris-HCl, pH 7.5; 2 mM EDTA, pH 7.5; 200 mM NaCl; add 0.1 mM PMSF and 200 μg/ml fresh lysozyme immediately prior to use.
Miniprep solution I	5 mM sucrose; 10 mM $Na_2EDTA\text{-}2H_20$; 25 mM tris; pH to 8.0 with NaOH.
Miniprep solution II	0.2 M NaOH; 1% SDS; prepare fresh.
Miniprep solution III	3 M sodium acetate, pH 4.8 made up with acetic acid.
Phosphate buffered saline (PBS), 50X	1.4 M NaCl, 27 mM KCl, 101 mM Na2HPO4, 18 mM KH2PO4, pH to 7.3 with HCl.
RIPA buffer	1% Nonidet p-40; 1% sodium deoxycholate; 0.1% SDS; made up with 1X PBS; add 0.5 mM PMSF on day of use.
SDS sample buffer (5X)	1 M Tris-HCl, pH 6.8; 10% glycerol; 10% SDS; β-mercaptoethanol; 1% bromophenol blue; store at 4ºC.
TAE: Tris acetate EDTA (50X)	2 M Tris base; 5.71% glacial acetic acid; 50 mM EDTA, pH 8.0.
Towbin buffer	25 mM Tris base; 192 mM glycine; 0.1% SDS; pH to 8.3 with HCl; 20% (v/v) methanol on day of use.

2.3 Chemicals and kits

Table 4. Chemicals, kits and their suppliers. All chemicals used during the project were of analytic grade and if not mentioned were purchased from either Sigma-Aldrich (South Africa) or Merck Biosciences (South Africa).

Supplier	**Chemical/Kit**
BIO-RAD	Bio-Rad protein assay reagent.
Boehringer	Tetracycline (Tet).
Calbiochem (Merck Biosciences)	Ubiquitin, recombinant GST-fusion in *E. coli*; ubiquitin-activating enzyme E1, human GST-fusion; ubiquitin conjugation enzyme set.
Fermentas	GeneRuler™ 100bp DNA ladder plus; PageRuler™ prestained protein ladder.
Invitrogen	GeneRacer™ kit; TOPO TA® cloning kit; TRIzol® reagent; SuperScript™ II reverse transcription system.
Millipore	Stirred Ultrafiltration Cell
Novagen (Merck Biosciences)	BugBuster® Protein Extraction Reagent; iFOLD™ Protein Refolding System 1.
Pierce	SnakeSkin™ pleated dialysis tubing; Slide-A-Lyzer® dialysis cassettes; SuperBlock® dry blend (TBS) blocking buffer; SuperSignal® West Pico Chemiluminescent Substrate.
Promega	pGEM®-T Easy vector system; ImProm-II™ reverse transcription system.
Roche Applied Science	Chloramphenicol (Cm); kanamycin (Kan).
Stratagene	*E. coli* XL-1 Blue and BL21(DE3)pLysS cells.

2.4 Bacterial Strains

Table 5. Bacterial strains.

Strain	**Genotype**
Escherichia coli XL-1 Blue	*recA1 endA1 gyrA96 thi-1 hsdR17 supE44 relA1 lac* [F´ *proAB lacI*qZΔ*M15* Tn*10* (Tet^r)]
Escherichia coli BL21(DE3)pLysS	F- *ompT hsdSB* (rB - mB-) *gal dcm* λ(DE3)pLysS T1R

2.5 Oligonucleotides

Oligonucleotides were purchased from Inqaba biotec unless otherwise stated. The GeneRacer™ 5´ primer and 5´ nested primer were supplied with the GeneRacer™ kit.

Table 6. Oligonucleotides used during PCR, RT-PCR, and sequencing. Restriction enzymes that were incorporated into the primers are underlined.

Oligonucleotide	**Sequence**
DWNN forward	5´-TTCATATGGATCCATGTCGGTACACTAT-3´
GeneRacer™ 5´	5´ -CGACTGGAGCACGAGGACACTGA-3´
GeneRacer™ 5´ nested	5´ -GGACACTGACATGGACTGAAGGAGTA-3´
M13 reverse	5´ -CAGGAAACAGCTATGAC-3´
RING finger reverse	5´ -CGAACAAAGCTTCTCCTTGCAATCG-3´
RF tail	5´ -AGTGAGTGCCCCGATTGCAAGGAG-3´
RF tail internal	5´ -CCGCAGCAGGGTATCATGACAGCAT-3´
T7	5´ -TAATACGACTCACTATAGGG-3´

2.6 Total RNA Extraction From Wild-Type *D. melanogaster*

Wild-type *Canton-S Drosophila melanogaster* flies were reared at 25ºC on standard cornmeal agar food with yeast added. For extraction of total RNA, 50 wild-type adult fruit flies were selected and homogenized in a 1.5 ml eppendorf tube using 500 µl TRIzol reagent. 150 µl chloroform was added to the homogenate and centrifuged at 13 000 x g for 10 minutes at 4ºC. The supernatant was retained and mixed with 350 µl isopropanol, left at room temperature for 2 minutes, and spun at 13 000 x g for 15 minutes at 4ºC. The supernatant was removed and the pellet resuspended in 200 µl ice-cold 70% ethanol after which it was centrifuged again for 15 minutes at 13 000 x g. The ethanol was removed by aspiration and the pellet allowed to dry for 3 minutes at 37ºC. The dried RNA pellet was resuspended in 50 µl of sterile, RNAse free water, heated at 65ºC for 10 minutes, and its concentration determined. 20 µg of RNA was then aliquoted into eppendorf tubes and placed at –20ºC until needed.

2.7 5´ Rapid Amplification of cDNA Ends (5´ RACE)

5´ RACE was used to determine the transcriptional start site and possible internal promoter regions of the SNAMA gene. 5´ RACE involved a number of consecutive steps that included the removal of 5´ - phosphates and 5´ -caps from RNA, followed by ligation of the GeneRacer™ RNA oligonucleotide, reverse transcription (RT), and polymerase chain reaction (PCR) respectively. All steps during 5´ RACE were carried out essentially as described in the GeneRacer™ kit, unless otherwise indicated.

(a) Removal of 5´ -terminal phosphates: Approximately 5 µg of total RNA from *Drosophila*, together with 1 µg HeLa mRNA from normal human tissues (as a positive control), was treated with calf intestinal phosphatase (CIP) to eliminate the 5´ -terminal phosphates.

(b) Removal of 5´-caps: Tobacco acid pyrophosphatase (TAP) was used to remove the 5´ -cap structure from the dephosphorylated RNA.

(c) Ligation of GeneRacer™ oligonucleotide: Removal of the 5´cap exposes the 5´-phosphate, which allows for the ligation of the GeneRacer RNA oligo to the decapped RNA in the presence of T4 RNA ligase.

(d) Reverse transcription: The ImProm-II™ or SuperScript™ II reverse transcription systems were used to generate cDNA from *Drosophila* RNA and the HeLa control mRNA. The RF tail primer was used as a gene-specific primer during the *Drosophila* RNA reverse transcription reaction, while an oligo(dT) primer was used for reverse transcription of the HeLa control mRNA. Extension temperatures for these reactions were 55ºC and 42ºC respectively.

(e) GeneRacer™ PCR: The PCR procedure for 5´ RACE is slightly different to that generally used. The reaction mixture consisted of 2 mM $MgCl_2$, 0.2 mM dNTP mix, 0.6 µM GeneRacer™ primers, 1 µM RF tail and RF tail internal primers, and 5 U *Taq* polymerase (section 2.12). In contrast, the cycling conditions were:

	5		5		30				No. of cycles
94	94	72	94	70	94	62	70	70	Temp (°C)
2	0.5	2	0.5	2	0.5	0.5	2	10	Time (minutes)

The PCR products generated from 5´ RACE were then run on an agarose gel, and the bands extracted, cloned and sequenced.

2.8 Agarose Gel Electrophoresis

Agarose gel electrophoresis is a technique that allows one to separate DNA and visualize the fragments as bands in the gel, therefore allowing DNA to be analyzed qualitatively. A 1% or 1.5% agarose gel, cast in 1X TAE buffer, was

used with between 0.5 and 1 μg of ethidium bromide added. Between 5 and 15 μg of DNA, mixed with 1X DNA loading dye, was added to the wells of the agarose gel. Electrophoresis was performed in a 1X TAE running buffer at a voltage of between 55 and 70 V. The DNA fragments within the gel were then visualized under UV light, and their image photographed, using the UVP BioDoc-It™ system. The size of the DNA fragments were then determined through visual comparison with the molecular weight markers or with the aid of a standard curve, constructed using the molecular weight markers.

2.9 DNA Extraction from Agarose Gel

DNA was excised from the agarose gel and purified using the GenElute™ Gel Extraction kit from Sigma. DNA was extracted following the procedure provided by the manufacturer. The kit combines silica based-membrane technology and the convenience of a spin column format to capture and purify the DNA from the gel.

2.10 Cloning

Cloning of DNA involved the ligation of a PCR product into a TA cloning vector and transformation into competent *E. coli* XL-1 Blue cells. The PCR product is in a more stable state and environment when incorporated in a plasmid within bacterial cells. The antibiotic resistance supplied by plasmids and cells also allows for accurate selection of transformed cells. Cloning an insert into an expression vector was more complex. Initially, the PCR product was cloned into a TA cloning vector, after which the fragment was restricted out with specific endonucleases, ligated into the pET41(a) expression vector, and transformed into *E. coli* BL21(DE3)pLysS cells. This allows the fragment to be inserted into the expression vector in the correct orientation and in-frame with the GST-gene.

2.10.1 Ligation

Purified PCR products were ligated into the pGEM®-T Easy or pCR®4-TOPO® TA cloning vectors using the pGEM®-T Easy vector TA-cloning system I and TOPO TA® cloning kit respectively (Appendix V). Both systems use T4 DNA ligase to ligate the PCR product, containing TA overhangs, into the TA cloning vector.

Ligation of the DCM of SNAMA into the pET41(a) expression vector (Appendix VI) initially involved the restriction of the fragment out of the cloning vector. The fragment was separated from the cloning vector through restriction with *Bam*HI and *Hind*III, after which the fragment was ligated into pET41(a) using T4 DNA ligase. Prior to ligation, pET41(a) was also restricted with *Bam*HI and *Hind*III, and dephosophorylated with alkaline phosphatase. This provided free phosphate groups needed for ligation of the fragment and insured that the fragment was inserted in the correct orientation.

2.10.2 Preparation of chemically competent cells

Chemically competent *E. coli* XL-1 Blue and BL21(DE)3pLysS cells were prepared by following a slightly altered procedure designed by the Fred Hutchinson Cancer Research Center. A single bacterial colony was used to inoculate 5 ml of LB and incubated overnight at 37°C with vigorous shaking. Following incubation, the starter culture was diluted 100X with 250 ml LB, supplemented with the appropriate antibiotic. The culture was then shaken at 37ºC until an OD_{600} of between 0.5 and 0.6 was reached, at which point they were transferred to GSA bottles and centrifuged at 5000 x g for 10 minutes at 4ºC. The supernatant was removed and the pellet resuspended in 100 ml of ice-cold 100 mM $MgCl_2$. This was followed by a 30 minute incubation on ice after which the cells were again pelleted by centrifugation at 4000 x g for 10 minutes at 4°C. The supernatant was discarded and cells resuspended in 10 ml of ice-cold 100 mM $CaCl_2$ containing 15% glycerol. The now competent cells were

aliquoted into small pre-cooled eppendorf tubes (200µl/tube) and stored, for a period of no longer than 6 months, at -70°C.

2.10.3 Transformation

The ligation reaction mixture of 10µl, containing approximately 50 ng of vector with insert, was added to 90µl of competent *E. coli* cells. The mixture was then incubated on ice for 20 minutes and heat shocked for 10 minutes at 37ºC, which caused the cells to take in the recombinant plasmids. The transformed cells were made up to 1 ml with 900 µl LB and shaken gently for 1 hour at 37ºC to allow for regeneration. 70 µl of transformed cells were then spread on LA-appropriate antibiotic plates, to select for those cells that took up the resistant recombinant plasmid. These plates were then incubated overnight at 37ºC.

2.11 Small Scale Preparation of Plasmid DNA (Miniprep)

The procedure for small scale preparation of plasmid DNA was derived from that published by Birnboim, 1983. A single bacterial colony containing the desired plasmid was used to inoculate 2 ml of LB, supplemented with the appropriate antibiotic, and incubated at 37ºC overnight with vigorous shaking. The next day the cells were harvested by centrifugation at 13 000 x g for one minute. The cells were resuspended in 100 µl of Miniprep solution I and then 200 µl Miniprep solution II, mixed, and incubated for 3 minutes at room temperature. 150 µl of Miniprep solution III was then added, mixed, and incubated on ice for 20 minutes. Following incubation, the mixture was microfuged at 13 000 x g for 5 minutes and the supernatant retained. RNA was removed through the addition of 50 µg RNaseA and incubation for 5 minutes at room temperature.

To remove protein contaminants an equal volume of phenol: chloroform: isoamyl alcohol (25:24:1) was added to the solution, mixed, and microfuged for 5 minutes at 13 000 x g. The aqueous layer was transferred to a fresh tube and an equal volume of chloroform added and mixed, before microfuging at 13 000 x g for 3

minutes. Once again the aqueous layer was transferred to a fresh tube and 2.5X the volume of 25:1 ethanol acetate acetate added, mixed by inversion, and placed at -70°C for 20 minutes. The mixture was then microfuged at 13 000 x g for 10 minutes, the supernatant aspirated, and the pellet resuspended in 500 µl of 70% ethanol. The DNA was once again pelleted by microfugation for 10 minutes at 13 000 x g at 4°C, and the supernatant aspirated. The pellet was allowed to dry at 55 °C for 10 minutes and then resuspended in 80-150 µl of ddH_2O depending on the size of the pellet.

2.12 Polymerase Chain Reaction (PCR)

Confirmation of 5´ RACE and cloning was determined by PCR on recombinant plasmid DNA obtained from miniprep, and/or colony PCR on the transformed cells. 0.6 µM of the GeneRacer^{TM} 5´ and 5´ nested primers as well as 1 µM of the RF tail and RF tail internal primers were used. The reaction mixture consisted of standard PCR reagents: 2 mM $MgCl_2$, 0.2 mM dNTP mix, 1X PCR reaction buffer, and 5 U *Taq* polymerase. Approximately 1 µg of DNA or a single colony of transformed cells was used as the template in the PCR reactions. PCR cycling conditions started with denaturation at 94ºC for 5 minutes. This was followed by 25 cycles of 94ºC for 30 seconds, 58ºC for 30 seconds, and 72ºC for 1 minute. PCR ended with a final extension of 72ºC for 7 minutes. The PCR product was subjected to agarose gel electrophoresis to separate the amplified product from the reaction mixture and visualize results.

PCR was also used to amplify the DCM of *SNAMA* that would later be expressed into recombinant protein. The reaction mixture and cycling conditions for the reaction were the same as mentioned above. However, 1 µM of the DWNN forward and RF reverse primers were used with 1 µg of pOT2 vector as the template. The pOT2 vector, 1665 bp in size, was obtained from the Flybase EST programme (accession AAF47162) and contains the entire *SNAMA* cDNA sequence.

2.13 Quantification of Nucleic Acid

Nucleic acid concentration was determined by spectroscopy. First, the spectrophotometer was calibrated with deionised water in a quartz cuvette. Thereafter, the absorbance of the prepared samples was taken at 260 nm (A_{260}) and 280 nm (A_{280}). The nucleic acid samples were prepared by diluting the RNA or DNA by a factor of 100 with ddH_2O. The samples were then placed in a quartz cuvette and the absorbance readings taken. The concentration was determined using the A_{260} reading, the dilution factor, and the optical density (OD) constant (A_{260} of 1 = 50 μg/ml for double-stranded DNA and 40 μg/ml for RNA). The purity of the DNA sample was determined using the A_{260}/A_{280} ratio, where a value greater than 1.8 indicated that the sample had little protein contamination and was thus of high purity.

2.14 Restriction Digestion of DNA

In order to confirm that the 5´ -RACE and SNAMA PCR products had been successfully cloned into the multiple cloning site (MCS) of the cloning vector, restriction digestion on the recombinant vectors were performed. The vectors were restricted with *Eco*RI, as it has recognition sites that flank the MCS of the cloning vectors. Reaction conditions followed those recommended by the manufacturer of the restriction enzyme. All reactions were incubated at 37ºC overnight and stopped by the addition of 1X DNA loading dye the next morning. The success of the digestion was then determined by agarose gel electrophoresis.

2.15 SDS-PAGE

SDS-PAGE (sodium dodecyl sulphate-polyacrylamide gel electrophoresis) is a technique that allows one to separate and visualize polypeptides in a gel matrix under denaturing conditions, thus allowing for qualitative analysis of protein (Laemmli, 1970). A discontinuous SDS-PAGE procedure was used with a 4% polyacrylamide stacking gel and 12% polyacrylamide separating gel. Protein

samples were suspended in 1X sample buffer, mixed, and boiled for 5 minutes before being loaded into the wells of the stacking gel. Electrophoresis was performed in 1X running buffer at a voltage of between 60 and 80 V. Proteins were visualized as bands in the gel by staining the gel with coomassie blue stain for 1 hour, followed by destaining overnight. If the protein sample could not be visualized with coomassie blue staining then the more sensitive silver staining technique was used as described by Morrissey (Morrissey, 1981). The size of the protein bands were then determined through visual comparison with the molecular weight marker.

2.16 Recombinant Protein Expression in *E. coli*

Protein expression in *E. coli* BL21(DE3)pLysS cells that have been transformed with the recombinant pET41(a) vector was induced by the addition of the galactose analog, isopropyl-β-D-thiogalactoside (IPTG). It was determined, through overexpression studies, that optimal expression of recombinant protein in these cells was achieved by induction with 0.2 mM IPTG for 4 hours at 37ºC. This provided the basis for the general procedure of recombinant protein expression in *E. coli* that was used during the course of this project.

Starter cultures of transformed BL21(DE3)pLysS cells were incubated overnight at 37ºC with vigorous shaking. The following morning the starter culture was used to inoculate LB of between 50 and 500 ml, supplemented with 50 μg/ml kanamycin and 100 μg/ml chloramphenicol. The culture was then grown with vigorous shaking, at 37ºC, until the OD_{600} of the culture was between 0.4 and 0.6. Recombinant protein expression was then induced by the addition of 0.2 mM IPTG and allowed to express for 4 hours at 37ºC with vigorous shaking. The recombinant protein was then extracted from the BL21(DE3)pLysS cells.

2.17 Recombinant Protein Extraction from *E. coli*

BugBuster® protein extraction reagent was initially used for the extraction of recombinant protein from *E. coli* cells. However, due to the rate at which the BugBuster® reagent was being exhausted and because of financial concerns, a new lysis buffer was developed and a protocol designed for extraction of recombinant protein. The lysis buffer technique was far more economical with only a slight loss in amount and purity of protein when compared to extraction with BugBuster® reagent.

2.17.1 Protein extraction using BugBuster® reagent

Recombinant protein extraction using the BugBuster® Extraction Reagent was accomplished by following the protocol provided by the manufacturer. SDS-PAGE was then used to determine whether the recombinant protein was soluble (in the supernatant) or insoluble (in the pellet). If the recombinant protein was insoluble they formed aggregates known as inclusion bodies. Purification of inclusion body protein was then performed using the BugBuster® reagent and following the manufacturers protocol.

2.17.2 Protein extraction using lysis buffer

Bacterial cells containing expressed protein were harvested by centrifugation at 5000 x g for 20 minutes. The cell paste was then resuspended in lysis buffer (5 ml lysis bufffer/100 ml cell culture) and incubated at room temperature for 20 minutes. The cell suspension was then sonicated for 3 cycles at 30 seconds each and then centrifuged at 16 000 x g for 20 minutes at 4ºC. Soluble protein present in the supernatant was retained and stored at –20ºC while insoluble inclusion body protein (pellet) was resuspended in the initial volume of lysis buffer and left at room temperature for 5 minutes. Three volumes of lysis buffer containing 1% triton X-100 was then added to the suspension and rotated slowly for 20 minutes at 4ºC. The inclusion body suspension was then centrifuged at 8 000 x g

for 15 minutes at 4ºC. The pellet was then washed with 2 volumes of lysis buffer with 1% triton X-100 and again centrifuged at 8 000 x g for 15 minutes at 4ºC. The pellet was then washed with one and a half volumes of lysis buffer that contained 1% triton X-100 and had been diluted 1:2 with distilled water. This was followed by a final centrifugation at 16 000 x g for 15 minutes at 4ºC. The inclusion body protein was then denatured to become soluble.

2.18 iFOLD™ Protein Refolding System 1

The iFOLD™ Protein Refolding System 1 is a simple, reliable, and comprehensive method to identify optimal protein refolding conditions. The system includes inclusion body purification reagents and a 96-well plate-based protein refolding buffer matrix (92 experimental and 4 control wells). By using the iFOLD™ Protein refolding system and following the manufacturers protocol the SNAMA inclusion body protein was denatured and rapidly diluted into the iFOLD 96-well buffer matrix. Absorbance readings at a wavelength of 340 nm were then taken for each of the 96 samples and recorded.

2.19 Inclusion Body Solubilization

Inclusion body protein was denatured and thereby solubilized using a urea based denaturation buffer and a procedure similar to that developed by Li and his colleagues (Li et al., 2004). 2 ml of denaturation buffer was added per gram of inclusion body protein. The mixture was then rotated at 4ºC overnight to allow for denaturation of the protein to occur. The following morning the mixture was centrifuged at 10 000 x g for 30 minutes to remove any debris. Solubilized protein was then analysed via SDS-PAGE.

2.20 Purification of Recombinant Protein

2.20.1 His-tag purification

Purification of recombinant protein that contained a histidine tag was achieved by nickel ion affinity chromatography using the HIS-Select™ Nickel Affinity Gel from Sigma. Purification of soluble protein without denaturant was accomplished by following the manufacturer's instructions provided. However, purification of protein under denaturing conditions followed a slightly different procedure to that supplied by the manufacturer of the affinity gel.

His-tag purification under denaturing conditions

Table 7. Buffers used during His-tag purification under denaturing conditions. All buffers were prepared fresh on the day of the procedure.

Buffer	**Composition**
Equilibration buffer	0.1 M sodium phosphate buffer, pH 8.0; 8 M urea.
Wash buffer 1	0.1 M sodium phosphate buffer, pH 6.3; 8 M urea.
Wash buffer 2	0.1 M sodium phosphate buffer, pH 4.5; 8 M urea.
Elution Buffer	50 mM sodium phosphate buffer, pH 8.0; 6 M Guanidine Hydrochloride.

Between 1 and 2 ml of affinity gel was transferred to a chromotography column and allowed to settle for approximately 2 hours. The column was then washed with 2 volumes deionised water followed by equilibration with 3 volumes of equilibration buffer. Between 5 and 7 volumes of denatured recombinant protein was then added onto the column at a flow rate of 2 to 10 column volumes/hour. After all the sample had been loaded the column was washed with 5 volumes of

wash buffer 1. This was followed by an additional abnormal column wash with 3 volumes of wash buffer 2. The histidine-containing sample was then eluted using 2 volumes of elution buffer. The column/affinity gel was then cleaned as described by the manufacturer and kept at 4ºC for future use.

2.20.2 GST-Tag Purification

The purification of recombinant protein containing a GST-tag was performed by glutathione affinity chromatography using glutathione agarose from Sigma. The procedure that was followed and buffers that were used are described in the product information manual supplied with the glutathione agarose.

2.21 Dialysis

Dialysis was performed to remove the denaturant, GuHCl, from purified recombinant protein thus refolding the recombinant protein. Pure recombinant protein was either added to SnakeSkin™ pleated dialysis tubing or Slide-A-Lyzer® dialysis cassettes and set-up as described by the manufacturer. Approximately 5 ml of sample was then dialyzed against 500 ml of dialysis buffer overnight at 4ºC. The following morning the sample was centrifuged at 10 000 x g for 30 minutes at 4ºC to remove any protein that might have precipitated out of solution. The dialysis buffer that was used for buffer exchange prior to CD spectroscopy differed from the norm as it lacked cyclodextrin, arginine, and EDTA, which interfered with the spectrophotometer readings at lower wavelengths.

2.22 Quantification of Protein

The concentration of an unknown protein was determined by the Bradford method, using a standard curve that was constructed from bovine serum albumin (BSA) standards and Bio-Rad Protein Assay. A BSA standard curve, ranging from 20-140 μg of protein (0.2-1.4 μg/μl), was constructed and stored in the UV-

160A UV-visible spectrophotometer. The protein samples were prepared in the same way as the standards by diluting the protein 100X with 1X Bio-Rad protein assay reagent and incubating for 30 minutes at room temperature. 1X Bio-Rad assay reagent was used to calibrate the spectrophotometer at A_{595} before the readings of the protein samples were taken. The concentration of the protein (in μg/ml) was then calculated automatically by the spectrophotometer using the BSA standard curve previously programmed. Protein was concentrated to required amounts using the Stirred Ultrfiltration Cell and following the manufactirer's instructions.

2.23 Circular Dichroism (CD) Spectroscopy

Circular dichroism (CD) spectroscopy is a valuable tool for the characetrization of protein structures in solution due to the inherent information content of the far UV CD spectra between 180 and 250 nm (Böhm et al., 2002). CD spectroscopy was used in order to gain important information concerning the secondary structure of the pure, recombinant GST-SNAMA fusion protein following dialysis in the absence of cyclodextrin, arginine and EDTA. Approximately 2.8 μM (~ 0.2 μg/μl) of GST-SNAMA fusion protein in 50 mM sodium phosphate buffer and 2.8 μM GST protein in 50 mM sodium phosphate buffer was used during the analysis. 50 mM sodium phosphate buffer was used as a blank for the GST-SNAMA and GST proteins. The GST protein without SNAMA was used both as a control to determine the accuracy of the procedure as well as a blank for the GST-SNAMA fusion protein. Circular dichroism spectra were recorded in the range from 190 to 250 nm at an interval of 0.5 nm with a Jasco J-810 Spectropolarimeter. Five scans were averaged for the sodium phosphate blank and ten scans averaged for each of the GST-SNAMA and GST proteins to obtain one spectrum for each sample. The CD spectra for each of the samples were then compared to known secondary structure spectra (Andrade et al., 2003; Bondesen and Schuh, 2001; Kelly and Price, 2000) in order to accurately predict the secondary structure of SNAMA.

2.24 Ubiquitin Conjugation Assay

An ubiquitin conjugation assay was performed in order to determine whether the recombinant SNAMA protein exhibited ubiquitin ligase activity. To determine the E2 that SNAMA would have optimal activity with, a series of E2s (UbcH2, UbcH3, UbcH5a, UbcH5b, UbcH5c, UbcH6, UbcH7, UbcH10) were initially used. The assay reaction mixture consisted of 7.2 µg ubiquitin, 0.1 µg E1, 0.4 µg E2, 4.6 µg GST-SNAMA fusion protein (E3), 2 mM DTT, 2 mM ATP, 5 mM $MgCl_2$, 250 µM $ZnCl_2$, and made up to 30 µl with 50 mM sodium phosphate buffer, pH 8.0. The reaction mixture was then incubated at 30ºC for 2 hours and stopped by the addition of sample buffer. To check for ubiquitin ligase activity the reaction mixture was run on an SDS-PAGE gel. Ubiquitin conjugation assays in the absence of the key components of the ubiquitin system, namely the E1, E2, E3, ubiquitin, ATP, and ZnCl2, were performed as controls.

2.25 Bioinformatic tools

Gene-specific primers were designed using Gene Runner (Version 3.05). Chromatograms of sequenced DNA obtained from Inqaba Biotech were visualized using Chromas (Vesion 1.45). Sequence alignments of both protein and DNA were carried out using DNAMAN version 4.03 (Lynnon Biosoft, Quebec, Canada) and ClustalX, using the optimal alignment setting. Secondary structure prediction for the DCM of SNAMA was achieved using the PSIPRED program version 2.5 (Bryson et al., 2005).

Table 8. Web addresses for various bioinformatic tools.

Bioinformatic Tool	**Web Address**
BLAST	http://www.ncbi.nlm.nih.gov/BLAST
Chromas	http://www.technelysium.com.au/chromas.html
ClustalX	http://www-igbmc.u-

	strasbg.fr/BioInfo/ClustalX/Top.html.
FlyBase	http://flybase.bio.indiana.edu
PSIPRED	http://bioinf.cs.ucl.ac.uk/psipred

3. TRANSCRIPTIONAL REGULATION OF *SNAMA*

The human RbBP6 homologue of SNAMA is expressed as three transcripts of 6.1, 6.0, and 1.1 kb (Pugh et al., 2006). These transcripts give rise to proteins of 1792, 1758, and 118 amino acids, designated RbBP6 isoforms 1, 2, and 3 respectively. The fact that human RbBP6 has various isoforms suggests that there might be additional isoforms of the SNAMA protein. Alternative splicing, poly-adenylation, or the presence of an internal promoter region and transcriptional start site within a gene would lead to the expression of isoforms. Internal promoters are usually present in more advanced and complex organisms where regulation of gene expression is intricate and under tight control (Neuman et al., 2005). These downstream internal promoters usually reside in the first introns, which are on average longer than other introns and are, sometimes, exceptionally long (Kriventseva and Gelfand, 1999). The annotated structure of *Drosophila* genes from chromosome 2R (where *SNAMA* is found) shows that more than 50% of the genes larger than 30 Kb contain large 5´ introns, and two or more predicted remote first exons regulated by alternative promoters (Neuman et al., 2005).

Determining the transcriptional start site of a gene makes it possible to examine the regulatory regions that define the promoter region and thereby gain further insight into how expression of protein is controlled. It is believed that during the course of evolution the sequences for promoter regulation have been preserved in the promoter region and that their occurrence frequencies are far from random (Gershenzon et al., 2006). There are six core promoter elements that have been discovered in eukaryotes thus far. These elements are TATA box, Initiator (Inr), Downstream Promoter Element (DPE), TFIIB recognition element (BRE), Downstream Core Element (DCE), and Motif Ten Element (MTE) (Smale and Kadonaga, 2003; Lim et al., 2004; Lewis et al., 2000). Four of these core promoter elements have been experimentally identified in *Drosophila* promoters: the TATA box, Inr, DPE and MTE (Smale and Kadonaga, 2003; Lim et al., 2004). Comparison between human and *Drosophila* shows consistent

percentages of promoters with TATA, Inr, DPE, and synergetic combinations thereof, as well as most of the same functional and mutual positions of the core elements (Gershenson et al., 2006).

The transcriptional initiation site of a gene can be determined by examining the 5´ -terminus of a transcript through the 5´ rapid amplification of cDNA ends (5´ RACE) technique (Bensing et al., 1996; Argaman et al., 2001; Gum et al., 2003; Aspegren et al., 2004). Analysis of the 5´ region of the *SNAMA* transcript was determined using the GeneRacer^{TM} 5´ RACE, which amplifies the beginning of the transcript to a point where the RF Tail primer binds. In this way it is possible to identify the core promoter elements that define the promoter region/s of *SNAMA*, thus providing valuable information into the transcriptional regulation of the gene.

3.1 5´ Rapid Amplification of cDNA Ends (5´ RACE)

5´ RACE using RNA from *Drosophila* embryos and the GeneRacer^{TM} (GR) kit resulted in the amplification of two distinct DNA fragments of varying size (Figure 10; see also Figure 12 for primer positions). The smaller fragment ranged from 650-700 bp while the larger ranged from 800-850 bp, depending on the combination of primers used. The DNA fragment between 800 and 850 bp in size was expected as the RF Tail primer that was used during reverse transcription was designed to bind at the end of the RFL motif (Appendix I). The presence of the DNA fragment from between 650 and 700 bp in size appeared to indicate that there was an additional promoter region and transcriptional start site, downstream the initial transcriptional start site. This sparked much interest as it would imply that there was an internal promoter in the *SNAMA* gene.

The slight variation in sizes between each of the two distinct 5´ RACE products can be attributed to the combination of primers that were used during GeneRacer^{TM} PCR. Amplification of the SNAMA cDNA resulted in fragments that were slightly smaller when using the GR 5´ Nested primer than when using

the GR 5´ primer. This was expected due to the GR 5´ Nested primer binding the GR oligo downstream the position where the GR 5´ primer binds. Similarly, amplification with the RF Tail Internal reverse primer resulted in slightly smaller fragments than that amplified using the RF Tail primer. This was due to the RF Tail Internal primer binding SNAMA upstream the RF Tail primer. Interestingly, the smaller DNA fragment was far more prominent when the RF Tail was used as the reverse primer. When the RF Tail Internal primer was used the smaller band was barely visible in the gel. In contrast, the larger DNA fragment was far more prominent when the RF Tail Internal primer was used as the reverse primer.

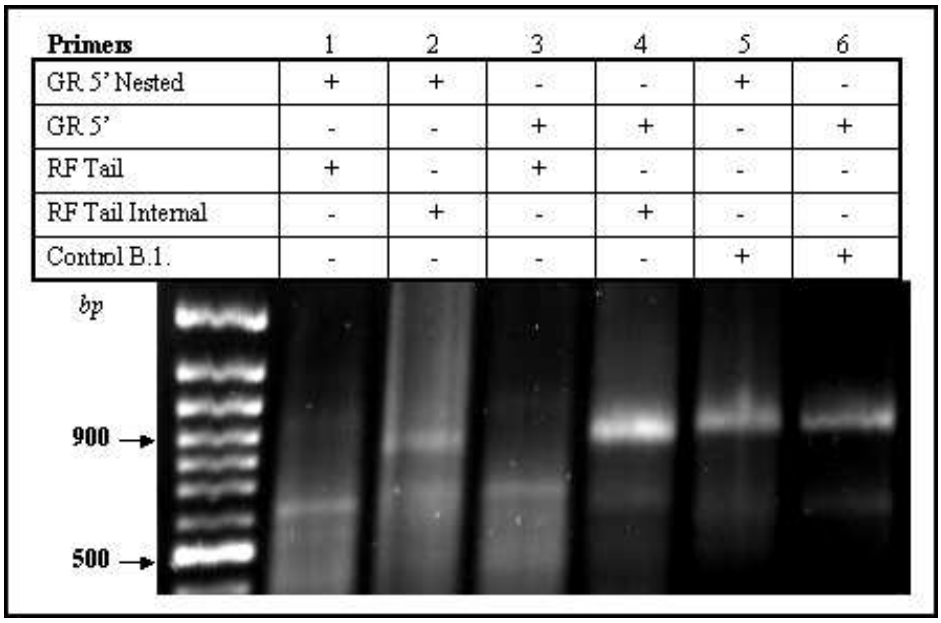


Figure 10. 5´ Rapid amplification of cDNA ends using *Drosophila* RNA. Two distinct fragments of different size were amplified when 5´ RACE was performed on *Drosophila* RNA from adults. The smaller fragment was between 650 and 700 bp in size while the larger was between 800 and 850 bp. Different combinations of primers resulted in slight variations in DNA fragment size and band intensities. A positive control using HeLa RNA and the Control B.1 primer resulted in the amplification of a fragment approximately 900 bp in size as expected (lanes 5 and 6).

5´ RACE using HeLa control RNA as a template resulted in the amplification of a DNA fragment approximately 900 bp in size when using the Control B.1 reverse primer together with the GR primers (Figure 10). This was the expected size for the 5´ RACE product of HeLa (according to manufacturer), thus confirming that 5´ RACE had occurred successfully.

3.2 Cloning of 5´ RACE Products

To confirm that the two DNA fragments were amplified from the *SNAMA* gene and determine the exact site of transcription initiation, they were both cloned and sequenced. The 800-850 bp fragment, that results from amplification with the GR 5´ and RF Tail Internal primers, was used when cloning the larger of the two 5´ RACE products. This fragment was used as it contained the most DNA when compared to the other 800-850 bp fragments, as is evident by its greater band intensity in the gel (Figure 10). For the same reason the 650-700 bp fragment that results from amplification with GR' Nested and RF Tail primers was used when cloning the smaller of the two 5´ RACE products.

The two DNA fragments were excised from the gel, ligated into TA cloning vectors and cloned for sequencing. Colony PCR was performed in order to confirm successful cloning and ensure DNA fragment sizes (Figure 11). The RF Tail was used as the reverse primer when amplifying the 650-700 bp DNA fragment, as this primer was most effective during initial amplification of the cDNA. For the same reason the RF Tail Internal primer was used during the amplification of the larger 800-850 bp fragment. As with 5´ RACE, a somewhat smaller fragment is amplified when using the GR 5´ Nested primer compared with the GR 5´ primer due to different positions at which the primers bind the product.

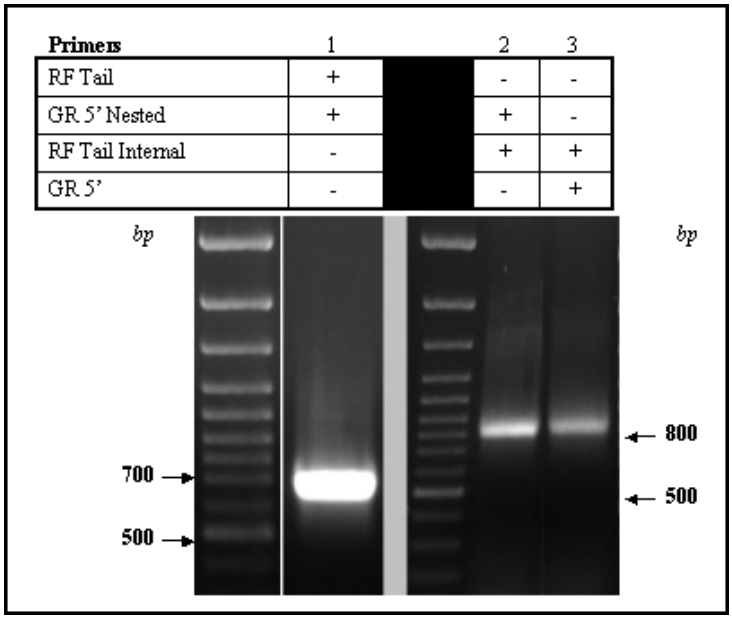


Figure 11. PCR amplification to verify cloning of 5´ RACE products. The 650-700 bp fragment was amplified using the RF Tail reverse primer (lane 1), in contrast to the 800-850 bp fragment, which was amplified using the RF Tail Internal primer (lanes 2 and 3).

3.3 Sequence Alignments of the 5´ RACE Clones

The two clones containing the products from 5´ RACE were sent to Inqaba Biotec for sequencing. The sequences for each of the clones were aligned with themselves, the GR oligo, the SNAMA cDNA sequence, and the primers, to ascertain whether the fragments were amplified from the *SNAMA* gene and determine where transcription begins (Figure 12). Alignment showed that the 800-850 bp clone was in fact 790 nucleotides in length and aligned completely with *SNAMA* cDNA, as did the RF Tail primer used during amplification (Figure 12 (b)). The transcriptional start site of the 790 bp fragment (GCATC) is indicated at the point where the GR oligo ends.

The 650-700 bp clone was shown to be 681 nucleotides in length and did not align significantly with *SNAMA*, yet the RF Tail primer showed complete binding to the amplified fragment (Figure 12 (a)). This was unfortunate as it suggested that this fragment was not amplified from *SNAMA* but rather from

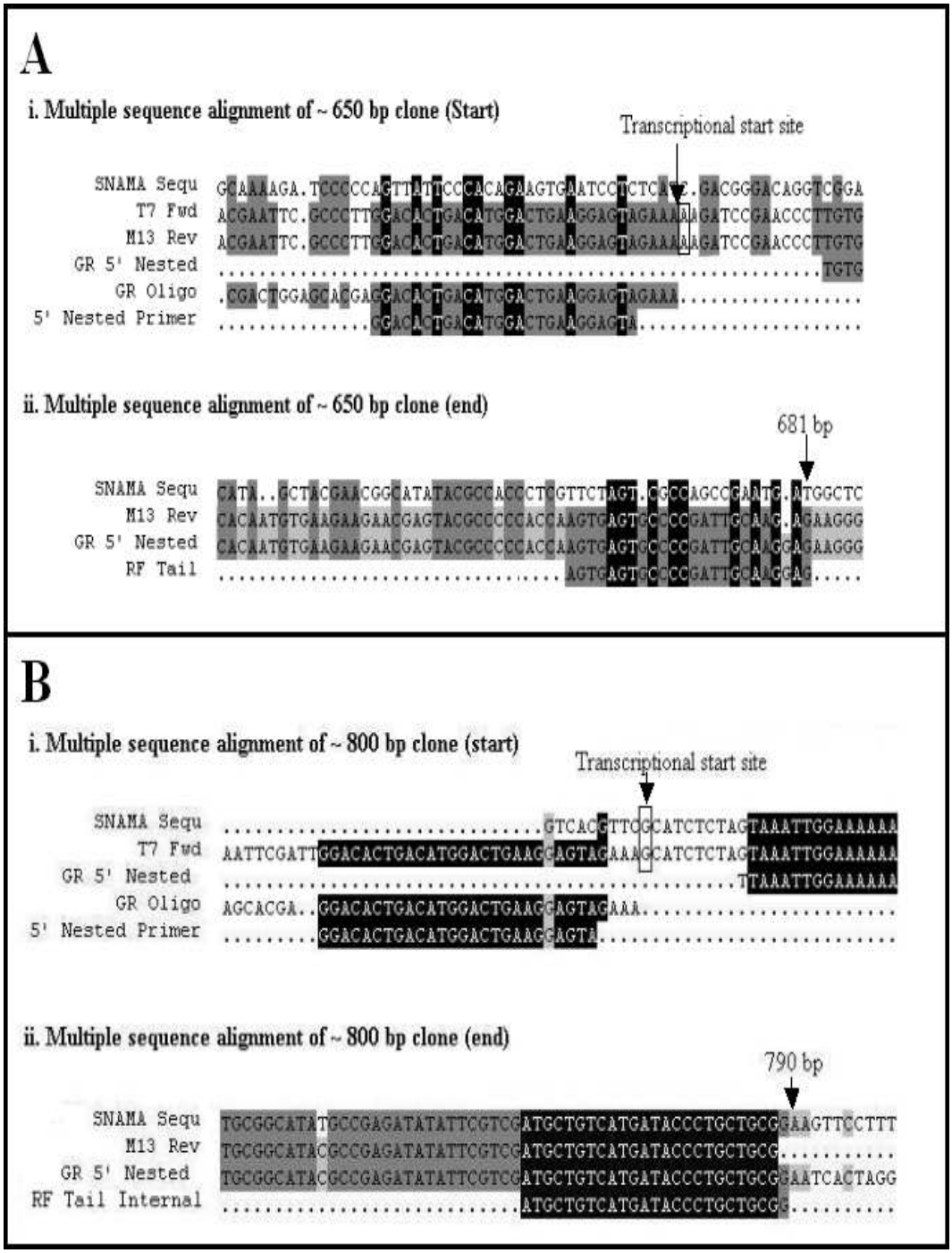


Figure 12. Multiple sequence alignment of cloned 5´ RACE products. (A) Alignment of the 650-700 bp clone shows a fragment 681 bp in size that does not have a significant alignment with the SNAMA sequence. In contrast, the alignment shows that the RF Tail primer binds completely to the fragment. (B) Alignment of the 800-850 bp clone shows a fragment of 790 bp that aligns completely with SNAMA and the RF Tail primer.

another gene within *Drosophila*. This was confirmed by BlastN searches against the *Drosophila* genome, which showed significant alignment of the 681 bp fragment with a gene approximately 4.6 Mbp upstream of *SNAMA*, in the right arm of chromosome 2 of *Drosophila* (ref: NT 033778) (Appendix II). This fragment was amplified during 5´ RACE due to the sequence of the reverse primer (RF Tail) that was used during reverse transcription of the *Drosophila* embryonic RNA. The first half of this primer shows complete homology to the gene identified upstream of *SNAMA*. Thus, the primer would have recognized and bound both the *SNAMA* gene and the gene upstream, which were both then reverse transcribed into the cDNA and later amplified. This also accounts for the virtual absence of a 650-700 fragment when 5´ RACE was performed using the RF Tail Internal primer (Figure 10), as this primer did not have homology to the other gene within the *Drosophila* genome.

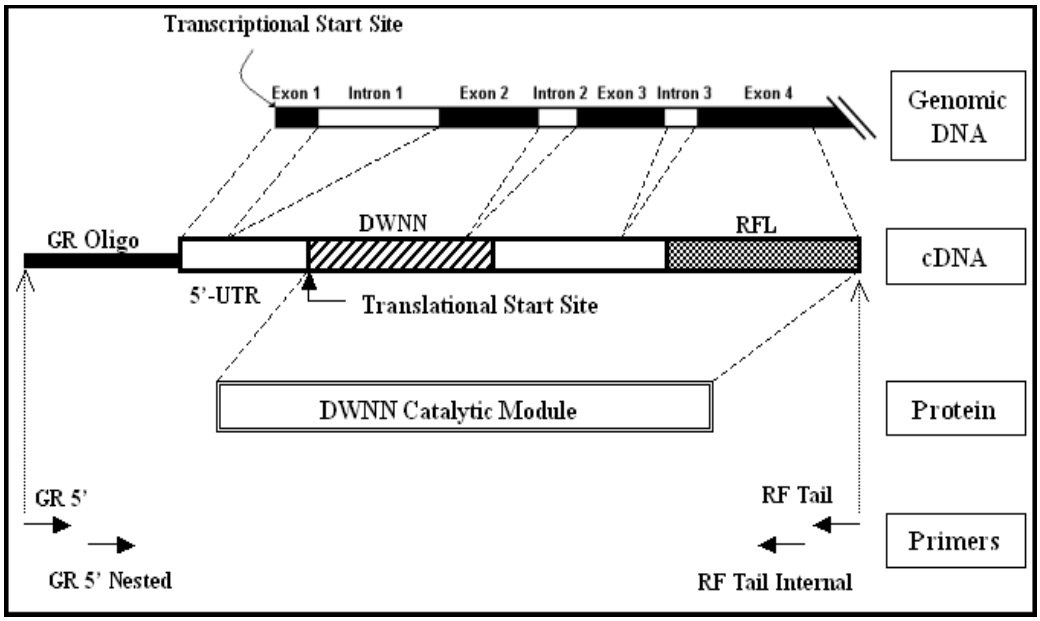


Figure 13. The 5´ region of the *SNAMA* gene that is ultimately translated into the DWNN catalytic module. The GeneRacer^{TM} (GR) oligo along with primers used during transcriptional start site determination are also shown.

It is evident that *SNAMA* contains a single transcriptional start site at the 5´ region of the gene. A summary of these results is illustrated in Figure 13, which indicates the 5´ region of *SNAMA* and its translation into the DWNN domain and RFL motif that comprise the DCM. Also shown are the primers used in determining the transcription start site of *SNAMA*.

4. DOES SNAMA EXHIBIT UBIQUITIN LIGASE ACTIVITY?

The modification of proteins by ubiquitin is essential for numerous cellular processes. For example, ubiquitin-dependent protein degradation is involved in the regulation of apoptosis, cell cycle progression, signal transduction, transcription, DNA repair, and protein quality control (Laney and Hochstrasser, 1999). Ubiquitination begins with the activation of ubiquitin by E1 in an ATP-dependent manner, resulting in the covalent attachment of ubiquitin to the E1 (Haas and Rose, 1982). Ubiquitin is subsequently transferred to an E2. Finally, the E3 attaches ubiquitin to its substrate by interacting with both the E2 and target protein (Hershko and Ciechanover, 1998).

The most common of the E3 ligases, the RING finger E3s, are dependent on their RING finger conformation for their ubiquitin ligase activity. The U-Box and PHD are referred to as derivatives of the RING finger E3 as they also form a RING finger conformation (Sun, 2003). However, these RING finger structures are stabilized in a different way to the characteristic RING finger.

SNAMA is a member of the RbBP6 superfamily. All members of this family contain a highly conserved N-terminal region known as the DWNN Catalytic Module (DCM). The module is comprised of the DWNN domain, zinc finger motif and RFL motif respectively (Mather et al., 2005). The RFL motif of SNAMA includes the highly conserved cysteine residues present in characteristic RING fingers but differs from the standard by substitution of a histidine residue in the fourth ligand with a serine residue (Mather et al., 2005).

The ability of a protein to exhibit ubiquitin ligase activity can be tested for by performing an ubiquitin conjugation assay using the protein as the E3 (Imai et al., 2003). A pure and active form of the protein is needed in order to perform this assay. The DCM of SNAMA was expressed as a recombinant protein in *E. coli* and formed insoluble inclusion body aggregates. The insoluble inclusion body protein was solubilized, purified and refolded into its native state. The pure

and active form of the recombinant SNAMA protein was then used as the E3 in an ubiquitin conjugation assay to determine whether it had ubiuqitin ligase activity.

4.1 Recombinant Expression and Extraction of SNAMA

The DCM of SNAMA was cloned and expressed in *E. coli* BL21(DE3)pLysS cells using the pET41(a) expression vector (Appendix VI). Optimal expression of recombinant protein in these cells was achieved through induction with 0.2 mM IPTG for 4 hours at 37ºC. The recombinant GST-fusion protein, representing the DCM of SNAMA, was referred to as GST-SNAMA (GST-S). Expression of GST-S resulted in the protein forming insoluble inclusion body aggregates, approximately 70 kDa in size, in the pellet (Figure 14). Expression of a GST protein (GST), in cells transformed with intact pET41(a), was used as a positive control that resulted in an approximately 38 kDa soluble protein, present in the supernatant (Figure 14). Whole cells lacking the pET41(a) vector were used as a negative control. Working with inclusion bodies is challenging as you have to solubilize and purify the protein before attempting to refold it back into its native state to use in activity assays.

The parameters under which protein expression occurs were changed in an attempt to solubilize the protein during expression. These parameters included induction temperature, protein expression time, and addition of zinc ions during expression. Protein expression was attempted at 30ºC, room temperature, and 18ºC. Protein expression was also induced at various temperatures for 2 hours, 6 hours, and overnight. Finally, expression of the protein was attempted in the presence of zinc ions. In all cases there was no affect on the solubility of the protein although levels of protein expression did fluctuate. The insoluble GST-S inclusion bodies were thus denatured using urea in order to solubilize the protein.

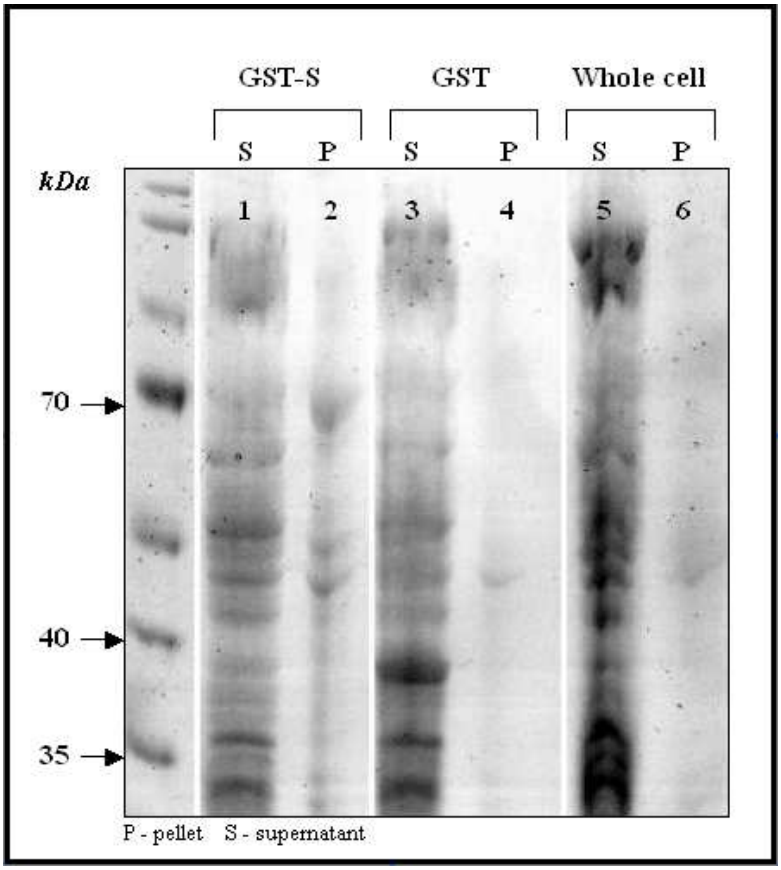


Figure 14. Recombinant expression of GST-fusion SNAMA protein. Recombinant protein was expressed in *E. coli* BL21(DE3)pLysS cells. GST-SNAMA (GST-S) is expressed as insoluble inclusion body protein approximately 70 kDa in size (lane 2). The GST protein (GST) is expressed as a 38 kDa soluble protein (lane 3). Protein extracted from the *E. coli* whole cell, lacking the pET41(a) vector, is used as a negative control (lanes 5 and 6).

4.2 His-Tag Purification of Denatured Recombinant SNAMA

The denatured, recombinant SNAMA protein was not very pure and was present amongst contaminating protein that included denatured membrane bound protein from *E. coli* (Figure 15). This could hinder both the refolding and activity of SNAMA and thus the recombinant protein was purified from the contaminating protein. Initially, glutathione agarose was used in an attempt to purify the GST-S through its affinity to the GST tag fused to SNAMA. However, this proved unsuccessful as GST-S was in its unfolded, denatured state and the glutathione

could therefore not recognize and bind the GST tag. Nickel charged agarose was then used in an attempt to purify the recombinant SNAMA protein through its affinity to the His_6 tag that is associated with the recombinant protein. Nickel ion affinity chromatography is capable of purifying His tag containing proteins in both the unfolded (denatured) and folded (native) states. In fact, purification of the protein is often more effective when it is its denatured state as the hexa-histidine residues are more exposed.

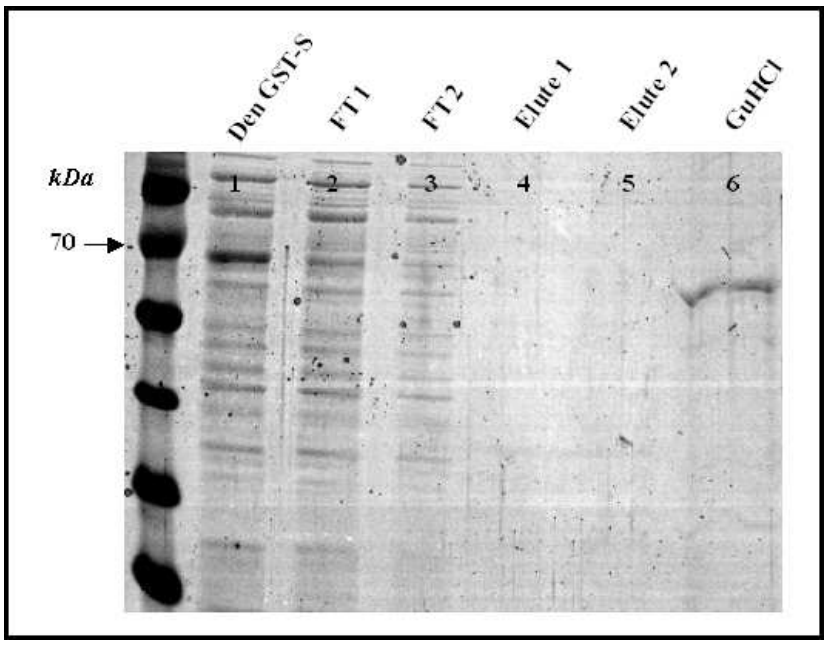


Figure 15. His-tag purification of denatured recombinant SNAMA protein. Denatured SNAMA protein was present amongst contaminating protein (lane 1). Ni^{+2} affinity chromatography under denaturing conditions was performed as described in the manufacturers protocol. Pure GST-SNAMA fusion protein was unexpectedly eluted using GuHCl (lane 6) rather than elution buffer in the step before (lanes 4 and 5). Note that the GST-SNAMA fusion protein appears smaller in size due to the gel being scewed.

Ni^{+2} affinity chromatography was used to purify the recombinant SNAMA protein under denaturing conditions. Results showed that there was specific binding of SNAMA to the affinity column, as was evident by very little recombinant protein eluted during the first washes (Figure 15). Unexpectedly,

recombinant SNAMA was not eluted during the typical, initial elution wash (wash buffer 2 in section 2.20.1). Instead, the recombinant SNAMA protein was eluted with buffer containing GuHCl as an extremely pure protein (Figure 15). Other than a denaturant, GuHCl is also commonly used to remove protein from the Ni^{+2} agarose during the cleaning process of the column. The GST-SNAMA fusion protein appears smaller in size when compared to the denatured SNAMA protein. This was due to the gel being placed at a slightly scew angel prior to its image being capured.

The imidazole ring present in the side chain of the histidine residues, contains a pKa of 6.04 and, is ultimately responsible for its affinity to the metal ions in the agarose. In buffers with a pH value greater than 6.04 the imidazole rings will be charged and thus bind specifically to the Ni^{+2} charged affinity gel. Normally, the elution buffer removes bound protein due to a drop in pH of the buffer to 4.5. This causes the imidazole rings of histidine residues to lose their charge as they become protonated and thus lose the ability to bind Ni ions in the affinity column. However, this drop in pH does not affect the binding of the recombinant SNAMA to the affinity column suggesting that the imidazole rings remain in their anionic state. Instead the bound protein is eluted with GuHCl. This is probably due to the presence of guanidinium cations (Gdm^{+}) in solution that bind with greater affinity to the imidazole rings of the histidine residues than the nickel ions, thus allowing for their elution from the column.

4.3 Optimal Refolding Conditions for SNAMA

Defining conditions that promote refolding of the denatured protein into its native conformation is empirical, difficult and time-consuming. To overcome these problems, the iFOLD^{TM} Protein Refolding System 1, together with the literature (Clark, 1998; Li et al., 2004; Karuppiah and Sharma, 1995; Chen et al., 2005; Cabrita and Bottomley, 2004), was used to determine the optimal refolding conditions for the recombinant SNAMA protein. Absorbance readings at 340 nm were recorded for 96 samples following the rapid dilution of SNAMA

protein into 96 different refolding buffers (Figure 16). The composition for each of the buffers within the 96-well plate can be seen in Appendix III. The lower the A_{340} value of the sample the more effective the refolding buffer as the absorbance of the solution is an indication of the degree of precipitation of protein out of solution. The composition of the top ten buffers with lowest absorbance were then examined to determine the best composition of additives for refolding recombinant SNAMA protein (Table 9).

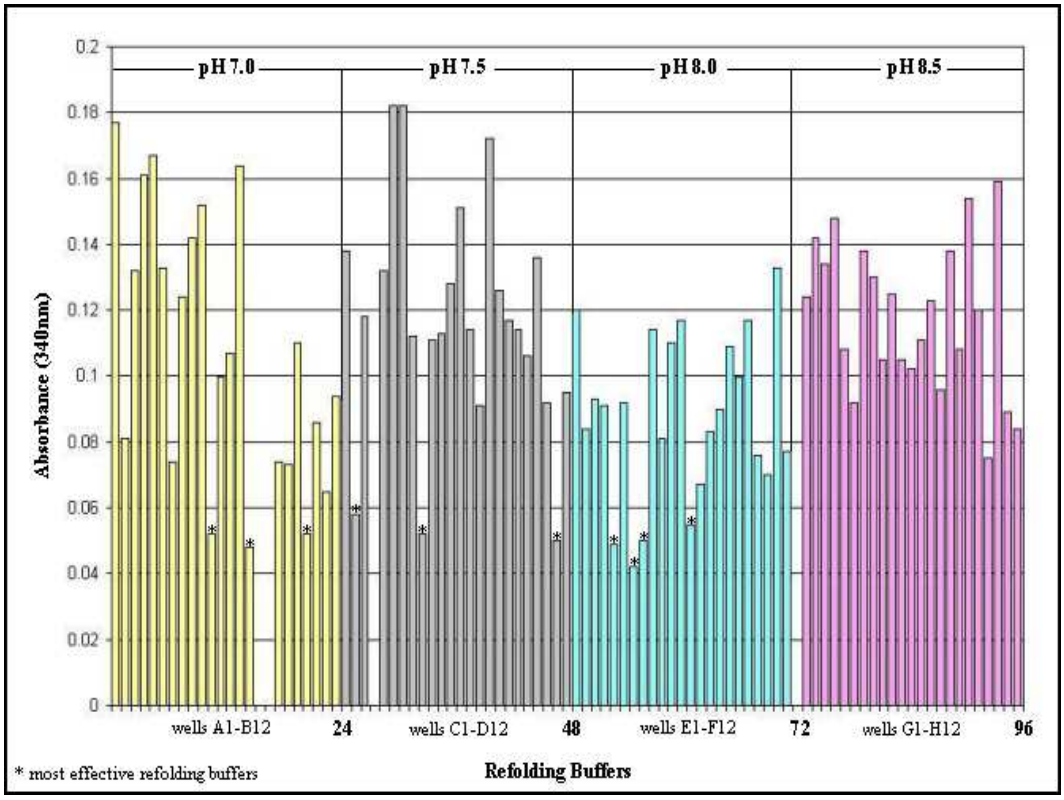


Figure 16. Refolding conditions for the recombinant SNAMA protein. GST-S protein was refolded by rapid dilution of the denatured protein into the 96-well iFOLD plate (Appendix III). The relative absorbance of samples was taken at 340 nm with the ten most effective refolding buffers indicated by an asterisk.

The iFOLD^{TM} protein refolding system showed that refolding buffers with a pH of 8 were the most effective when refolding SNAMA (Figure 16). SNAMA is most stable at this pH as precipitation levels of the protein remain low on a regular basis across various refolding buffers. This is illustrated by the high

consistency of low peaks ($A_{340} < 0.12$) at this pH. In addition, majority of the top ranked refolding buffers for SNAMA had this pH (Table 9). Other buffers with a pH of 7 and/or 7.5 appear to be effective refolding buffers. However, these buffers do not refold SNAMA with the same consistency as a buffer with a pH of 8 and SNAMA is not as stable throughout a broad range of buffers. Furthermore, the effeciveness of the buffers with a pH of 7 and 7.5 is most likely due to the refolding components within the buffer.

Cyclodextrin is by far the most successful refolding additive of SNAMA as it appeared most frequently in the best refolding buffers for SNAMA. This is not surprising as cyclodextrin is both a stripping agent, used for the removal of detergents (Rozema and Gellman, 1995), and a suppressing agent, preventing aggregation of protein during refolding (Karuppiah and Sharma, 1995).

Independently, the L-arginine and buffer solutions alone were successful in causing SNAMA to refold well (Table 9). L-arginine is mentioned in a great deal of published literature involving protein refolding (Arakawa and Tsumoto, 2003; Bell et al., 2002). Arginine plays an important role by not facilitating the actual refolding of the protein but rather suppresses aggregation of the protein during refolding. Additives that facilitate disulphide bond formation include combinations of reduced and oxidized forms of glutathione (GSG/GSSG), cysteine and cystine, or DTT/oxidized glutathione. These redox systems are usually added to accelerate shuffling of disulphide bonds. However, they are not pivotal as air is also suitable to promote disulphide bond formation through air oxidation (Cabrita and Bottomley, 2004). Furthermore, “shuffling” of disulphide bonds is generally catalyzed by trace amounts of metal ions and also by slightly alkaline pH of between 8 and 9. Conversely, EDTA was added to the refolding buffer to scavenge unwanted metal ions, which could cause oxidation reactions.

Table 9. The most effective refolding buffers for recombinant SNAMA. The composition of the top ten refolding buffers for SNAMA when using the iFOLD Refolding Protein System 1 were compared. Cyclodextrin appeared most frequently while 100 mM NaCl, L-arginine and EDTA appear to be amongst the most significant of the additives.

Composition\Buffer	A11	B3	B9	C2	C9	D11	E5	E7	E8	F1
Rank	5	2	5	7	5	4	3	1	4	6
PH	7	7	7	7.5	7.5	7.5	8	8	8	8
100 mM NaCl	+	+					+			
250 mM NaCl			+					+		
Cyclodextrin	+		+	+	+		+	+		
L-Arginine			+						+	
EDTA		+			+					+
GSH/GSSG		+								+
TCEP				+			+	+		
GuHCl							+			+
Buffer						+				
Glycerol				+						

4.4 Refolding the Pure, Denatured SNAMA

A pure form of the recombinant SNAMA protein was acquired in its denatured form and needed to be refolded into its native state. Dialysis of the His-tag purified SNAMA protein was performed to slowly remove GuHCl from the sample through buffer exchange with the dialysis (refolding) buffer, thus refolding SNAMA. Many dialysis buffers were designed using the information obtained from the iFOLD^{TM} Protein Refolding System 1 combined with information gathered from literature (Clark, 1998; Li et al., 2004; Karuppiah and Sharma, 1995; Chen et al., 2005; Cabrita and Bottomley, 2004). Most buffers that were tried caused precipitation of the SNAMA protein out of solution. This was determined confirmed through visualization of the protein in the polyacrylamide gel and through spectrophotometric quantification. However, after much trial and error it was ultimately discovered that denatured SNAMA protein could be successfully refolded by dialysis against a phosphate-based refolding buffer of pH 8.0, containing cyclodextrin, L-arginine, NaCl and EDTA. This resulted in only a slight precipitation of recombinant SNAMA with majority of the protein remaining in a soluble, refolded form (Figure 17). Refolding took place at 4ºC as this temperature minimizes protein aggregation best.

4.5 Confirmation of Correctly Refolded SNAMA Protein

Once refolded, it had to be determined whether GST-S had refolded correctly into its native conformation or misfolded into a non-active form. This was confirmed through affinity binding and secondary structure determination of the recombinant protein. Binding of GST-S to the glutathione agarose column and elution from the column with reduced glutathione illustrated that the GST tag of the recombinant protein had specificity for the glutathione (Figure 18). This confirms that the GST portion of the recombinant protein refolded into its native state, which is shown by its ability to recognize and bind glutathione. However, this does not prove that the SNAMA fraction of the recombinant protein has

refolded correctly but suggests that it could have due to the GST portion having refolded correctly.

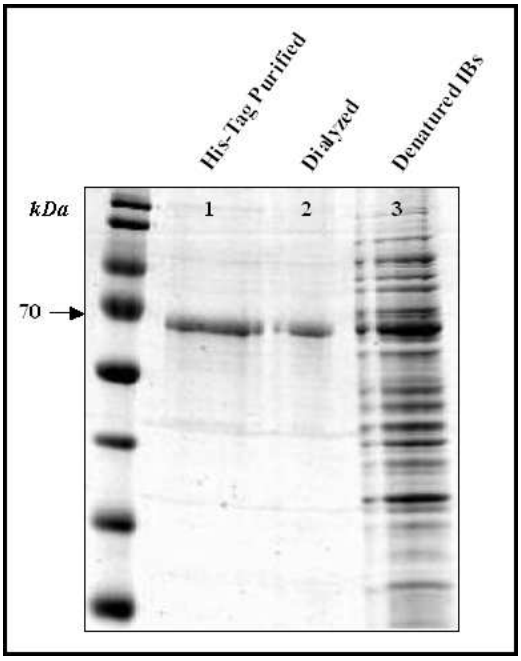


Figure 17. Dialysis of His-tag purified SNAMA protein. The His-tag purified SNAMA sample before dialysis can be seen in lane 1. Following dialysis the now refolded SNAMA sample shows a slight decrease in amount of protein, which was confirmed by spectrophotometric quantification (lane 2). Denatured inclusion bodies (IBs) prior to purification and dialysis can be seen in lane 3.

Circular dichroism (CD) spectroscopy was used to determine the secondary structure of the recombinant SNAMA protein by far UV CD spectra (between 190 and 250 nm). Initially poor readings were obtained due to the buffer components of the sample interfering with the absorbance of light by the protein at the lower, more significant wavelengths. These components within the buffer included sodium phosphate buffer concentration, cyclodextrin, L-arginine and EDTA. Dialysis in the absence of cyclodextrin, L-arginine and EDTA was therefore attempted and proved successful, but at a price. Large amounts of protein was lost during the dialysis due to absence of the refolding agents, and thus protein was concentrated in order to obtain the large amounts that were needed in order to perform CD spectroscopy.

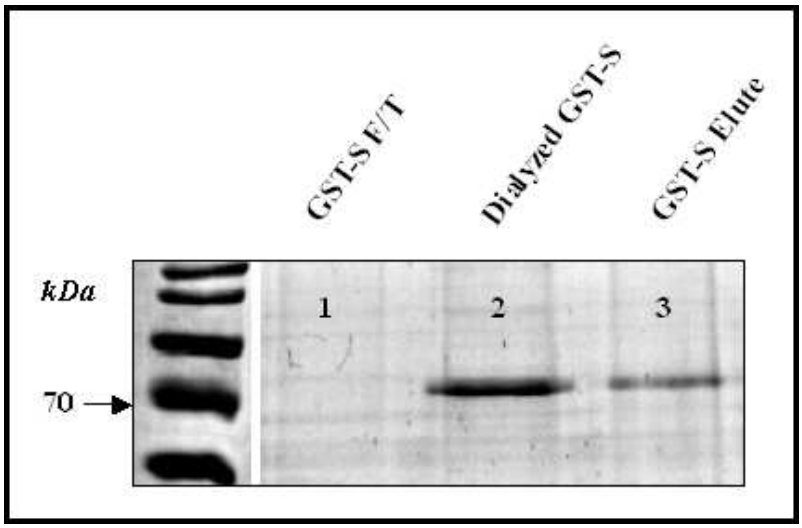


Figure 18. Glutathione affinity chromatography of refolded GST-S protein. The GST-S protein was eluted during the elution wash using glutathione (lane 3), with no protein present in the flow through wash (lane 1). The dialyzed GST-S protein sample prior to loading onto the glutathione agarose column can be seen in lane 2.

The fact that there were CD spectra for both the refolded GST-S protein sample and the GST protein proved that the protein had a secondary structure and that refolding had occurred (Figure 19). A CD spectrum with no troughs or peaks (zero absorbance) was obtained for the denatured GST-S protein sample, indicating that there was no secondary structure (results not shown). This is what was expected from a non-folded protein. The CD spectra for each of the samples was then compared to typical secondary structures defined in literature in order to determine the secondary structure for the DCM of the SNAMA protein (Kelly and Price, 2000) (Appendix VII).

The GST protein was used both as a positive control and a blank during CD spectroscopy studies. As a positive control it portrayed the characteristic α-helical spectrum having a trough between 200 and 240 nm with lows at 220 nm and 210nm, and a slight peak between them. Furthermore, the spectrum increased to an immense peak at 190 nm much like classical α-helical proteins. This was expected as GST is predominantly an α-helical protein. The GST

protein was also used as a blank against the GST-SNAMA protein to eliminate the effect of the GST tag secondary structure from the secondary structure determination of SNAMA.

The CD spectrum for the GST-SNAMA protein was very similar to that of the GST protein as it represented a protein that was predominantly α-helical. However, the GST-SNAMA spectrum was different in that it showed a large trough just below 200 nm that is indicative of a protein containing random coils. The spectrum for only the DCM of SNAMA (GST-S – GST) was very different to that observed when including the GST tag as it lost all of its α-helical characteristics. On the contrary, the spectrum was indicative of a protein that is made up mostly of β-turns, random coils and β-sheets. The presence of β-turns is represented by a slight trough between 220 nm and 230 nm, a peak at approximately 202 nm, and a trough at 190 nm (Figure 19). Random coils are represented by a major low at 198 nm while the presence of β-sheets is represented by a slight peak at 196 nm.

The secondary structure determined for the DCM of SNAMA by CD spectroscopy is similar to that predicted by bioinformatic analysis and the literature (Appendix IV). The DWNN domain is expected to contain three and a half α-helices, five β-sheet strands and seven reverse turns (Pugh et al., 2006). The zinc finger knuckle usually has two short β-strands followed by a short α-helix and connected by a turn (Krishna et al., 2003). The RING finger motif is usually made up of three β-strands, a α-helix and long loops. The secondary structure predicted using the PSIPRED bioinformatic program was very similar for these domains within the DCM. Overall, the predicted secondary structure for SNAMA showed a protein that consisted predominantly of random coils and turns with a greater presence of β-sheets than α-helices. This data is similar to that acquired from CD spectroscopy and thus it was concluded that the protein had refolded into its native conformation. This would ultimately be confirmed by testing for the activity of the pure refolded protein in an activity assay.

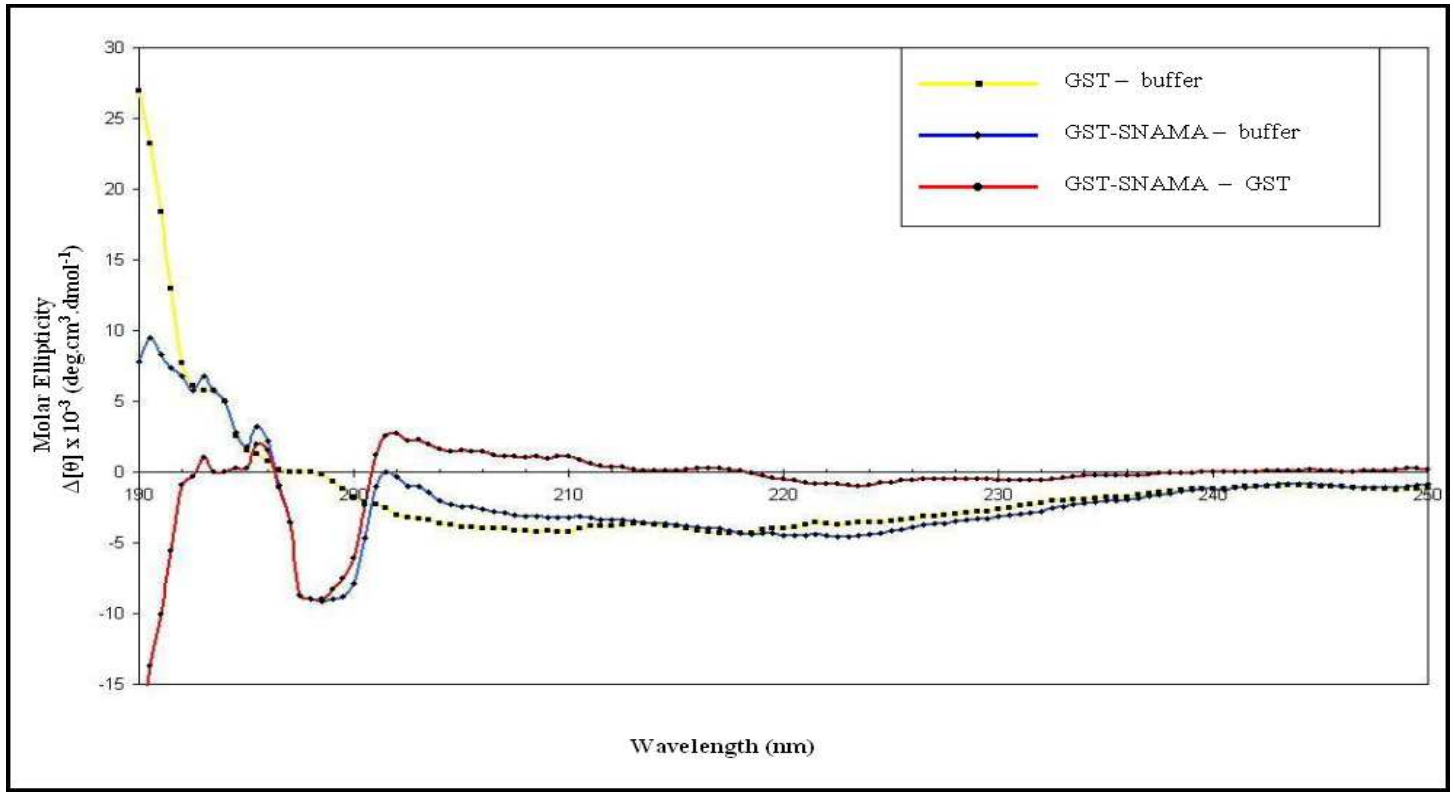


Figure 19. CD spectra for the recombinant GST-S and GST proteins. The yellow spectrum (square) represents the GST protein blanked against its buffer and is predominantly α-helical with a trough between 200 nm and 240 nm, lows at ~ 220 nm and 210 nm with a slight peak between them, and a large peak at 190 nm. The blue spectrum (diamond) represents the GST-S sample blanked against its buffer also shows α-helical characteristics with a trough between 202 nm and 240 nm, and peaking around 190 nm. However, this spectrum also indicates the presence of random coils by the large trough at ~ 200 nm. The red spectrum (circle) represents the GST-S sample blanked against the GST-protein and is indicative of β-turns, random coils, as shown by a slight trough between 220 nm and 230 nm, a peak at ~ 202 nm, a major low at ~ 198 nm, a peak at ~ 196 nm, and a trough at 190 nm.

4.6 Ubiquitin Conjugation Assays Using SNAMA as the E3

The pure and correctly folded recombinant SNAMA protein was used as the ubiquitin ligase (E3) in an ubiquitin conjugation assay to ascertain whether the protein has ubiquitin ligase activity. Initially the assay was performed with a set of various ubiquitin conjugation enzymes (E2s) to determine which of the E2s would function best with SNAMA as an E3. The key components of the ubiquitination process were then examined by performing conjugation assays in the absence of an E1, E2, E3, ubiquitin, $ZnCl_2$, and ATP.

4.6.1 Specificity of SNAMA E3 activity to various E2s

SNAMA ubiquitin ligase activity was initially determined using refolded GST-S as the E3 and 8 different E2s in an ubiquitin conjugation assay (Figure 20). Recombinant SNAMA (E3) is visible as an approximately 70 kDa protein, with a ~ 23 kDa protein contaminant also visible in the sample. The various E2s that were used are marked with an asterisk while the ubiquitin activating enzyme (E1) is visible as an approximately 140 kDa protein. Ubiquitin is visible at approximately 35 kDa with a slightly smaller peptide of ~ 25 kDa also visible in the sample.

The ubiquitin conjugation assays led to the ubiquitination of the SNAMA protein itself through a process known as autoubiquitination. This was evident by the formation of “smears” in the SDS-PAGE gel that indicate various degrees of poly-ubiquitinated SNAMA protein (Figure 20). The smears depicting ubiquitinated protein began at 100 kDa and increased in size according to the degree of poly-ubiqutination. Majority of ubiquitinated protein appeared to be greater than 170 kDa in size, illustrated by intense smears in the gel representing a number of different sized proteins (Figure 20). This was expected as SNAMA alone was 70 kDa in size while the ubiquitin molecules, which were fused to GST, were each approximately 30 kDa in size. Thus, a poly-ubiqutinated SNAMA protein tagged with only 3 or 4 ubiquitin molecules would already

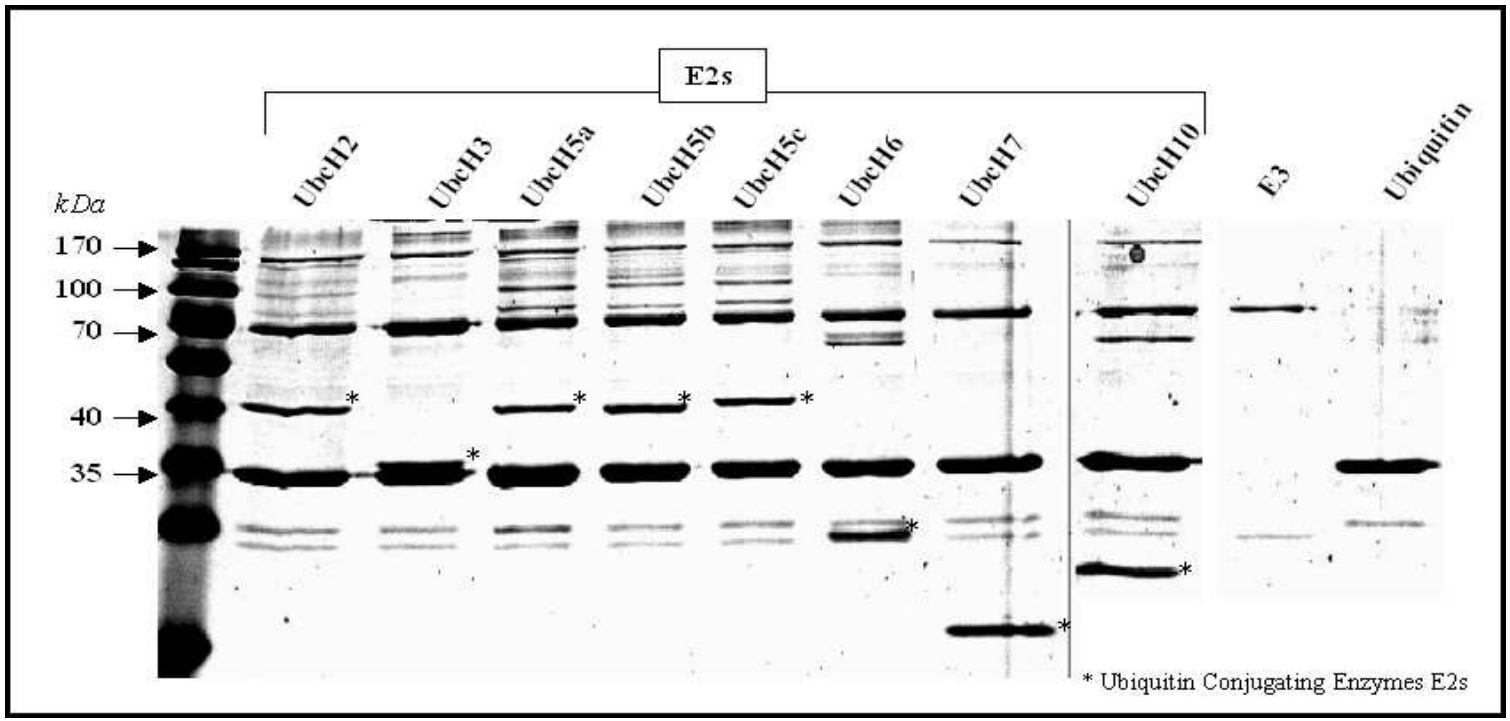


Figure 20. The test for ubiquitin ligase activity of SNAMA, and its specificity towards various E2s. Ubiquitin conjugation assays were performed using recombinant SNAMA as the E3 (~ 70 kDa) with 8 different E2s (marked with an asterisk). Ubiquitin and E1 are visible as approximately 35 kDa and 140 kDa peptides respectively. “Smears” representing multiple polypeptides as a result of polyubiquitination are seen getting larger from approximately 100 kDa. SNAMA catalyses the ubiquitination of itself (autoubiquitination), illustrated by majority of the polypeptides being larger than 170 kDa in size. Ubiquitination occurs optimally with UbcH5 E2s, in particular UbcH5a.

have molecular weights of 160 kDa and 190 kDa respectively. It is therefore easy to see that there would be many poly-ubiquitinated SNAMA protein larger than 170 kDa in size as was represented by the smear.

Recombinant SNAMA E3 had activity in the presence of a number of E2s, which include UbcH2, UbcH3, UbcH5 and UbcH6. However, SNAMA E3 had the greatest specificity for the UbcH5 family of E2s, in particular UbcH5a (Figure 20). This was evident through the appearance that the greatest amount of poly-ubiquitination occurs in the presence of the E2 UbcH5a. The formation of E2-ubiqutin complexes was observed during conjugation assays as is evident by 57 kDa, 60 kDa, 70 kDa, and 75 kDa polypeptides that represent the UbcH10-Ub, UbcH6-Ub, UbcH3-Ub, and UbcH5-Ub complexes respectively. This was not surprising as ubiquitin is known to bind E2 prior to transfer of the ubiquitin moiety onto the target protein during the ubiquitin conjugation reaction (Figure 9).

4.6.2 Key components involved in SNAMA E3 ubiquitination

Ubiquitin is capable of forming poly-ubiquitin chains of 2 to 3 molecules, 70 kDa and ~ 100 kDa in size respectively, in the presence of E1 and E2 and in the absence of the E3 (SNAMA) (Figure 21). The 75 kDa peptide in this sample represents the UbcH5a-Ub complex as described earlier. However, reaction mixtures in which E3 was present show far more prominent bands as well as the presence of additional polypeptides, particularly the bigger polypeptides greater than 170 kDa (Figure 22). This indicates unequivocally that SNAMA E3 is essential for ubiquitination and catalyses self-ubiquitination.

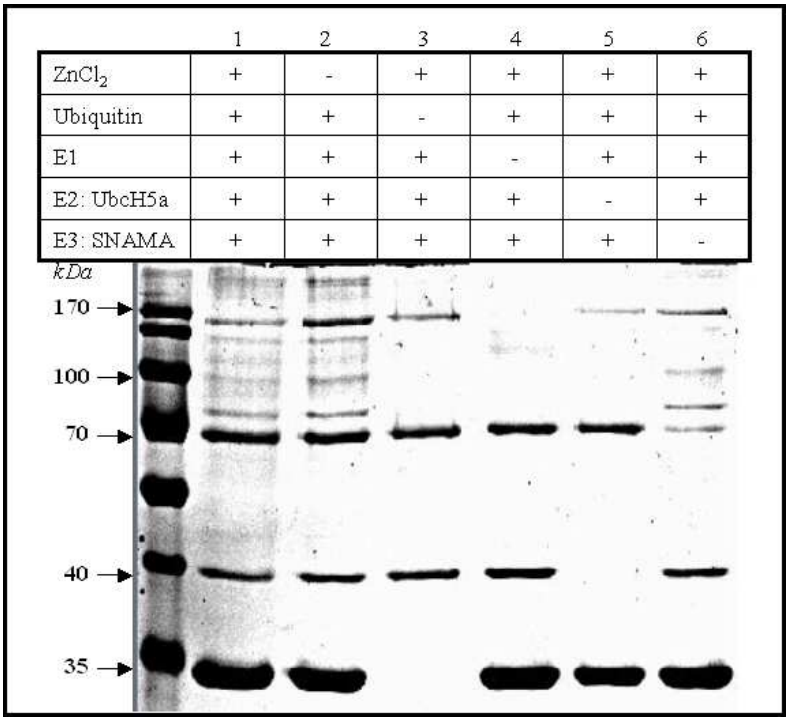


Figure 21. The dependence of SNAMA E3 activity on key ubiquitination factors. Ubiquitin conjugation assays using SNAMA E3 were performed in the absence of each of the key players involved in ubiquitination including E1, E2, ubiquitin, or zinc ions. Ubiquitination does not occur in the absence of ubiquitin, E1 or E2 (lanes 3, 4 and 5 respectively). However, ubiquitination takes place in the absence of zinc ions (lane 2). Poly-ubiquitin chains of 2 to 3 molecules and the Ubc5a-Ub complex still form in the absence of the E3 (SNAMA) as is indicated by the three additional peptides of approximately 70 kDa, 75 kDa, and 100 kDa (lane 6).

The dependence of SNAMA E3 activity on key factors involved in the ubiquitination process (E1, E2, ubiquitin, ZnCl2, ATP) was examined by performing conjugation assays in the absence of each of these factors (Figure 21 and 22). E1, E2 and ubiquitin are crucial for ubiquitination to occur as is indicated by no ubiquitination occurring at all in their absence (Figure 21). However, a polypeptide of approximately 110 kDa does arise in the absence of the ubiquitin activating enzyme (E1). This polypetide probably represents the interaction between E3 SNAMA (70 kDa) and the E2 (40 kDa) to form a E3-E2 complex and further confirms the specificity of SNAMA E3 for the E2 UbcH5a. ATP is

essential for ubiquitination as no ubiquitination occurs in its absence (Figure 22). Furthermore, the formation of the E3-E2 complex is dependent on ATP as no E3-E2 complex formed in the absence of ATP. This is not surprising as ATP is required for the activation of ubiquitin by E1..

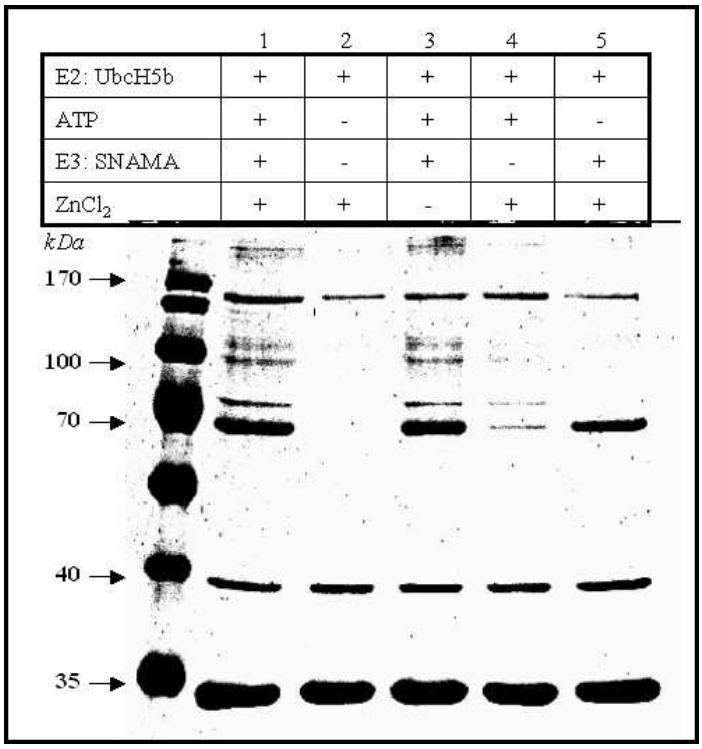


Figure 22. The effect of ATP on SNAMA E3 activity. Ubiquitin conjugation assays using SNAMA E3 in the presence of ATP results in ubiquitination as is evident by the additional polypeptides present as a "smear" in the sample (lanes 1 and 3). Reaction mixtures without ATP showed no sign of ubiquitination at all as there were no additional polypeptides when the sample was separated (lanes 1 and 5). Ubiquitin and the E1 were present in all the reaction mixtures when testing for the dependence of SNAMA activity on ATP.

Surprisingly, SNAMA E3 mediated ubiquitination is not dependent on zinc ions for its activity as polyubiquitination occurs in the absence of $ZnCl_2$ (Figure 21). In fact, ubiquitination appears more prominent when zinc is absent than when it is present reaction mixture.

5. DISCUSSION

Evidence suggests that SNAMA plays a role in *Drosophila* development and in apoptosis, probably as a suppressor of apoptosis or negative regulator of an activator of apoptosis (Mather et al., 2005; Jones et al., 2006). Recently, *SNAMA* was characterized by Jones and his colleagues, who named the gene *mini-me* (*mnm*) (Jones et al., 2006). They identified *SNAMA/mnm* as a dominant modifier of *hedgehog* loss-of-function. Furthermore, they go on to show that *SNAMA/mnm* is required for normal cell proliferation and for cell survival anterior to the furrow of the *Drosophila* eye, but not posterior to it. Thus, their findings go hand-in-hand with our hypothesis that SNAMA/mnm is involved in cell proliferation as a negative regulator of apoptosis.

Preliminary studies have shown that SNAMA probably interacts with Dmp53 and is involved in apoptosis via the Dmp53 pathway (Mather thesis, 2005). Further preliminary studies illustrated that the interaction between Dmp53 and SNAMA occurs through the DWNN domain within the DCM (Rakgotho, thesis, 2007). Groundwork has also shown that increased levels of SNAMA mRNA and protein probably result in decreased levels of Dmp53 and vice versa (Hull, personal communication). Thus, SNAMA appears to regulate apoptosis through the negative regulation of the pro-apoptotic protein, Dmp53. This is consistent with other members of the RbBP6 family of proteins, which are involved in tumorigenesis through the negative regulation of p53 and Rb (Li et al., 2007).

Transcriptional regulation of *SNAMA* was examined through analysis of the core promoter elements surrounding the transcription start site of the gene (Ntwasa and Antunes, in preparation). This was achieved by 5´ RACE, which allowed for analysis of the 5´ region of the gene by ensuring the amplification of capped transcripts.

Further elucidation of the functional role of SNAMA was determined by confirming whether it exhibits ubiquitin ligase activity. SNAMA contains an ubiquitin-like DWNN domain followed closely by a RFL motif within its DCM at its N-terminus (Mather et al., 2005). The RING finger conformation is responsible for supplying RING finger E3s and U-box E4s with their activity, as they play an essential role in conjugation of ubiquitin to target proteins (Joazeiro and Weissman, 2000; Aravind and Koonin, 2000). The notion that the RFL motif would supply SNAMA with ubiquitin ligase activity was tested by ubiquitin conjugation assays using pure and active recombinant SNAMA as the E3. Furthermore, the dependence of SNAMA E3 activity on key components of the ubiquitination process was determined.

5.1 A Single TATA-less Promoter Regulates Expression of *SNAMA*

The transcription start site of *SNAMA* was initially predicted to be approximately 2.2 kb from the translation start site, which would have given rise to mRNA of approximately 4.6 kb (Mather et al., 2005). Determination of the transcriptional start site by 5´ RACE implies that the *SNAMA* transcript would be approximately 3.9 kb in size. This finding was supported by Jones and his colleagues who identified the expression of 3.9 kb transcript throughout development in *Drosophila* (Jones et al., 2006). Thus, the *SNAMA* transcript has a 5´ UTR of 81 nucleotides, interrupted by a large first intron of 0.84 kb, and giving rise to an mRNA sequence of approximately 3.9 kb.

Determining the transcription start site of a gene makes it possible to identify regulatory regions of that gene and ultimately the promoter region. We show that there is a single site of transcription initiation for the *SNAMA* gene (Figure 12; Appendix I). A sequence extending 1000 bases upstream and 70 bases downstream from the transcription start site was used to search for potential

transcription factor binding sites and core promoter elements (Ntwasa and Antunes, in preparation).

No plausible TATA box was identified in the expected region 23-33 bp upstream of the transcription start site, however, it is known that less than 40% of *Drosophila* promoters do not contain a recognizable TATA box (Gershenzon et al., 2006). Furthermore, the sequence at the transcription start site (GCATC) matches the published initiator element (Inr) consensus sequence, which is present in approximately 65% of *Drosophila* promoters (Gershenzon et al., 2006). There is also a good sequence match (GTCG) with the downstream promoter element (DPE) consensus sequence, 32 residues downstream from the transcription start site (Appendix I).

In order for transcription initiation to occur in *Drosophila* the general transcription factor TFIID must first bind the promoter, thereby creating a platform for the assembly of additional components of the initiation complex. TFIID requires one of three elements or combination of them in order for this to occur, namely the TATA box, Inr and the DPE. Thus, *SNAMA* has a TATA-less promoter region containing a combination of the core elements Inr-DPE that is needed for the binding of the transcription initiation factor TFIID.

This work shows that *SNAMA* is regulated by a single TATA-less promoter that gives rise to a transcript of approximately 3.9 kb. However, an additional transcript of *SNAMA*, approximately 1.8 kb in size, has also been identified in *Drosophila* during devlopment (Jones et al., 2006). The size of this additional transcript seems to indicate the independent expression of the DWNN domain, much like its mammalian RbBP6 counterpart. However, further experimental evidence is needed in order to confirm this hypothesis.

5.2 SNAMA Exhibits Ubiquitin Ligase Activity

The release of sequence data, particularly from a number of medically and biotechnologically important genomes such as that of *Drosophila*, is increasing in an exponential fashion. In light of this, elucidating the structure and function of proteins in these organisms is important. Determining whether the DCM of SNAMA portrayed ubiquitin ligase activity was extensive and complex. It involved a number of consecutive processes that ultimately led to a pure and active form of the SNAMA protein that could be used as the ubiquitin ligase in an ubiquitin conjugation assay.

5.2.1 SNAMA has E3 activity capable of auto-ubiquitination

The DCM of SNAMA exhibits ubiquitin ligase activity that is capabe of self-ubiquitination (Figure 20). Auto-ubiquitination of SNAMA during the ubiquitin conjugation assays is most likely due to the ubiquitin-like DWNN domain within the DCM. This domain probably serves as the substrate for the covalent attachment of ubiquitin molecules by the RFL motif of SNAMA. This attachment most likely occurs at the conserved K^{29} residue and not the more common K^{48} residue as this conserved lysine is absent in the DWNN domain. The choice of the lysine residue used to form the ubiquitin chain influences the fate of the ubiquitinated protein (Stone et al., 2005). The fate of K^{48} and K^{29} poly-ubiquitinated proteins is degradation by the 26S proteasome (Pugh et al., 2006), whereas protein modification with a poly-ubiquitin K^{63} chain has been implicated in protein activation (Deng et al., 2000). It is possible that SNAMA utilizes different lysine residues on ubiquitin for poly-ubiquitination in comparison to characteristic RING finger E3s. Further investigation is needed to determine the exact lysine residue that is used during ubiquitination.

5.2.2 SNAMA demonstrates optimal activity with UbcH5a

The presence or absence of polypeptides in the gel at sizes greater than 100 kDa indicates whether poly-ubiquitination has occurred or not occurred respectively (Figure 20). Using this information it can be noted that SNAMA has ubiquitin ligase activity in the presence of a number of E2s that include UbcH2, UbcH3, UbcH5 and UbcH6. However, SNAMA has no activity in the presence of the E2s UbcH7 and UbcH10. Furthermore, it appears as though the activity of SNAMA is greatest when using the UbcH5a conjugating enzyme due to the greater intensity of the bands, thus confirming that SNAMA has greatest specificity for UbcH5a. RING finger ubiquitin ligases bind specifically to an E2 in addition to a target protein in order to promote ubiquitination of the target protein. SNAMA probably binds UbcH5a and forms an E3-E2 complex through contacts between a groove in the RING domain and the two loops in the E2 fold (Zhou and Howley, 1998). The function of SNAMA ubiquitin ligase activity is therefore dependent on its RING finger-like motif within the DCM that forms a RING finger structure.

5.2.3 SNAMA is a classical RING fingerE3

SNAMA mediated ubiquitination occurs in the presence and absence of zinc ions. Typical RING fingers are known for their dependence on divalent metal ions, such as zinc, in order to exhibit their ligase activity (Freemont, 1993) whilst U-box E4s are capable of ubiquitination in the absence of divalent ions (Hatakeyama et al., 2001). The reason for this can be attributed to the way in which each ligase stabilizes its RING finger conformation, which is dependent on the sequence composition of their domains. Characteristic RING finger E3s rely on conserved cysteine and histidine residues, that co-ordinate two zinc ions to maintain their RING finger conformation (Borden, 2000; Saurin et al., 1996). In contrast, U-box E4s stabilize their RING finger fold through hydrogen bonds, salt-bridges and conserved hydrophobic residues within its consensus.

The fact that SNAMA has ubiquitin ligase activity in the absence of zinc ions seems to indicate that the RFL motif still forms a RING finger structure in the absence of zinc ions. It is easy to assume that SNAMA is a U-box E4 due to it having activity in the absence of zinc ions. However, closer investigation shows that the primary structure of the RFL motif resembles that of a RING finger domain and not a U-box domain. Multiple sequence alignments between the SNAMA RFL motif and the RFL motifs of other RbBP6 proteins show that they all have a consensus sequence like that of the "classical" RING finger domain (Figure 23). This is evident by the presence of highly conserved cysteine residues in the correct positions within their sequences. In contrast, the characteristic U-box domain from Ufd2 showed no significant homology to either the SNAMA RFL motif or other RbBP6 family proteins.

SNAMA can be defined as a RING finger-like protein that functions as a chracteristic RING finger E3 and not a U-box E4. There is no experimental evidence to demonstrate exactly how the RING finger conformation of the RFL motif is being stabilized. However, the RING finger fold is probably maintained by salt-bridges, hydrogen-bonds and disulphide bonds between cysteine residues, that form during refolding of denatured recombinant SNAMA into its native state. To assume that SNAMA is a U-box protein would be bold, especially with no experimental evidence of how the RING conformation is stabilized. Further research of the crystal structure of the DCM of SNAMA would confirm the characterization of SNAMA as a RING finger E3.

This work represents the first evidence of a member of the RbBP6 family of proteins having ubiquitin ligase activity. It has been suggested on a number of occasions, by various groups, that RbBP6 proteins would exhibit ubiquitin ligase activity due to the presence of a RING finger-like motif in the DCM of these proteins. Li and his colleagues showed that the mouse RbBP6 protein (PACT) interacts with Hdm2 and enhances Hdm2-mediated ubiquitination and degradation of p53 as a result of an increase in p53-Hdm2 affinity (Li et al.,

2007). However, no group has shown that a member of the RbBP6 protein family has ubiquitin ligase activity on its own until now, where it is shown that SNAMA is capable of ubiquitination. SNAMA is also one of very few proteins that contains a RFL motif capable of exhibiting ubiquitin ligase activity. Furthermore, SNAMA is the first protein to exhibit "classical" RING finger ligase activity *in vitro*, in the absence of zinc ions.

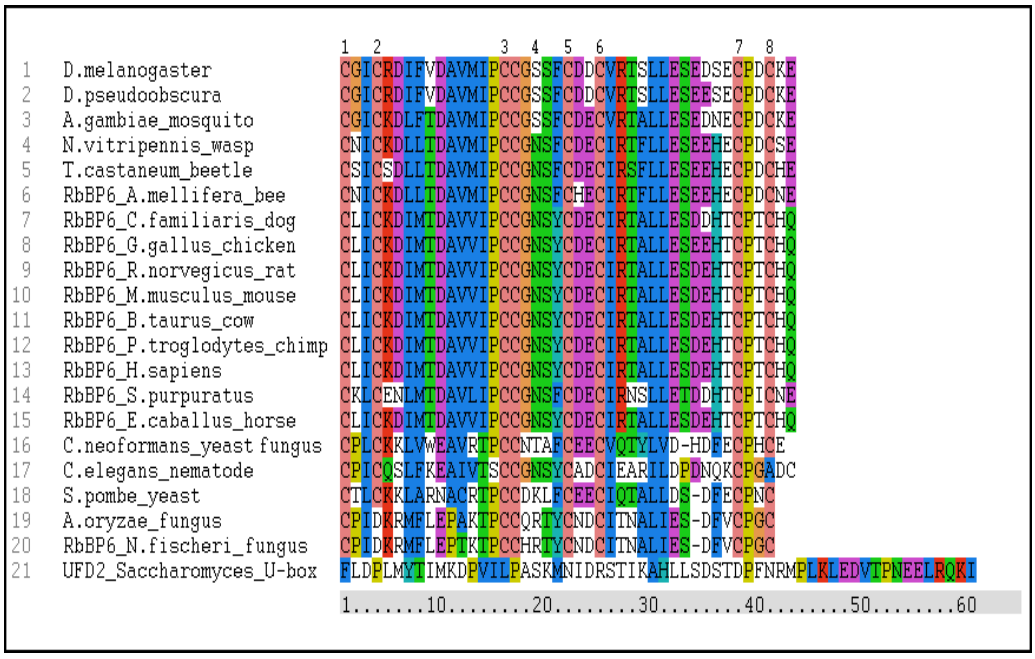


Figure 23. Multiple alignment of RING finger motifs from the RbBP6 superfamily. Orthologues of the SNAMA RFL motif were generated from the BlastP bioinformatic tool followed by alignment of the sequences using ClustalX. The conserved cysteine residues involved in the formation of the cross-brace structure of the RING finger are numbered at the top of the sequences. The conserved histidine in the fourth ligand has been substituted in all the RFL motifs of the RbBP6 family of protein. The classical U-box protein, Ufd2, was also included in the alignment.

SNAMA is involved in regulatory pathways that affect apoptosis and cell proliferation. A number of preliminary studies also show a definite association between SNAMA and Dmp53, much like other members of the RbBP6

superfamily. Furthermore, SNAMA functions as a target-specific RING finger E3 capable of ubiquitination. Ubiquitination is pivotal for the modification of proteins that are involved in a wide variety cellular process, thereby maintaining the homeostasis within the cell. Thus, SNAMA represents a desirable target for drug therapy and pharmaceutical intervention due to its high specificity and ubiquitination of target proteins that are involved in important cell signalling pathways, that include apoptosis.

5.3 Conclusion

- The *SNAMA* gene is regulated by a single TATA-less promoter that gives rise to a single characterized transcript of approximately 3.9 kb.

- SNAMA is a characteristic RING finger ubiquitin ligase that it is capable of auto-ubiquitination, particularly in the presence of UbcH5a.

- SNAMA is the first identified RING finger E3 that is capable of ubiquitination in the absence of zinc ions *in vitro*.

- This work represents the first evidence of a member of the RbBP6 family of proteins having ubiquitin ligase activity and shows that SNAMA is one of few proteins to exhibit ubiquitin ligase activity having a RFL motif.

- SNAMA is an important target for drug therapy and pharmaceutical intervention.

5.4 Future Work

The first objective would be to generate a pure and active recombinant Dmp53 protein that could be used as a substrate during the ubiquitin conjugation reaction.

Dmp53 has already been shown to bind SNAMA *in vivo* and increased levels of SNAMA results in decreased levels of Dmp53 and vice versa. Therefore, determining whether SNAMA catalyzes the ubiquitination of Dmp53 would increase the understanding of programmed cell death in *Drosophila* through Dmp53. Furthermore, Dmp53 ubiquitination by SNAMA would confirm an interaction between the two proteins and the involvement of SNAMA in programmed cell death through Dmp53 regulation.

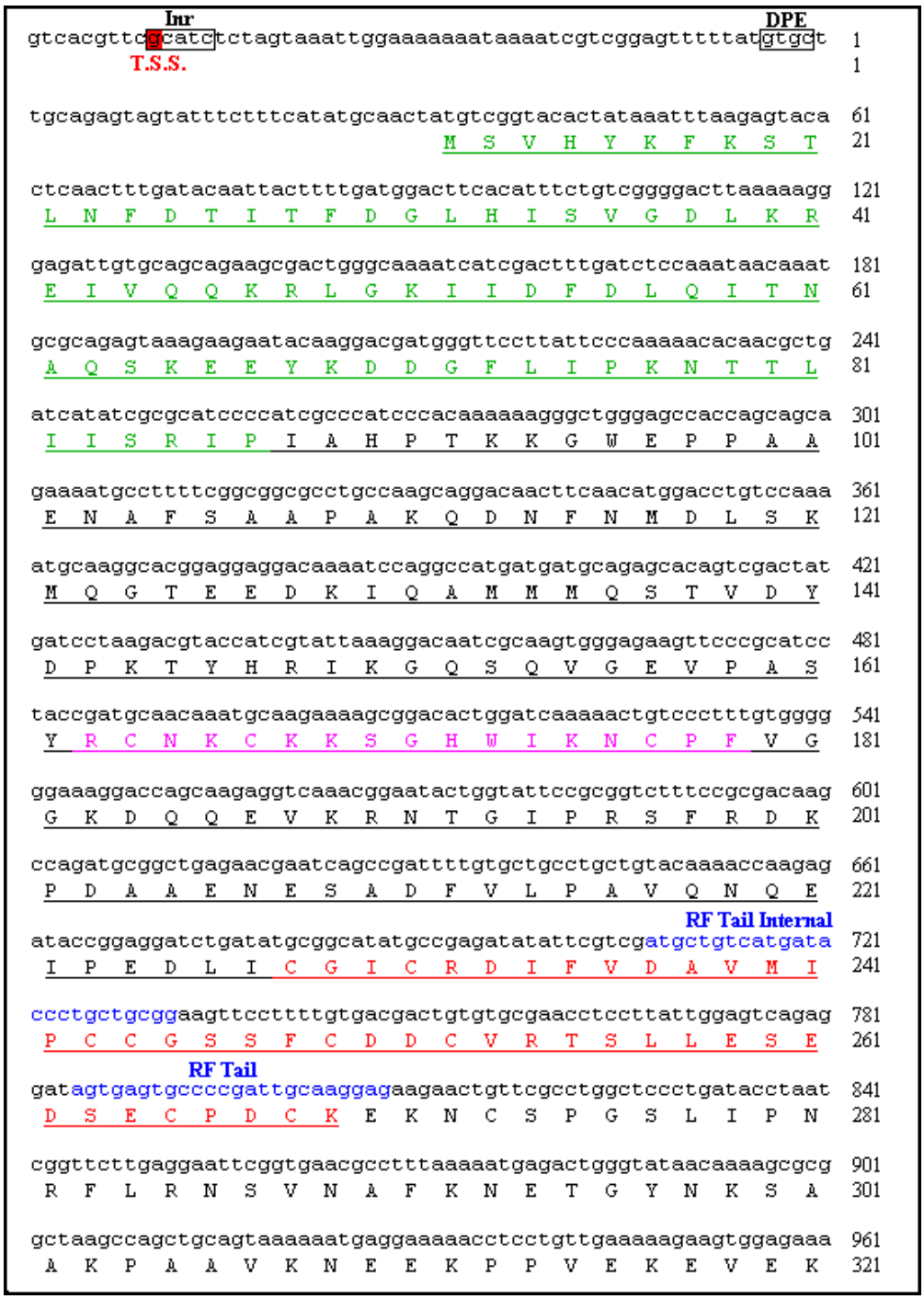
The determination of the lysine residues utilized during auto-ubquitination of SNAMA and formation of poly-ubiquitin chains would be useful in providing insight into the fate of proteins that are ubquitinated by SNAMA. This could be determined by mutational analysis of lysine residues in the DWNN domain of SNAMA, or lysine residues in the ubiquitin molecules that are used during the ubiquitination process. Alternatively, the crystal structure of the auto-ubiquitinated SNAMA would illustrate the lysine residues that are being utilized during ubiquitination.

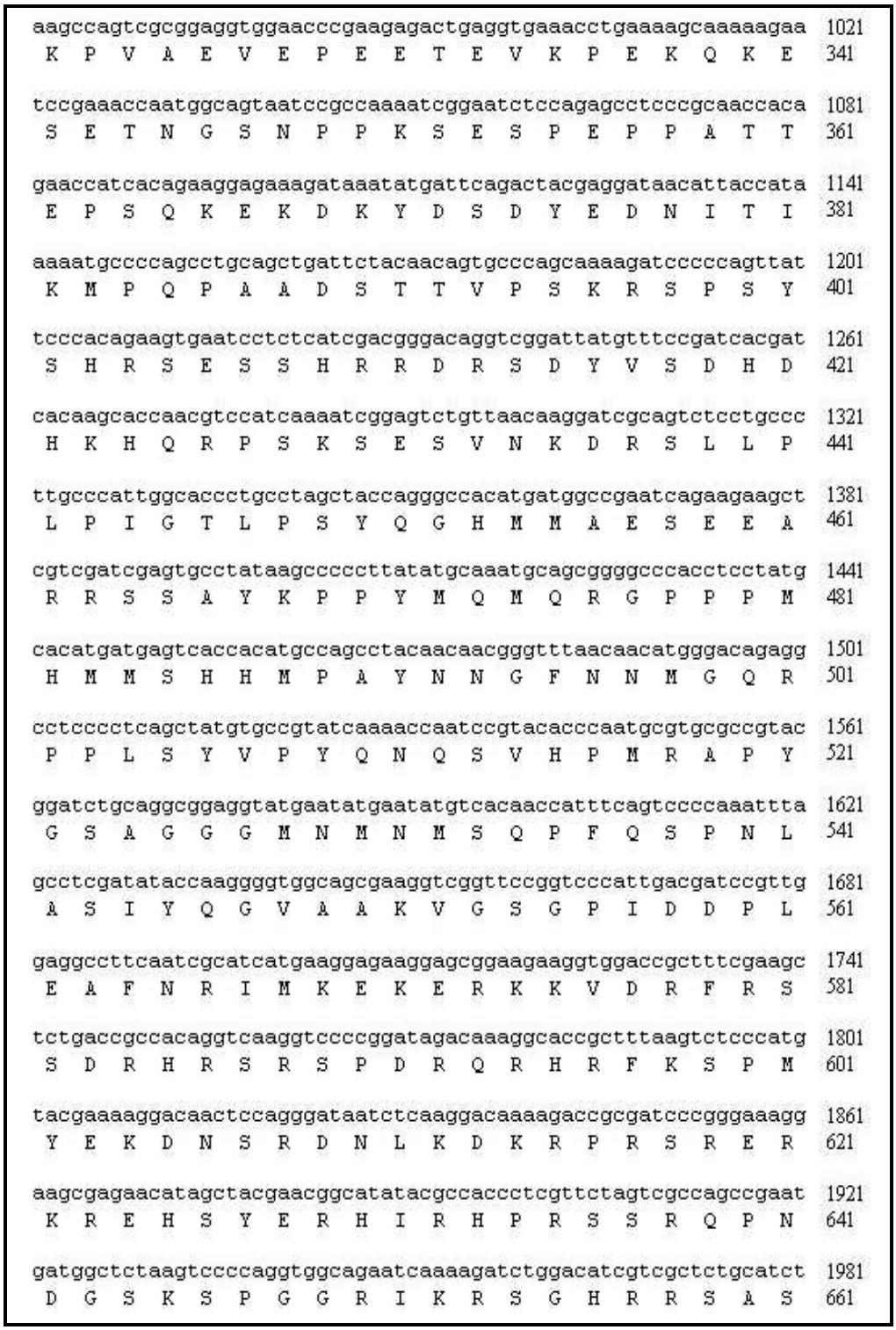
Examining the way in which the RING finger conformation of the RFL motif is stabilized could be another important investigation. This would support the fact that SNAMA functions as a RING finger E3 and not a U-box E4. This would most easily be achieved by examining the crystal structure of the DCM of SNAMA. However, it would be possible to examine how the RFL motif is stabilized through mutational analysis of important residues (such as the conserved cysteines) in the RFL of the DCM.

6. APPENDIX

6.1 Appendix I

The SNAMA Protein and cDNA Sequence (NCBI, Locus no. NM_138040)




aagccagtcgcggaggtggaacccgaagagactgaggtgaaacctgaaaagcaaaaagaa 1021
K P V A E V E P E E T E V K P E K Q K E 341
tccgaaaccaatggcagtaatccgccaaaatcggaatctccagagcctcccgcaaccaca 1081
S E T N G S N P P K S E S P E P P A T T 361
gaaccatcacagaaggagaaagataaatatgattcagactacgaggataacattaccata 1141
E P S Q K E K D K Y D S D Y E D N I T I 381
aaaatgccccagcctgcagctgattctacaacagtgcccagcaaaagatcccccagttat 1201
K M P Q P A A D S T T V P S K R S P S Y 401
tcccacagaagtgaatcctctcatcgacgggacaggtcggattatgtttccgatcacgat 1261
S H R S E S S H R R D R S D Y V S D H D 421
cacaagcaccaacgtccatcaaaatcggagtctgttaacaaggatcgcagtctcctgccc 1321
H K H Q R P S K S E S V N K D R S L L P 441
ttgcccattggcaccctgcctagctaccagggccacatgatggccgaatcagaagaagct 1381
L P I G T L P S Y Q G H M M A E S E E A 461
cgtcgatcgagtgcctataagccccttatatgcaaatgcagcggggcccacctcctatg 1441
R R S S A Y K P P Y M Q M Q R G P P P M 481
cacatgatgagtcaccacatgccagcctacaacaacgggtttaacaacatgggacagagg 1501
H M M S H H M P A Y N N G F N N M G Q R 501
cctcccctcagctatgtgccgtatcaaaaccaatccgtacacccaatgcgtgcgccgtac 1561
P P L S Y V P Y Q N Q S V H P M R A P Y 521
ggatctgcaggcggaggtatgaatatgaatatgtcacaaccatttcagtccccaaattta 1621
G S A G G G M N M N M S Q P F Q S P N L 541
gcctcgatataccaaggggtggcagcgaaggtcggttccggtcccattgacgatccgttg 1681
A S I Y Q G V A A K V G S G P I D D P L 561
gaggccttcaatcgcatcatgaaggagaaggagcggaagaaggtggaccgctttcgaagc 1741
E A F N R I M K E K E R K K V D R F R S 581
tctgaccgccacaggtcaaggtccccggatagacaaaggcaccgctttaagtctcccatg 1801
S D R H R S R S P D R Q R H R F K S P M 601
tacgaaaaggacaactccagggataatctcaaggacaaaagaccgcgatcccgggaaagg 1861
Y E K D N S R D N L K D K R P R S R E R 621
aagcgagaacatagctacgaacggcatatacgccaccctcgttctagtcgccagccgaat 1921
K R E H S Y E R H I R H P R S S R Q P N 641
gatggctctaagtccccaggtggcagaatcaaaagatctggacatcgtcgctctgcatct 1981
D G S K S P G G R I K R S G H R R S A S 661

```
ccaaagccgggctacaagagtgattacagagacaagccgtacaacaagcctagtgctccc 2041
 P  K  P  G  Y  K  S  D  Y  R  D  K  P  Y  N  K  P  S  A  P  681

aaaacggaggcagttgagcctcctccccccggattcgagccgttgcagctgacggatgaa 2101
 K  T  E  A  V  E  P  P  P  P  G  F  E  P  L  Q  L  T  D  E  701

gacggctacaggaacaagcacccgaccagttcggaagcatcacaaagcagcaagggtgat 2161
 D  G  Y  R  N  K  H  P  T  S  S  E  A  S  Q  S  S  K  G  D  721

agcagcaagaagagaggggaaaacaggcacgaagaggcgccacgaaagaggcacaggtct 2221
 S  S  K  K  R  G  E  N  R  H  E  E  A  P  R  K  R  H  R  S  741

cgcagcattagcaaggaaccgaagccgaatgacagcaactacaggagcctgactccacca 2281
 R  S  I  S  K  E  P  K  P  N  D  S  N  Y  R  S  L  T  P  P  761

gcaaagatcaccacaccgaaaatgactgctgcccagttgaggcaacgcgaaagttcaccg 2341
 A  K  I  T  T  P  K  M  T  A  A  Q  L  R  Q  R  E  S  S  P  781

aagacgccggaaaagagtcacgacgattatctgaccgcgaaggccagaattatggcctcc 2401
 K  T  P  E  K  S  H  D  D  Y  L  T  A  K  A  R  I  M  A  S  801

cagcccgtcatcaacgacacggaaatggagaccaatgtgggcaaggagaacaaggccaag 2461
 Q  P  V  I  N  D  T  E  M  E  T  N  V  G  K  E  N  K  A  K  821

agtccgttgtcaaaagatcgcaagaagaagaagaaggacaaggacaaggctgagcgcaag 2521
 S  P  L  S  K  D  R  K  K  K  K  K  D  K  D  K  A  E  R  K  841

aaaaacaagaaggacaagcgcgctaagaaggagaaaggggatcgccagaagaagagctcc 2581
 K  N  K  K  D  K  R  A  K  K  E  K  G  D  R  Q  K  K  S  S  861

tcagttaatcgatctgactcggatattaacaacagctcactaatgaacgagtcaaattat 2641
 S  V  N  R  S  D  S  D  I  N  N  S  S  L  M  N  E  S  N  Y  881

aaagtattgtctcccagggctcaaagtcccagcattgagatcaatgcggctcaactttcc 2701
 K  V  L  S  P  R  A  Q  S  P  S  I  E  I  N  A  A  Q  L  S  901

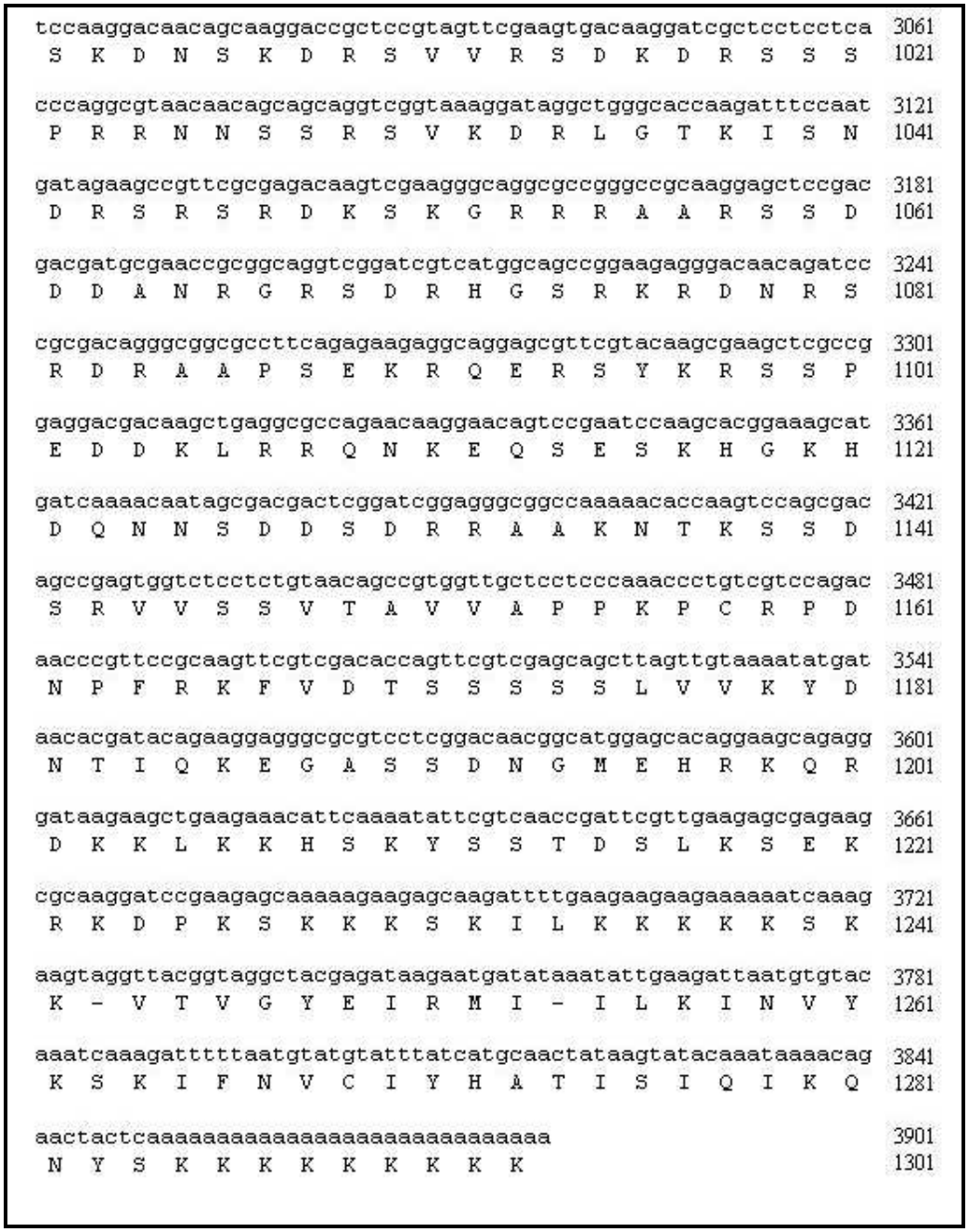
cctactcacaacgctactgaaaacgttaatccgaagagtcattccatccttactgtgggt 2761
 P  T  H  N  A  T  E  N  V  N  P  K  S  H  S  I  L  T  V  G  921

gctgctagcgacgataatcttggcccaagaagcaaactcagcgaggctaattctgtcaat 2821
 A  A  S  D  D  N  L  G  P  R  S  K  L  S  E  A  N  S  V  N  941

ctatccaaatgggaaatcgacgagaatatcttaggtttggaggattcctccaaaaaagct 2881
 L  S  K  W  E  I  D  E  N  I  L  G  L  E  D  S  S  K  K  A  961

gccggggcctccgacgatccgtcggaaataacttcagacgtcctgcgaaaggctgagaac 2941
 A  G  A  S  D  D  P  S  E  I  T  S  D  V  L  R  K  A  E  N  981

gcaatatttgcaaaggctattaatgccatcaggcctatggagtttcaagttattatcaat 3001
 A  I  F  A  K  A  I  N  A  I  R  P  M  E  F  Q  V  I  I  N 1001
```

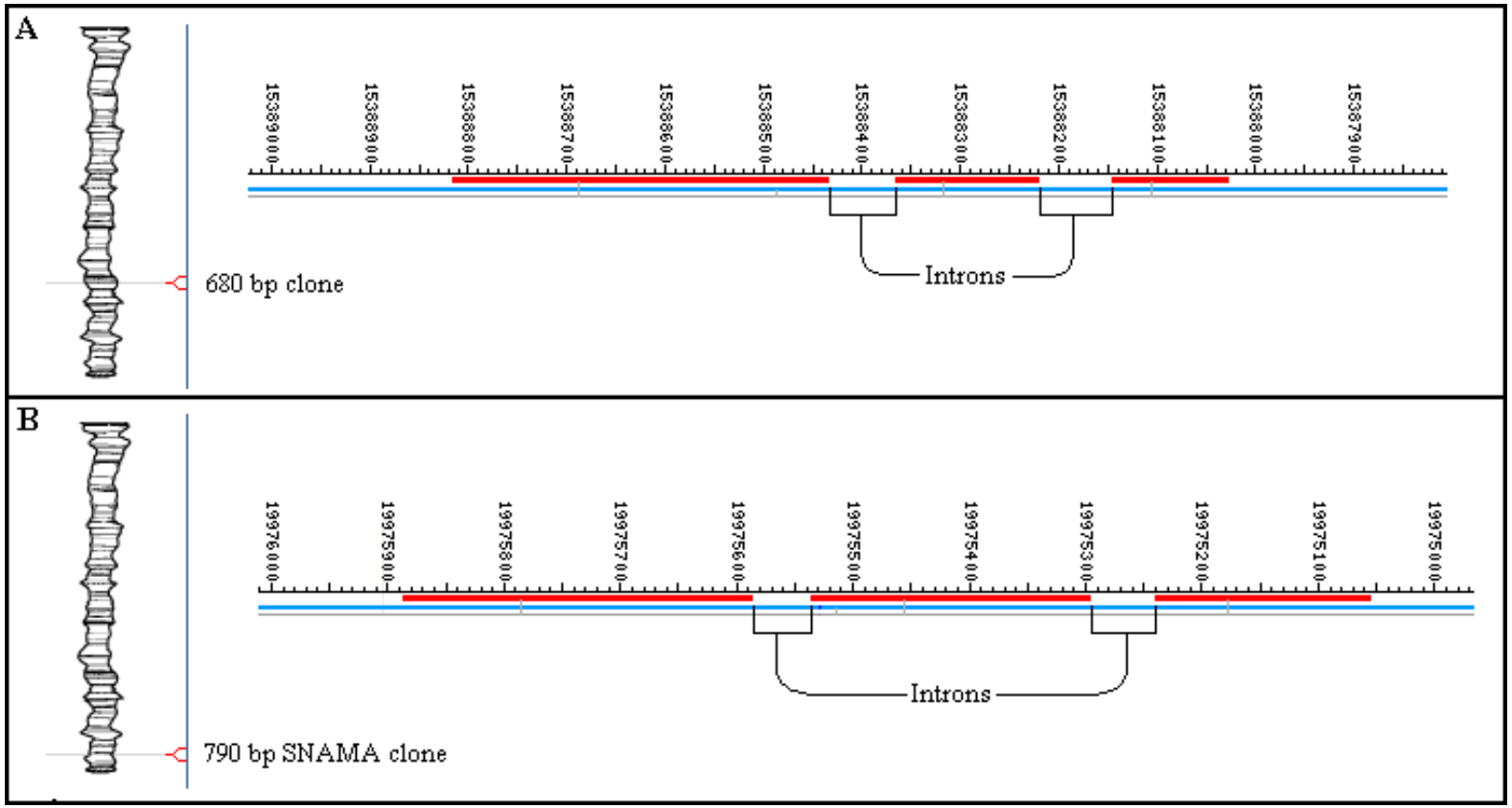


KEY

Blue:	Reverse primers used for 5´ RACE and sequencing
Underlined:	DWNN Catalytic Module (DCM) of SNAMA
Green:	DWNN domain
Purple:	Zinc finger motif
Red:	RING finger-like motif
Red Block:	Transcriptional start site (T.S.S.)
Inr & DPE:	Initiator and Downstream Promoter Element

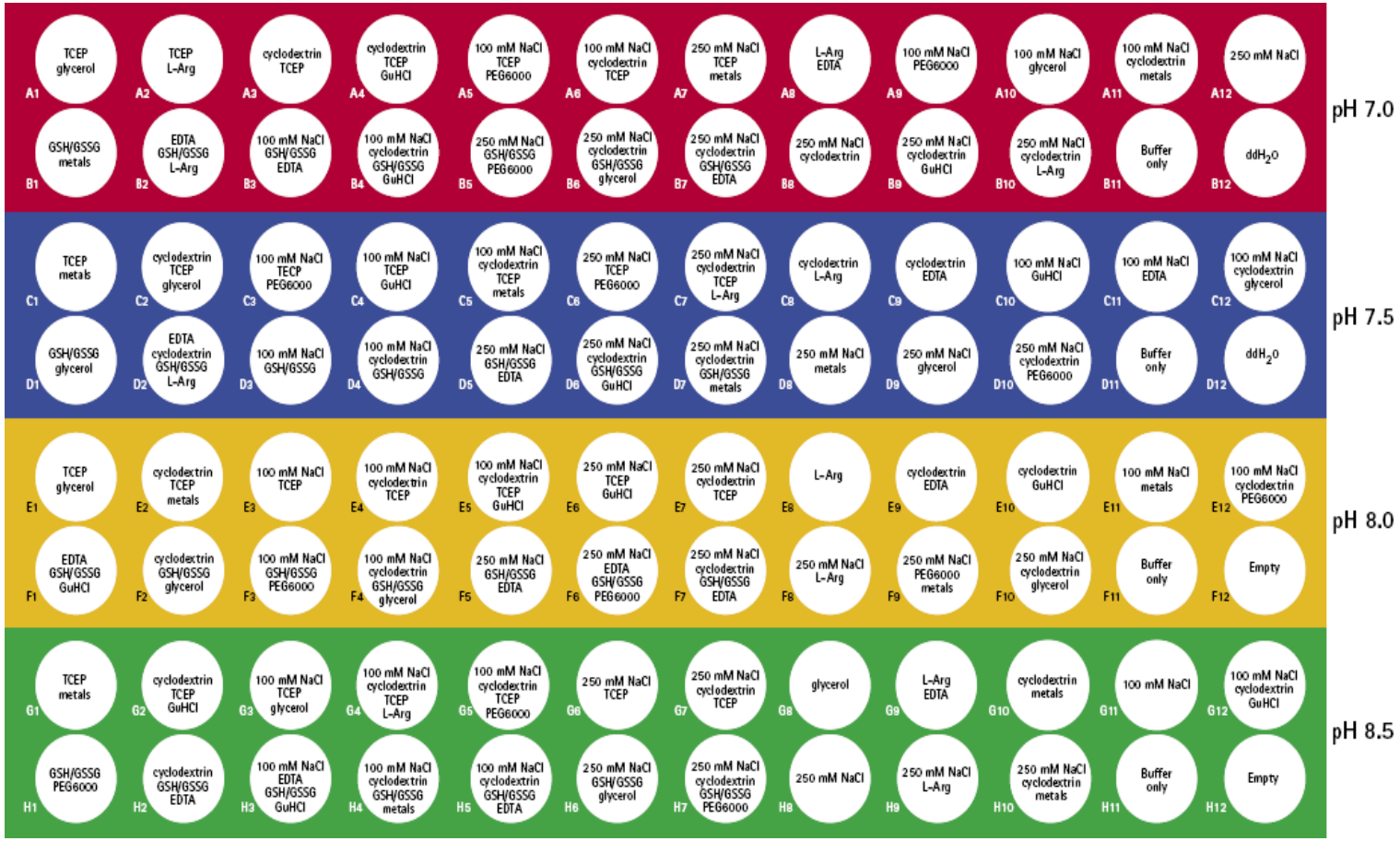
6.2 Appendix II

Chromosome Map of the 5´ RACE Products



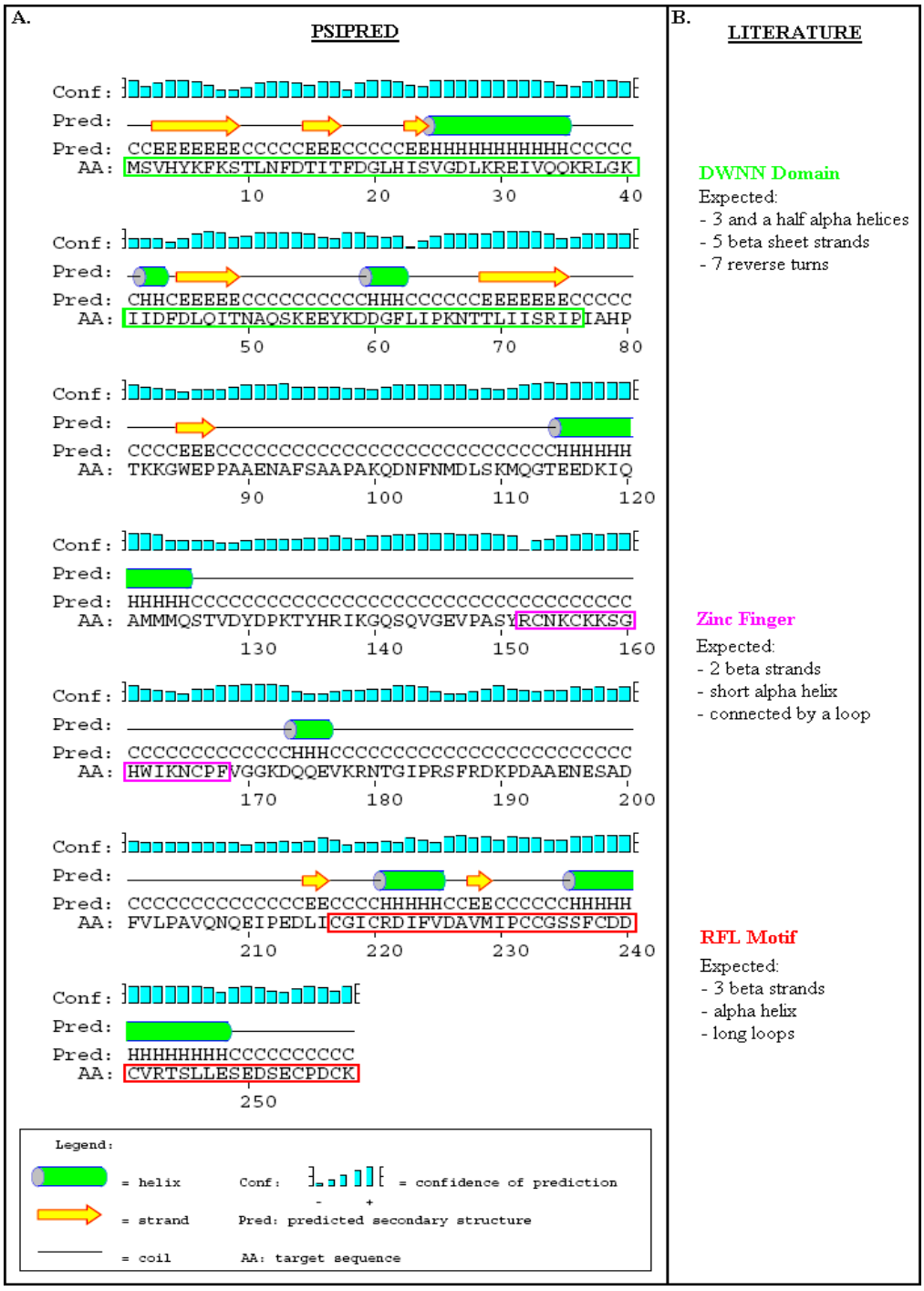
6.3 Appendix III

iFOLD™ Protein Refolding System Plate Layout



6.4 Appendix IV

Secondary structure prediction for SNAMA DCM

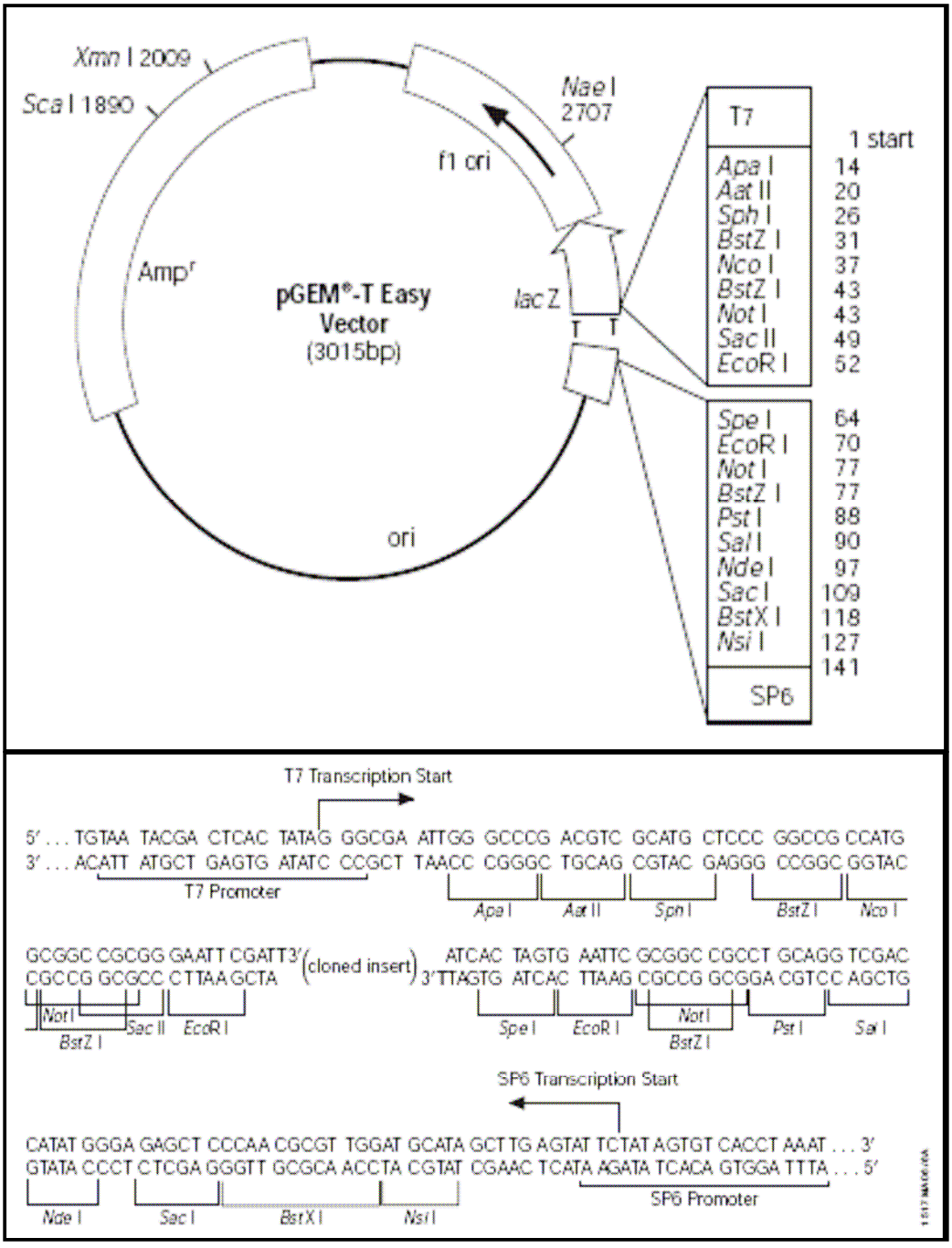


(A) Prediction of the DCM secondary structure using PSIPRED

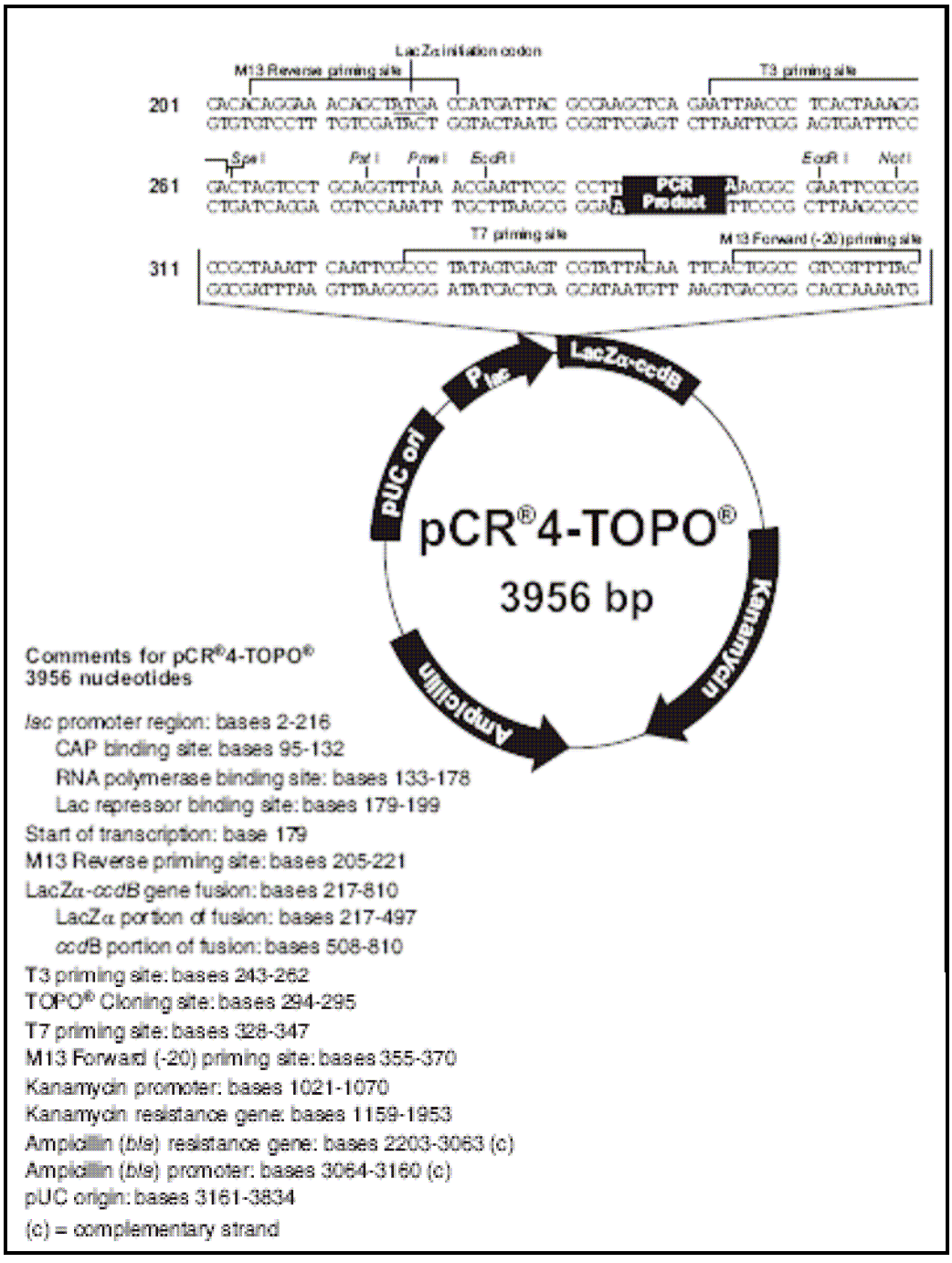
(B) The secondary structures of the domains within the DCM as mentioned in the literature.

6.5 Appendix V

TA cloning vectors



pGEM®-T easy cloning vector map and MCS (Promega, A 1360)



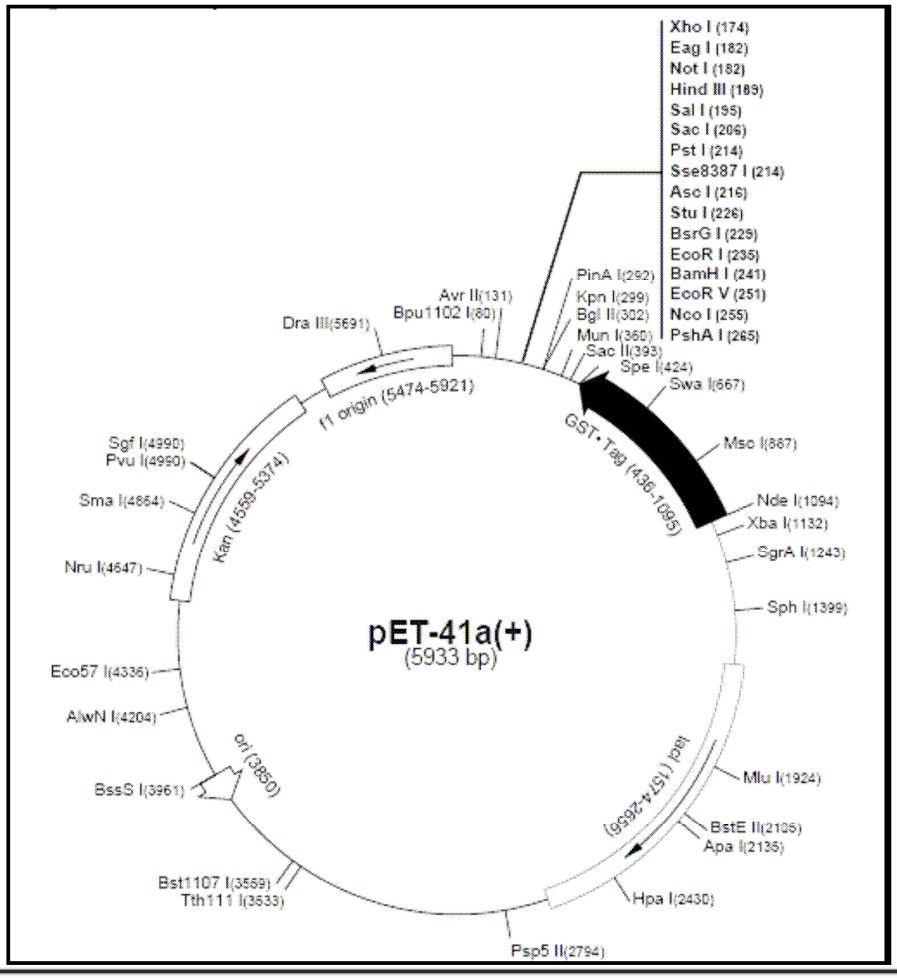
Comments for pCR®4-TOPO®
3956 nucleotides

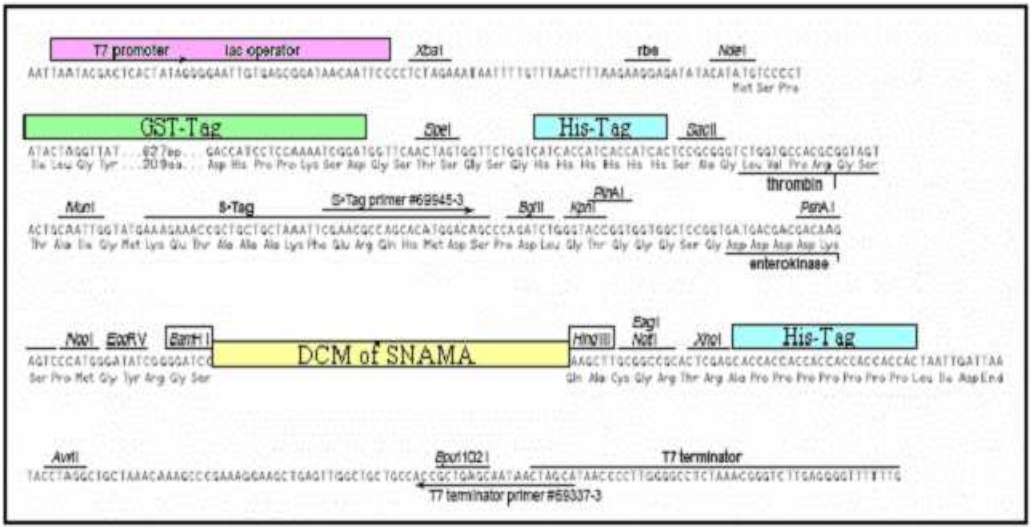
lac promoter region: bases 2-216
CAP binding site: bases 95-132
RNA polymerase binding site: bases 133-178
Lac repressor binding site: bases 179-199
Start of transcription: base 179
M13 Reverse priming site: bases 205-221
LacZα-*ccdB* gene fusion: bases 217-810
LacZα portion of fusion: bases 217-497
ccdB portion of fusion: bases 508-810
T3 priming site: bases 243-262
TOPO® Cloning site: bases 294-295
T7 priming site: bases 328-347
M13 Forward (-20) priming site: bases 355-370
Kanamycin promoter: bases 1021-1070
Kanamycin resistance gene: bases 1159-1953
Ampicillin (*bla*) resistance gene: bases 2203-3063 (c)
Ampicillin (*bla*) promoter: bases 3064-3160 (c)
pUC origin: bases 3161-3834
(c) = complementary strand

pCR®4-TOPO® cloning vector and MCS

6.6 Appendix VI

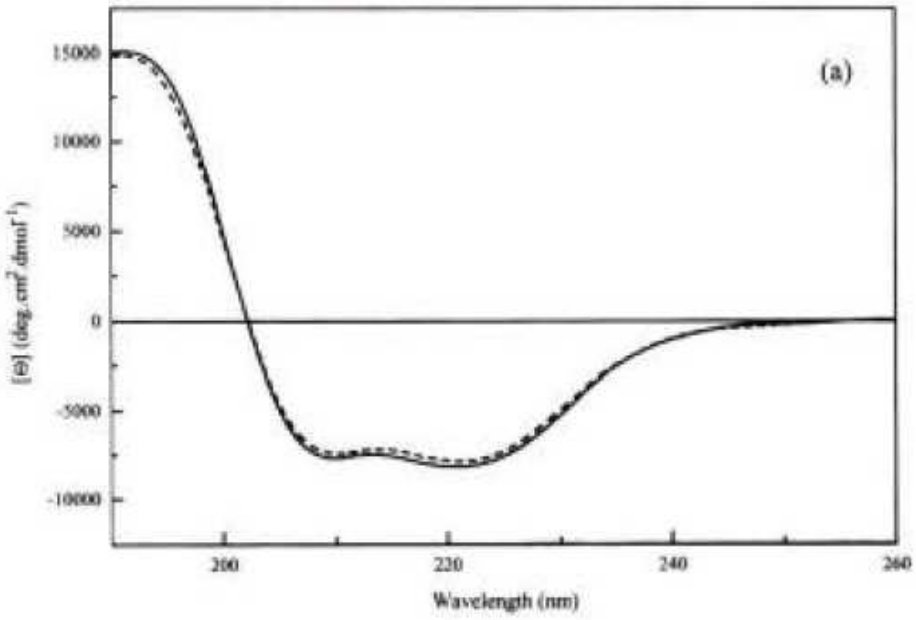
pET41(a) expression vector map and MCS (Novagen, 70556-3)



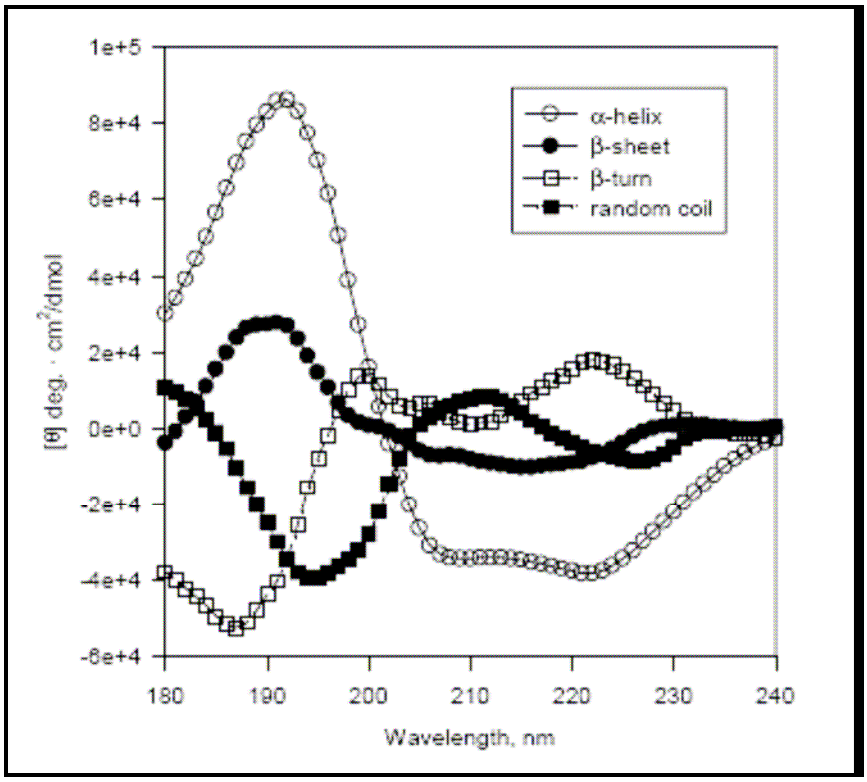


6.7 Appendix VII

CD spectra of characteristic secondary structures



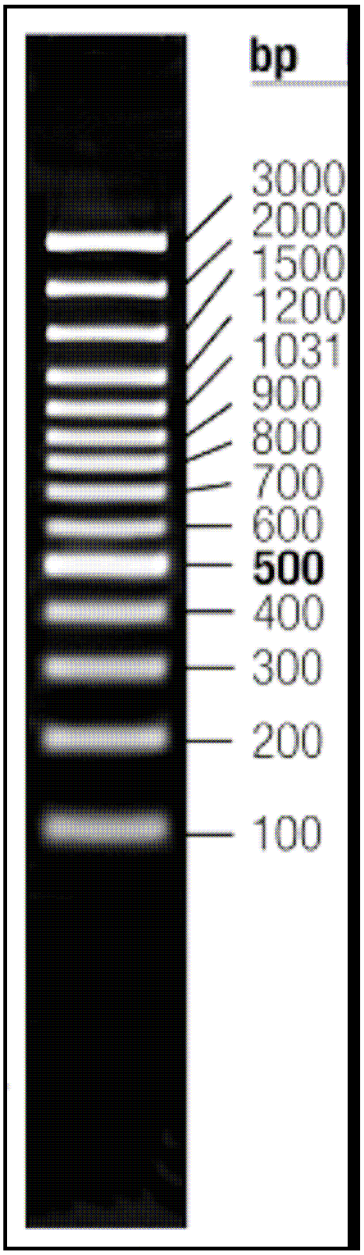
Typical CD spectra for an α-helical protein (Kelly and Price, 2000)



Basic CD spectra extrapolated from spectra from 16 proteins (Greenfield, 2004)

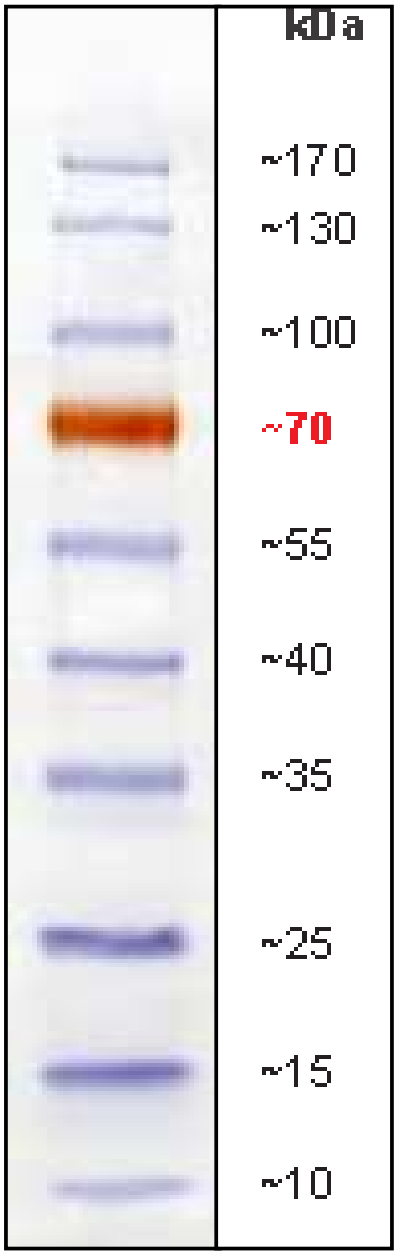
6.8 Appendix VIII

The molecular weight markers



GeneRuler™ 100 bp DNA Ladder Plus Ladder

(Fermentas, SM0321)



PageRuler™ Prestained Protein

(Fermentas, SM0671)

7. REFERENCES

Aasland, R., Gibson, T.J., and Stewart, A.F. (1995). The PHD finger: implications for chromatin-mediated transcriptional regulation. *TRENDS Biochem. Sci.* **20**, 56-59.

Albert, T.K., Hanzawa, H., Legtenberg, Y.I.A., de Ruwe, M.J., van den Heuvel, F.A.J., Collart, M.A., Boelens, R. and Timmers, H.T. (2002). Identification of a ubiquitin-protein ligase subunit within the CCR4-NOT transcription repressor complex. *EMBO J.* **21**, 355-364.

Andrade, M.A., Chacón, P., Merelo, J.J., and Morán, F. (1993). Evaluation of secondary structure of proteins from UV circular dichroism spectra using an unsupervised learning neural network. *Protein Engng* **6**, 383-390.

Arakawa, T. and Tsumoto, K. (2003). The effects of arginine on refolding of aggregate proteins: not facilitate refolding, but suppress aggregation. *Biochem. Biophys. Res. Communic.* **304**, 148-152.

Aravind, L. and Koonin, E.V. (2000). The U box is a modified RING finger – a common domain in ubiquitination. *Curr. Biol.* **10**, 132-134.

Argaman, L., Hershberg, R., Vogel, J., Bejerano, G., Wagner, E.G.H., Margalit, H., and Altuvia, S. (2001). Novel small RNA-encoding genes in the intergenic regions of *Escherichia coli*. *Curr. Biol.* **11**, 941-950.

Aspegren, A., Hinas, A., Larsson, P., Larsson, A., and Söderbom (2004). Novel non-coding RNAs in *Dictyostelium discoideum* and their expression during development. *Nucleic Acids Res.* **32**, 4646-4656.

Bell, S., Hansen, S, and Buchner, J. (2002). Refolding and structural characterization of the human p53 tumor suppressor protein. *Biophys. Chem.* **96**, 243-257.

Bensing, B.A., Meyer, B.J., and Dunny, G.M. (1996). Sensitive detection of bacterial transcription initiation sites and differentiation from RNA processing sites in the pheromone-induced plasmid transfer system of *Enterococcus faecalis*. *Proc. Natl. Acad. Sci. U.S.A.* **93**, 7794-7799.

Bergmann, A., Agapite, J., McCall, K., and Steller, H. (1998). The *Drosophila* gene *hid* is a direct target of Ras-dependent survival signalling. *Cell* **95**, 331-341.

Bernards, A. and Hariharan, I.K. (2001). Of flies and men – studying human disease in *Drosophila*. *Curr. Opin. Gen. Dev.* **11**, 274-278.

Biggins, S., Ivanovska, I., and Rose, M.D. (1996). Yeast ubiquitin-like genes are involved in duplication of the microtubule organising center. *J. Cell Biol.* **133**, 1331-1346.

Birnboim, H.V. (1983). A rapid alkaline extraction method for the isolation of plasmid DNA. *Methods Enzymol*. **100**, 243-255.

Böhm, G., Muhr, R., and Jaenicke, R. (1992). Quantitative analysis of protein far UV circular dichroism spectra by neural networks. *Protein Engng.* **5**, 191-195.

Bondesen, B.A. and Schuh, M.D. (2001). Circular dichroism of globular proteins. *J. Chem. Ed.* **78**, 1244-12247.

Borden, K.L.B. (2000). RING domains: master builders of molecular scaffolds? *J. Mol. Biol.* **295**, 1103-1112.

Bourdon, J.C., Fernandes, K., Murray-Zmijewski, F., Liu, G., Diot, A., Xirodimas, D.P., Saville, M.K., and Lane, D.P. (2005). p53 isoforms can regulate p53 transcriptional activity. *Genes Dev.* **19**, 2122-2137.

Brodsky, M.H., Nordstrom, W., Tsang, G., Kwan, E., Rubin, G.M., and Avrams, J.M. (2000). *Drosophila* p53 binds a damage response element at the *reaper* locus. *Cell* **101**, 103-113.

Brodsky, M.H., Weinert, B.T., Tsang, G., Rong, Y.S., McGinnis, N.M., Golic, K.G., Rio, D.C., and Rubin, G.M. (2004). *Drosophila melanogaster* MNK/Chk2 and p53 regulate multiple DNA repair and apoptotic pathways following DNA damage. *Mol. Cell. Biol.* **24**, 1219-1231.

Brooks, C.L., and Gu, W. (2006). p53 ubiquitination: Mdm2 and beyond. *Mol. Cell.* **21**, 307-315.

Bryson, K., McGuffin, L.J., Marsden, R.L., Ward, J.J., Sodhi, J.S. and Jones, D.T. (2005). Protein strucure prediction servers at University College London. *Nucl. Acids. Res.* **33** (Web Server Issue), 36-38.

Cabrita, L. D. and Bottomley, S.P. (2004). Protein expression and refolding – a practical guide to getting the most out of inclusion bodies. *Biotechol. Annu. Rev.* **10**, 31-50.

Canman, C.E., Lim, D.S., Cimprich, K.A., Taya, Y., Tamai, K., Sakaguchi, K., Appella, E., Kastan, M.B., and Siliciano, J.D. (1998). Activation of the ATM kinase by ionising radiation and phosphorylation of p53. *Science* **281**, 1677-1679.

Cashio, P., Lee, T.V., and Bergmann, A. (2005). Genetic control of programmed cell death in *Drosophila melanogaster*. *Semin. Cell Dev. Biol.* **16**, 225-235.

Cavener, D.R. (1987). Comparison of the consensus sequence flanking translational start sites in *Drosophila* and vertebrates. *Nucleic Acids Res.* **15**, 459-472.

Celniker, S.E. (2000). The *Drosophila* genome. *Curr. Opin. Gen. Dev.* **10**, 612-616.

Chai, J., Yan, N., Huh, J.R., Wu, J.W., Li, W., Hay, B.A., and Shi, Y. (2003). Molecular mechanism of Reaper-Grim-Hid-mediated suppression of DIAP1-dependent Dronc ubiquitination. *Nat. Struct. Biol.* **10**, 892-898.

Chen, D., Kon, N., Li, M., Zhang, W., Qin, J., and Gu, W. (2005). ARF-BP1/Mule is a critical mediator of the ARF tumor suppressor. *Cell* **121**, 1071-1083.

Chen, J., Lin, J., and Levine, A.J. (1995). Regulation of transcription functions of the p53 tumor suppressor by the *mdm*-2 oncogene. *Mol. Med.* **1**, 1142-1152.

Chen, P., Nordstrom, W., Gish, B., and Abrams, J.M. (1996). *grim*, a novel cell death gene in *Drosophila*. *Genes & Dev*. **10**, 1773-1782.

Chung, C.H. and Baek, S.H. (1999). Deubiquitinating enzymes: their diversity and emerging roles. *Biochem. Biophys. Res. Commun.* **266**, 633-640.

Ciechanover, A. (1998). The ubiquitin-proteasome pathway: on protein death and cell life. *EMBO J*. **17**, 7151-7160.

Clark, E.D. (1998). Refolding of recombinant proteins. *Curr. Opin. Biotech.* **9**, 157-163.

Colombani, J., Polesello, C., Josue, F., and Tapon, N. (2006). Dmp53 activates the Hippo pathway to promote cell death in response to DNA damage. *Curr. Biol.* **16**, 1453-1458.

D'Andrea, A. and Pellman, D. (1998). Deubiquitinating enzymes: a new class of biological regulators. *Crit. Rev. Biochem. Mol. Biol.* **33**, 337-352.

Darlix, J.C., Lapadat-Tapolsky, M., de Rocquigny, H., and Roques, B.P. (1995). First glimpses at structure-function relationships of the nucleocapsid protein of retroviruses. *J. Mol. Biol.* **254**, 523-537.

Degterev, A., Boyce, M. and Yuan, J. (2003). A decade of caspases. *Oncogene* **22**, 8543-8567.

Deng, L., Wang, C., Spencer, E., Yang, L., Braun, A., You, J., Slaughter, C., Pickart, C., and Chen, Z.J. (2000). Activation of the IκB kinase complex by TRAF6 requires a dimeric ubiquitin-conjugating enzyme complex and a unique polyubiquitin chain. *Cell* **103**, 351-361.

Ditzel, M., Wilson, R., Tenev, T., Zachariou, A., Paul, A., Deas, E., and Meier, P. (2003). Degradation of DIAP1 by the N-end rule pathway is essential for regulating apoptosis. *Nat. Cell Biol.* **5**, 373-376.

Dornan, D., Wertz, I., Shimizu, H., Arnott, D., Frantz, G.D., Dowd, P., O'Rourke, K., Koeppen, H., and Dixit, V.M. (2004). The ubiquitin ligase COP1 is a critical negative regulator of p53. *Nature* **429**, 86-92.

Dorstyn, L., Colussi, P.A., Quinn, L.M., Richardson, H., and Kumar, S.

(1999). DRONC, an ecdysone-inducible *Drosophila* caspase. *Proc. Natl. Acad. Sci. U.S.A.* **96**, 4307-4312.

Doumanis, J., Quinn, L., Richardson, H., and Kumar, S. (2001). STRICA, a novel *Drosophila melanogaster* caspase with an unusual serine/threonine-rich prodomain, interacts with DIAP1 and DIAP2. *Cell Death & Differ*. **8**, 387-394.

Du, W. and Dyson, N. (1999). The role of RBF in the introduction of G1 regulation during *Drosophila* embryogenesis. *EMBO J.* **18**, 916-925.

Edgar, B.A. (2006). From cell structure to transcription: Hippo forges a new path. *Cell* **124**, 267-273.

Eytan, E., Armon, T., Heller, H., Beck, S., and Hershko, A. (1993). Ubiquitin C-terminal hydrolase activity associated with the 26 S protease complex. *J. Biol. Chem.* **268**, 4668-4674.

Fang, S., Jensen, J.P., Ludwig, R.L., Vousden, K.H., and Weissman, A.M. (2000). Mdm2 is a RING finger-dependent ubiquitin protein ligase for itself and p53. *J. Biol. Chem.* **275**, 8945-8951.

Feng, L., Lin, T., Uranishi, H., Gu, W., and Xu, Y. (2005). Functional analysis of the roles of posttranslational modifications at the p53 C terminus in regulating p53 stability and activity. *Mol. Cell. Biol.* **25**, 5389-5395.

Folberg-Blum, A., Sapir, A., Shilo, B.Z., amd Oren, M. (2002). Overexpression of mouse Mdm2 induces development phenotypes in *Drosophila*. *Oncogene* **21**, 2413-2417.

Freemont, P.S. (1993). The RING finger: a novel protein sequence motif related to the zinc finger. *Ann. N Y Acad. Sci.* **11**, 174-192.

Freemont, P.S., Hanson, I.M. and Trowsdale, J.A. (1991). Novel cysteine-rich sequence motif. *Cell* **64**, 483-484.

Fribourg, S., Kellenberger, E., Rogniaux, H., Poterszman, A., Van Dorsselaer, A., Thierry, J.C., Egly, J.M., Moras, D. and Kieffer, B. (2000). Structural characterization of the cysteine-rich domain of TFIIH p44 subunit. *J. Biol. Chem.* **275**, 31963-31971.

Furukawa, K., Mizushima, N., Noda, T., and Ohsumi, Y. (2000). A protein conjugation system in yeast with homology to biosynthetic enzyme reaction of prokaryotes. *J. Biol. Chem.* **275**, 7462-7465.

Furukawa, M., Ohto, T., and Xiong, Y. (2002). Activation of UBC5 ubiquitin-conjugating enzyme by the RING finger of ROC1 and assembly of active ubiquitin ligases by all cullins. *J. Biol. Chem.* **227**, 15758-15785.

Gao, S. and Scott, R.E. (2002). P2P-R protein overexpression restricts mitotic progression at prometaphase and promotes mitotic apoptosis. *J. Cellular Physiology* **193**, 199-207.

Gao, S., Witte, M.M., and Scott, R.E. (2002). P2P-R protein localizes to the nucleolus of interphase cells and the periphery of chromosomes in mtotic cells which show maximum P2P-R immunoreactivity. *J. Cellular Physiology* **191**, 145-154.

Gershenzon, N.I., Trifonov, E.N., and Ioshikhes, I.P. (2006). The features of *Drosophila* core promoters revealed by statistical analysis. *BMC Gen.* **7**, 161.

Glickman, M.H. and Ciechanover, A. (2002). The ubiquitin-proteasome proteolytic pathway: destruction for the sake of construction. *Physiol. Rev.* ***82***, 373-428.

Goldstein, G., Steed, M., Hammerling, U., Boyse, E.A., Schlesinger, D.H. and Niall, H.D. (1975). Isolation of a polypeptide that has lymphocyte-differentiating properties and is probably represented universally in living cells. *Proc. Natl. Acad. Sci. U.S.A.* **72**, 11-15.

Grether, M.E., Abrams, J.M., Agapite, J., White, K., and Steller, H. (1995). The *head involution defective* gene of *Drosophila melanogaster* functions in programmed cell death. *Genes & Dev.* **9**, 1694-1708.

Gum, J.R., Hicks, J.W., Crawley, S.C., Dahl, C.M., Yang, S.C., Robertson, A.M., and Kim, Y.S. (2003). Initiation of transcription of the *MUC*3A human intestinal mucin from a TATA-less promoter and comparison with the *MUC*3B amino terminus. *J. Biol. Chem.* **278**, 49600-49609.

Haas, A.L. and Rose, I.A. (1982). The mechanism of ubiquitin activating enzyme. *J. Biol. Chem.* **257**, 10329-10337.

Hamaratoglu, F., Willecke, M., Kango-Singh, M., Nolo, R., Hyun, E., Tao, C., Jafar-Nejad, H., and Halder, G. (2006). The tumour-suppressor genes NF2/Merlin and Expanded act through Hippo signaling to regulate cell proliferation and apoptosis. *Nat. Cell Biol.* **8**, 27-36.

Hatakeyama, S., Yada, M., Matsumoto, M., Ishida, N., and Nakayama, K.I. (2001). U box proteins as a new family of ubiquitin-protein ligases. *J. Biol. Chem.* **276**, 33111-33120.

Haupt, Y., Maya, R., Kazaz, A. and Oren, M. (1997). Mdm2 promotes the rapid degradation of p53. *Nature* **387**, 296-299.

Hay, B.A., Wassarman, D.A., and Rubin, G.M. (1995). *Drosophila* homologs of baculovirus inhibitor of apotosis proteins function to block cell death. *Cell* **83**, 1253-1262.

Hershko, A. and Ciechanover, A. (1998). The ubiquitin system. *Annu. Rev. Biochem.* **67**, 425-479.

Hershko, A., Heller, H., Elias, S., and Ciechanover, A. (1983). Components of the ubiquitin protein ligase system: resolution, affinity purification and role in protein breakdown. *J. Biol. Chem.* **258**, 8206-8214.

Hölzl, H., Kapelari, B., Kellermann, J., Seemüller, E., Sümegi, M., Udvardy, A., Medalia, O., Sperling, J., Müller, S.A., Engel, A., and Baumeister, W. (2000). The regulatory complex of *Drosophila melanogaster* 26S proteasomes: subunit composition and localization of a debubiquitylating enzyme. *J. Cell. Biol.* **150**, 119-129.

Honda, R., Tanaka, H., and Yasuda, H. (1997). Oncoprotein MDM2 is a ubiquitin ligase E3 for tumor suppressor p53. *FEBS. Lett.* **420**, 25-27.

Hori, T., Osaka, F., Chiba, T., Miyamoto, C., Okabayashi, K., Shimbara, N., Kato, S., and Tanaka, K. (1999). Covalent modification of all members of human cullin family proteins by NEDD8. *Oncogene* **18**, 6829-6834.

Hu, M., Li, P., Li, M., Li, W., Yao, T., Wu, J.W., Gu, W., Cohen, R.E., and Shi, Y. (2002). Crystal structure of a UBP-family deubiquitinating enzyme in isolation and in complex with ubiquitin aldehyde. *Cell* **111**, 1041-1054.

Huang, J., Wu, S., Barrera, J., Matthews, K., and Pan, D. (2005). The Hippo signalling pathway co-ordinately regulates cell proliferation and apoptosis by inactivating Yorkie, the *Drosophila* homolog of YAP. *Cell* **122**, 421-434.

Igaki, T., Kanda, H., Yamamoto-Goto, Y., Kanuka, H., Kuranaga, E., Aigaki, T., and Miura, M. (2002). Eiger, a TNF superfamily ligand that triggers the *Drosophila* JNK pathway. *EMBO J.* **21**, 3009-3018.

Imai, N., Matsuda, N., Tanaka, K., Nakano, A., Matsumoto, S., and Kang, W. (2003). Ubiquitin ligase activities of *Bombyx mori* Nucleopolyhedrovirus RING finger proteins. *J. Virol.* **77**, 923-930.

Jacobson, M.D., Weil, M., and Raff, M.C. (1997). Programmed cell death in animal development. *Cell* **88**, 347-354.

Jentsch, S. and Pyrowolakis, G. (2000). Ubiquitin and its kin: how close are the family ties? *Trends Cell Biol.* **10**, 335-342.

Jeszenszky, W. A. (1997). Managing the fruit fly experiment. *American Biology Teacher* **59**, 292-294.

Jiang, C., Lamblin, A.F.J., Steller, H., and Thummel, C.S. (2000). A steroid-triggered transcriptional hierarchy controls salivary gland cell death during *Drosophila* metamorphosis. *Mol. Cell* **5**, 445-455.

Jin, S., Martinek, S., Joo, W.S., Wortman, J.R., Mirlovic, N., Sali, A., Yandell, M.D., Pavletich, N.P., Young, M.W., and Levine, A.J. (2000). Identification and characterization of a p53 homologue in *Drosophila melanogaster*. *Proc. Natl. Acad. Sci. U.S.A.* **97**, 7301-7306.

Joazeiro, C.A.P. and Weismann, A.M. (2000). RING finger proteins: mediators of ubiquitin ligase activity. *Cell* **102**, 549-552.

Johnson, E.S. and Gupta, A.A. (2001). An E3-like factor that promotes SUMO conjugation to the yeast septins. *Cell* **106**, 735-744.

Johnson, E.S., Schwienhorst, I., Dohmen, R.J., and Blobel, G. (1997). The ubiquitin-like protein Smt3p is activated for conjugation to other proteins by an Aos1p/Uba2p heterodimer. *EMBO J.* **16**, 5509-5519.

Johnson, P.R. and Hochstrasser, M. (1997). SUMO-1: ubiquitin gains weight. *trends Cell Biol.* **7**, 408-413.

Jones, C., Reifegerste, R., and Moses, K. (2006). Characterization of Drosophila *mini-me*, a gene required for cell proliferation and survival. *Genetics* **173**, 793-808.

Kamitani, T., Kito, K., Nguyen, H.P., Wada, H., Fukuda-Kamitani, T., and Yeh, E.T.H. (1998). Identification of three major sentrinization sites in PML. *J. Biol. Chem.* **273**, 26675-27782.

Karuppiah, N. and Sharma, A. (1995). Cyclodextrins as protein refolding aids. *Biochem. Biophys. Res. Commun.* **211**, 60-66.

Kawakami, T., Chiba, T., Suzuki, T., Iwai, K., Yamanaka, K., Minato, N., Suzuki, H., Shimbara, N., Hidaka, Y., Osaka, F., Omata, M., and Tanaka, K. (2001). NEDD8 recruits E2-ubiquitin to SCF E3 ligase. *EMBO J.* **20**, 4003-4012.

Kelly, S.M. and Price, N.C. (2000). The use of circular dichroism in the investigation of protein structure and function. *Curr. Protein Peptide Science* **1**, 349-384.

Khorasanizadeh, S., Peters, I.D., Butt, T.R., and Roder, H. (1993). Folding and stability of a tryptophan-containing mutant of ubiquitin. *Biochemistry* **32**, 7054-7063.

Kirschner, M. (1999). Intracellular proteolysis. *Trends Cell Biol.* **9**, M42-M45.

Kleijnen, M.F., Shih, A.H., Zhou, P., Kumar, S., Soccio, R.E., Kedersha, N.L., Gill, G., and Howley, P.M. (2000). The hPLIC protins may provide a link between the ubiquitination machinery and the proteasome**.** *Mol. Cell.* **6**, 409-419.

Klein, D.J., Johnson, P.E., Zollars, E.S., De Guzman, R.N., and Summers, M.F. (2000). The NMR structure of the nucleocapsid protein from the mouse mammary tumor virus reveals unusual folding of the C-terminal zinc knuckle. *Biochemistry* **39**, 1604-1612.

Koegl, M., Hoppe, T., Schlenker, S., Ulrich, H.D., Mayer, T.U., and Jentsch, S. (1999). A novel ubiquitination factor, E4, is involved in multiubquitin chain assembly. *Cell* **96**, 635-644.

Kramer, C.D. (1986). The classroom animals – fruit flies. *Science and Children*, 30-33.

Krantz, B.A. and Sosnick, T.R. (2000). Distinguishing between two state and three state models for ubiquitin folding. *Biochemistry* **39**, 11696-11701.

Krishna, S.S., Majumdar, I., and Grishin, N.V. (2003). Structural classification of zinc fingers: Survey and summary. *Nucleic Acids Res.* **31**, 532-550.

Kriventseva, E.V. and Gelfand, M.S. (1999). Statistical analysis of the exon-intron structure of higher and lower eukaryotes genes. *J. Biom. Struct. Dyn.* **17**, 281-288.

Krummel, K.A., Lee, C.J., Toledo, F., and Wahl, G.M. (2005). The C-terminal lysines fine-tune p53 stress responses in a mouse model but are not required for stability control or transactivation. *Proc. Natl. Acad. Sci. U.S.A.* **102**, 10188-10193.

Kumar, S. and Doumanis, J. (2000). The fly caspases. *Cell Death Differ.* **7**, 1039-1044.

Kurada, P. and White, K. (1998). Ras promotes cell survival in *Drosophila* by downregulating *hid* expression. *Cell* **95**, 319-329.

Laemmli, U.K. (1970). Cleavage of structural proteins during the assembly of the head of bacteriophage T4. *Nature* **227**, 680-685.

Lambertson, D., Chen, L., and Madura, K. (1999). Pleiotropic defects caused by loss of the proteasome-interacting factors Rad23 and Rpn10 of *Saccharomyces cerevisiae*. *Genetics* **153**, 69-79.

Laney, J.D. and Hochstrasser, M. (1999). Substrate targeting in the ubiquitin system. *Cell* **97**, 427-430.

Lee, J.H., Lee, E., Park, J., Kim, E., Kim, J., and Chung, J. (2003). In vivo p53 function is indispensable for DNA damage-induced apoptotic signalling in *Drosophila*. *FEBS Lett.* **550**, 5-10.

Lee, T. A. and Tyers, M. (2001). Ubiquitin junction, what's your function? *Genome Biol.* **2**, 40251-40253.

Leng, R.P., Lin, Y., Ma, W., Wu, H., Lemmers, B., Chung, S., Parant, J.M., Lozano, G., Hakem, R., and Benchimol, S. (2003). Pirh2, a p53-induced ubiquitin-protein ligase, promotes p53 degradation. *Cell* **112**, 779-791.

Leulier, F., Rodriguez, A., Khush, R.S., Abrams, J.M., and Lemaitre, B. (2000). The *Drosophila* caspase Dredd is required to resist gram-negative bacterial infection. *EMBO Rep.* **1**, 353-358.

Levine, A.J. (1997). p53, the cellular gatekeeper for growth and division. *Cell* **88**, 323-331.

Lewis, B.A., Kim, T.K., and Orkin, S.H. (2000). A downstream element in the human β-globin promoter: Evidence of extended sequence-specific transcription factor IID contacts. *Proc. Natl. Acad. Sci. U.S.A.* **97**, 7172-7177.

Li, D.W., Yu, J.F., Chen, Y.J., Ma, H.B., Wang, Z.F., Zhu, Y.B., and Zhang, X.G. (2004). Refolding and characterization of recombinant human GST-PD-1 fusion protein expressed in *Escherichia coli*. *Acta Biochim. Biophys. Sin.* **36**, 141-146.

Li, L., Deng, B., Xing, G., Teng, Y., Tian, C., Cheng, X., Yin, X., Yang, J., Gao, X., Zhu, Y., Sun, Q., Zhang, L., Yang, X., and He, F. (2007). PACT is a negative regulator of p53 and essential for cell growth and embryonic development. *Proc. Natl. Acad. Sci U.S.A.* **104**, 7951-7956.

Liakopoulos, D., Doenges, G., Matuschewski, K., and Jentsch, S. (1998). A novel protein modification pathway related to the ubiquitin system. *EMBO J.* **17**, 2208-2214.

Lim, C.Y., Santoso, B., Boulay, T., Dong, E., Ohler, U., and Kadonaga, J.T. (2004). The MTE, a new core promoter element for transcription by RNA polymerase II. *Genes Dev.* **18**, 1606-1617.

Lopato, S., Gattoni, R., Fabini, G., Stevenin, J., and Barta, A. (1999). A novel family of plant splicing factors with a Zn knuckle motif: examination of RNA binding and splicing activities. *Plant Mol. Biol.* **39**, 761-773.

Lorick, K.L., Jensen, J.P., Fang, S., Ong, A.M., Hatakeyama, S., and Weissman, A.M. (1999). RING fingers mediate ubiquitin-conjugating enzyme (E2)-dependent ubiquitination. *Proc. Natl. Acad. Sci. U.S.A.* **96**, 11364-11369.

Lu, Z., Xu, S., Joazeiro, C., Cobb, M.H., and Hunter, T. (2002). The PHD domain of MEKK1 acts as an E3 ubiquitin ligase and mediates ubiquitination and degradation of ERK1/2. *Mol. Cell* **9**, 945-956.

Lüders, J., Pyrowolakis, G., and Jentsch, S. (2003). The ubiquitin-like protein HUB1 forms SDS-resistant complexes with cellular proteins in the absence of ATP. *EMBO rep.* **4**, 1169-1174.

Martinez-Noel, G., Niedenthal, R., Tamura, T., and Harbers, K. (1999). A family of structurally related RING finger proteins interacts specifically with the ubiquitin-conjugating enzyme UbcM4. *FEBS Lett.* **454**, 257-261.

Mather, A. *The identification and characterisation of a novel apoptotic gene, SNAMA, in Drosophila melanogaster*, University of the Witwatersrand, Johannesburg, South Africa, 2005.

Mather, A., Rakgotho, M., and Ntwasa, M. (2005). SNAMA, a novel protein with a DWNN domain and a RING finger-like motif: A possible role in apoptosis. *Biochim. Biophys. Acta* **1727**, 169-176.

Matthews, J.M., Kowalski, K., Liew, C.K., Sharpe, B.K., Fox, A.H., Crossley, M., and Mackay, J.P. (2000). A class of zinc fingers involved in protein-protein interactions. *Eur. J. Biochem.* **267**, 1030-1038.

McNally, T., Huang, Q., Janis, R.S., Liu, Z., Olejniczak, E.T. and Reilly, R.M. (2003). Structural analysis of UBL5, a novel ubiquitin-like modifier. *Protein Sci.* **12**, 1562-1566.

Meier, P., Silke, J., Leevers, S.J. and Evan, G.I. (2000). The *Drosophila* caspase DRONC is regulated by DIAP1. *EMBO J.* **19**, 598-611.

Michael, D. and Oren, M. (2002). The p53-Mdm2 module and the ubiquitin system. *Sem. Cancer Biol.* **13**, 49-58.

Midgley, C.A. and Lane, D.P. (1997). p53 protein stability in tumour cells is not determined by mutation but is dependent on Mdm2 binding. *Oncogene* **15**, 1179-1189.

Miller, L.K. (1999). An exegesis of IAPs: salvation and surprises from BIR motifs. *Trends Cell Biol.* **9**, 323-328.

Miyashita, T. and Reed, J.C. (1995). Tumor suppressor p53 is a direct transcriptional activator of the human *bax* gene. *Cell* **80**, 293-299.

Morett, E. and Bork, P. (1999). A novel transactivation domain in parkin. *TRENDS Biochem. Sci.* **24**, 229-231.

Morgan, T. H., Sturtevant, A. H., Muller, H. J. and Bridges, C. B. (1915). The mechanism of mendelian heredity. Henry Bolt, New York, reproduced in Johnson Reprints, New York, 1972.

Morrissey, J.H. (1981). Silver stain for proteins in polyacrylamide gels: a modified procedure with enhanced uniform sensitivity. *Anal. Biochem.* **117**, 308-310.

Mortin, L.I. and Sedat, J.W. (1982). Structure of *Drosophila* polytene chromosomes. *J. Cell Sci.* **57**, 73-113.

Muro, I., Hay, B.A. and Clem, R.J. (2002). The *Drosophila* DIAP1 protein is required to prevent accumulation of a continuously generated, processed form of the apical caspase DRONC. *J. Biol. Chem.* **277**, 49644-49650.

Nakayama, K.I. and Nakayama, K. (2006). Ubiquitin ligases: cell-cycle control and cencer. *Nature Rev. Cancer* **6**, 369-381.

Neuman, S., Kovalio, M., Yaffe, D., and Nudel, U. (2005). The *Drosophila* homologue of the dystrophin gene – Introns containing promoters are the major contributors to the large size of the gene. *FEBS Letters* **579**, 5365-5371.

Nijman, S.M.B., Luna-Vargas, M.P.A., Velds, A., Brummelkamp, T.R., Dirac, A.M.G., Sixma, T.K., and Bernards, R. (2005). A genomic and functional inventory of deubiquitinating enzymes. *Cell* **123**, 773-786.

Nordstrom, W. and Abrams, J.M. (2000). Guardian ancestry: fly p53 and damage-inducible apoptosis. *Cell Death Diff.* **7**, 1035-1038.

Nordstrom, W., Chen, P., Steller, H., and Abrams, J.M. (1996). Activation of the *reaper* gene during ectopic cell killing in *Drosophila*. *Dev. Biol.* **180**, 213-226.

Ollmann, M., Young, L.M., Di Como, C.J., Karim, F., Belvin, M., Robertson, S., Whittaker, K., Demsky, M., Fisher, W.W., Buchman, A., Duyk, G.,

Friedman, L., Prives, C., and Kopczynski, C. (2000). *Drosophila* p53 is a structural and functional homolog of the tumor suppressor p53. *Cell* **101**, 91-101.

Olson, M.R., Holley, C.L., Yoo, S.J., Huh, J.R., Hay, B.A., and Kornbluh, S. (2003). Reaper is regulated by IAP-mediated ubiquitination. *J. Biol. Chem.* **278**, 4028-4034.

Oren, M. (2003). Decision making by p53: life, death and cancer. *Cell Death Differ*. **10**, 431-442.

Peters, J.M. (1998). SCF and APC: the Yin and Yang of cell cycle regulated proteolysis. *Curr. Opin. Cell Biol.* **10**, 759-768.

Peters, M., DeLuca, C., Hirao, A., Stambolic, V., Potter, J., Zhou, L., Liepa, J., Snow, B., Arya, S., Wong, J., Bouchard, D., Binari, R., Manoukian, A.S., and Mak, T.W. (2002). Chk2 regulates irradiaion-induced, p53-mediated apoptosis in *Drosophila*. *Proc. Natl. Acad. Sci U.S.A.* **99**, 11305-11310.

Pickart, C.M. (2001). Mechanisms underlying ubiquitination. *Annu. Rev. Biochem.* 70503-70555.

Pugh, D., Ab, E., Faro, A., Lutya, P.T., Hoffmann, E., and Rees, J.G. (2006). DWNN, a novel ubiquitin-like domain, implicates RBBP6 in mRNA processing and ubiquitin-like pathways. *BMC Struc. Biol.* **6**,

Quinn, L.M., Dorstyn, L., Mills, K., Colussi, P.A., Chen, P., Coombe et al. (2000). An essential role for the capsase dronc in developmentally programmed cell death in *Drosophila*. *J. Biol. Chem.* **275**, 40416-40424.

Rakgotho, P.M. *Identification of proteins that interact with DWNN domain of SNAMA a member of a novel protein superfamilyi*, University of the Witwatersrand, Johannesburg, South Africa, 2007.

Ramelot, T.A., Cort, J.R., Yee, A.A., Semesi, A., Edwards, A.M., Arrowsmith, C.H., and Kennedy, M.A. (2003). Solution structure of the yeast ubiquitin-like modifier protein Hub1. *J. Struc. Func. Genomics* **4**, 25-30.

Richardson, H. and Kumar, S. (2002). Death to flies: *Drosophila* as a model system to study programmed cell death. *J. Immunol. Meth.* **265**, 21-38.

Rozema, D. and Gellman, S.H. (1995). Artificial chaperones: protein refolding via sequential use of detergent and cyclodextrin. *J. Am. Chem. Soc.* **117**, 2373-2374.

Ryan, K.M., Phillips, A.C., and Vousden, K.H. (2001). Regulation and function of the p53 tumor suppressor protein. *Curr. Opin. Cell Biol.* **13**, 332-337.

Sakai, Y., Saijo, M., Coelho, K., Kishino, T., Niikawa, N., and Taya, Y. (1995). cDNA sequence and chromosomal localisation of a novel human protein, RBQ-1 (RBBP6), that binds to the retinoblastoma gene product. *Genomics* **30**, 98-101.

Salvesen, G.S. and Abrams, J.M. (2004). Caspase activation – stepping on the gas or releasing the brakes? Lessons from humans and flies. *Oncogene* **23**, 2774-2784.

Salvesen, G.S. and Duckett, C.S. (2002). IAP proteins: blocking the road to death's door. *Nat. Rev. Mol. Cell Biol.* **3**, 401-410.

Saurin, A.J., Borden, K.L.B., Boddy, M.N., and Freemont, P.S. (1996). Does this have a familiar RING? *Trends Biochem. Sci.* **21**, 208-214.

Scheffner, M., Huibregtse, J.M., Vierstra, R.D., and Howley, P.M. (1993). The HPV-16 E6 and E6-AP complex functions as a ubiquitin-protein ligase in the ubiquitination of p53. *Cell* **75**, 495-505.

Schwartz, D.C. and Hochstrasser, M. (2003). A superfamily of protein tags: ubiquitin, SUMO and related modifiers. *TRENDS Biochem. Sci.* **28**, 321-328.

Scott, R.E., Giannakouros, T., Gao, S., and Peidis, P. (2003). Functional potential of P2P-R: a role in the cell cycle and cell differentiation related to its interactions with protein that bind to matrix associate regions of DNA. *J. Cellular Biochem.* **90**, 6-12.

Shieh, S.Y., Ahn, J., Tamai, K., Taya, Y., and Prives, C. (2000). The human homologs of checkpoint kinases Chk1 and Cds1 (Chk2) phosophorylate p53 at multiple DNA damage-inducible sites. *Genes Dev.* **14**, 289-300.

Shimura, H., Hattori, N., Kubo, S.I., Mizuno, Y., Asakawa, S., Minoshima, S., Shimizu, N., Iwai, T.C., Tanaka, K., and Suzuki, T. (2000). Familial Parkinson disease gene product, Parkin, is a ubiquitin-protein ligase. *Nat. Genet.* **25**, 302-305.

Simons, A., Melamed-Bessudo, C., Wolkowicz, R., Sperling, J., Sperling, R., Eisenbach, L., and Rotter, V. (1997). PACT: cloning and characterization of a cellular p53 binding protein that interacts with Rb. *Oncogene* **14**, 145-155.

Smale, S.T. and Kadonaga, J.T. (2003). The RNA polymerase II core promoter. *Annu. Rev. Biochem.* **72**, 449-479.

Sofer, W. and Tompkins, L. (1994). Genetics in the classroom – *Drosophila* genetics in the classroom. *Genetics* **136**, 417-422.

Srinivasula, S.M., Datta, P., Kobayashi, M., Wu, J.W., Fujioka, M., Hegde, R., Zhang, Z., Mukattash, R., Fernandes-Alnemri, T., Shi, Y., Jaynes, J.B., and Alnemri, E.S. (2002). *sickle*, a novel *Drosophila* death gene in the *reaper*/*hid*/*grim* region, encodes an IAP-inhibitory protein. *Curr. Biol.* **12**, 125-130.

Staub, O., Dho, S., Henry, P., Correa, J., Ishikawa, T., McGlade, J. and Rotin, D. (1996). WW domains of Nedd4 bind to the proline-rich PY motifs in the epithelial Na+ channel deleted in Liddle's syndrome. *EMBO J.* **15**, 2371-2380.

Stone, S.L., Hauksdóttir, H., Troy, A., Herschleb, J., Kraft, E., and Callis, J. (2005). Functional analysis of the RING-type ubiquitin ligase family of *Arabidopsis Plant Phys.* **137**, 13-30.

Sun, Y. (2003). Targeting E3 ubiquitin ligases for cancer therapy. *Cancer Biol. Ther*. **2**, 623-629.

Sutcliffe, J.E., and Brehm, A. (2004). Of flies and men: p53, a tumour suppressor. *FEBS Lett.* **567**, 86-91.

Sutcliffe, J.E., Korenjak, M., and Brehm, A. (2003). Tumour suppressors – a flies perspective. *Eur. J. Cancer* **39**, 1355-1362.

Tenev, T., Zachariou, A., Wilson, R., Paul, A., and Meier, P. (2002). Jafrac2 is an IAP antagonist that promotes cell death by liberating Dronc from DIAP1. *EMBO J.* **21**, 5118-5129.

Thompson, B.J. and Cohen, S.M. (2007). The Hippo pathway regulates the *bantam* microRNA to control cell proliferation and apoptosis in *Drosophila*. *Cell* **126**, 767-774.

Thress, K., Henzel, W., Shillinglaw, W., and Kornbluth, S. (1998). Scythe: a novel reaper-binding apoptotic regulator. *EMBO J.* **17**, 6135-6143

Varshavsky, A. (2003). The N-end rule and regulation of apoptosis. *Nat. Cell Biol.* **5**, 467-473.

Vernooy, S.Y., Copeland, J., Ghaboosi, N., Griffin, E.E., Yoo, S.J., and Hay, B.A. (2000). Cell death regulation in *Drosophila*: conservation of mechanism and unique insights. *J. Cell Biol.* **150**, 69-75.

Vidal, M. and Cagan, R.L. (2006). *Drosophila* models for cancer research. *Curr. Opin. Gen. Dev.* **16**, 10-16.

Vijay-Kumar, S., Bugg, C.E. and Cook, W.J. (1987). Structure of ubiquitin refined at 1.8 Å resolution. *J. Mol. Biol.* **194**, 531-544.

Vo, L.T.A., Minet, M., Schmitter, J., Lacroute, F., and Wyers, F. (2001). Mpe1, a zinc knuckle protein, is an essential component of yeast cleavage and polyadenylation factor required for the cleavage and adenylation of mRNA. *Mol. Cell. Biol.* **21**, 8346-8356.

Vousden, K.H. (2000). p53: death star. *Cell* **103**, 691-694.

Wang, S.I., Hawkins, C.J., Yoos, S.J., Muller, H.A., and Hay, B.A. (1999). The *Drosophila* caspase inhibitor DIAP1 is essential for cell survival and is negatively regulated by HID. *Cell* **98**, 453-463.

Watkins, J.F., Sung, P., Prakash, L., and Prakash, S. (1993). The *Saccharomyces cerevisiae* DNA repair gene *RAD23* encodes a nuclear protein containing a ubiquitin-like domain required for biological funcion. *Mol. Cell. Biol.* **13**, 7757-7765.

Weber, P.L., Brown, S.C. and Mueller, L. (1987). Sequential H-1-NMR assignments and secondary structure identification of human ubiquitin. *Biochemistry* **26**, 7283-7290.

Weismann, A.M. (1997). Regulating protein degradation by ubiquitination. *Immunol. Today* **18**, 189-198.

White, K., Grether, M.E., Abrams, J.M., Young, L., Farrell, K., and Steller, H. (1994). Genetic control of programmed cell death in *Drosophila*. *Science* **264**, 677-683.

Wilkinson, K.D., Urban, M.K., and Haas, A.L. (1980). Ubiquitin is the ATP-dependent proteolysis factor I of rabbit reticulocytes. *J. Biol. Chem.* **255**, 7529-7532.

Wing, J.P., Karres, J.S., Ogdahl, J.L., Zhou, L., Schwartz, L.M., and Nambu, J.R. (2002). *Drosophila sickle* is a novel *grim-reaper* cell death activator. *Curr. Biol.* **12**, 131-135.

Wing, J.P., Schwartz, L.M., and Nambu, J.R. (2001). The RHG motifs of *Drosophila* Reaper and Grim are important for their distinct cell death-inducing abilities. *Mech. Dev.* **102**, 193-203.

Witte, M.M. and Scott, R.E. (1997). The proliferation potential protein-related (P2P-R) gene with domains encoding heterogeneous nuclear ribonucleoprotein

association and Rb1 binding shows repressed expression during terminal differentiation. *Proc. Natl. Acad. Sci. U.S.A.* **94**, 1212-1217.

Wu, X., Bayle, J.H., Olson, D., and Levine, A.J. (1993). The p53-mdm-2 autoregulatory feedback loop. *Genes & Dev.* **7**, 1126-1132.

Xu, J., Xin, S., and Du, W. (2001). *Drosophila* Chk2 is required for DNA damage-mediated cell cycle arrest and apoptosis. *FEBS Lett.* **508**, 394-398.

Yan, N., Wu, J.W., Chai, J., Li, W., and Shi, Y. (2004). Molecular mechanisms of DrICE inhibition by DIAP1 and removal of inhibition by Reaper, Hid and Grim. *Nat. Struct. & Mol. Biol.* **11**, 420-428.

Yeh, E.T.H., Gong, L., and Kamitani, T. (2000). Ubiquitin-like proteins: new wines in new bottles. *Genes* **248**, 1-14.

Yi, C. and Deng, X.W. (2005). COP1 – from plant photomorphogenesis to mammalian tumorigenesis. *TRENDS Cell Biol.* **15**, 618-625.

Yoshitake, Y., Nakatsura, T., Monji, M., Senju, S., Matsuyoshi, H., Tsukamoto, H., Hosaka, S., Komori, H., Fukuma, D., Ikuta, Y., Katagiri, T., Furukawa, Y., Ito, H., Shinohara, M., Nakamura, Y., and Nishimura, Y. (2004). Proliferation potential-related protein, an ideal esophageal cancer antigen for immunotherapy, identified using complementary DNA microarray analysis. *Clinical Cancer Res.* **10**, 6437-6448.

Zachariou, A., Tenev, T., Goyal, L., Agapite, J., Steller, H., and Meier, P. (2003). IAP-antagonists exhibit non-redundant modes of action through differential DIAP1 binding. *EMBO J.* **22**, 6642-6652.

Zhou, P. and Howley, P.M. (1998). Ubiquitination and degradation of the substrate recognition subunits of SCF ubiquitin-protein ligases. *Mol. Cell* **2**, 571-580.